

LOW OXIDATION POTENTIAL ELECTROACTIVE POLYMERS

By

JENNIFER ALLISON ASH IRVIN

A DISSERTATION PRESENTED TO THE GRADUATE SCHOOL  
OF THE UNIVERSITY OF FLORIDA IN PARTIAL FULFILLMENT  
OF THE REQUIREMENTS FOR THE DEGREE OF  
DOCTOR OF PHILOSOPHY

UNIVERSITY OF FLORIDA

1998

*This dissertation is dedicated to my family:*

*To my parents, who encouraged me to reach for the sky*

*To my grandparents, who didn't get to see me finish*

*and*

*To my husband, whose love means everything*

## ACKNOWLEDGEMENTS

This work would not have been possible without the excellent guidance of Dr. John Reynolds. His advice was instrumental in all the work found in this dissertation. The guidance of other faculty at the University of Florida has also been crucial to this work, especially the members of my committee, who made sure I had the knowledge necessary to complete my education. This includes Dr. Kenneth Wagener, Dr. James Deyrup, Dr. Robert Kennedy, and Dr. Anthony Brennan.

The support for graduate students in the Chemistry Department at the University of Florida is second to none. I would especially like to thank Donna Balkcom for her tireless support, as well as Lorraine Williams and Carol Lowe for their fantastic efforts and attention to detail. My thanks also go to all my professors at the University of Florida for their guidance and extreme patience.

Collaborations outside the Reynolds research group have been crucial to the success of this project. This includes the assistance of Dr. Youngkwan Lee, who was instrumental in the synthesis of one monomer. Dr. Alex Angerhofer's insights into EPR have been very helpful. Dr. Khalil Abboud's expertise in X-ray crystallography has been greatly appreciated.

The comments and assistance of members of the Reynolds research group have made the work presented in this dissertation much easier; off-hand observations often lead to great results. This project was initiated in part by work done by Dr. Balasubramanian Sankaran and Dr. Gregory Sotzing; their early assistance was helpful. Dr. Mark Morvant and Fabienne Piroux studied the *in situ* conductivity of polymers prepared herein. Mike Ramey's expertise in the areas of Stille and Suzuki polymerizations was essential and very timely. Irina Giurgiu's studies of ion effects in the glyme polymer were highly insightful and greatly appreciated. I had the pleasure to guide the research of two undergraduates, Norbert Correa and Chad Jones, whose precursor syntheses saved me countless hours. Former group member Dr. Andrew Child provided expert assistance in the areas of chemical polymerization and EPR spectroscopy. Other members of the group who helped incredibly in many ways include Dr. Anil Kumar, Dr. Peter Balandi, Dr. Seungho Kim, Don Cameron, Dean Welsh, Dr. Ashebir Fiseha, Dr. Hiep Ly, Dr. Fatma Selampinar, Carl Gaupp, and Chris Thomas.

I wish to extend my extreme gratitude to Debra Tindall and Jonathan Penney, without whom I would have been homeless during the writing of this dissertation.

Finally, I would like to thank my family, who always told me I could be anything I wanted. My husband, David, has been with me through the entire experience, and without his love, support, and fruitful conversations, none of this would have been possible.

## TABLE OF CONTENTS

	<u>page</u>
ACKNOWLEDGEMENTS .....	iii
LIST OF TABLES.....	viii
LIST OF FIGURES.....	ix
ABSTRACT .....	xii
CHAPTERS	
1 INTRODUCTION .....	1
Brief History of Conducting Polymers.....	1
Oxidative Polymerization Mechanism .....	2
Non-Oxidative Polymerizations.....	8
Conjugation and Conduction in Electroactive Polymers.....	11
Substituent Effects.....	14
Polymers Derived from 3,4-Ethylenedioxythiophene .....	15
Extended Conjugation Monomers.....	17
Applications .....	21
Thesis of this Work .....	22
2 MONOMER SYNTHESIS.....	23
Motivation for Research.....	23
Synthetic Method.....	23
Synthesis of 1,4-Dialkoxy-2,5-dibromobenzenes.....	23
Transition Metal-Mediated Coupling Reactions .....	25
Synthesis of BEDOT-B(OR) <sub>2</sub> .....	28
X-Ray Crystal Structure of PBEDOT-B(OG) <sub>2</sub> .....	31
Experimental.....	33
Materials.....	33
Structural Identification of Monomers and Polymers.....	34
Synthesis .....	35
3 ELECTROCHEMISTRY.....	43

Motivation for Research.....	43
Cyclic Voltammetry.....	43
Background .....	43
Techniques .....	46
Electropolymerization of BEDOT-B(OR) <sub>2</sub> .....	48
Polymer Cyclic Voltammetry .....	52
Electrochemical Stability of Polymers .....	58
In-situ Optoelectrochemistry.....	62
Background .....	62
Techniques .....	64
Optoelectrochemistry of polymers <b>4a-f</b> .....	65
Polymer Modified Electrodes.....	75
In-Situ EPR Electrochemistry .....	78
Background .....	79
Techniques .....	80
Experimental.....	81
EPR-Electrochemistry of polymers <b>4a-c, f</b> .....	83
In-Situ Conductivity.....	90
Background .....	90
Techniques and Instrumentation .....	93
In-situ conductivity of polymers <b>4a,c, d</b> and <b>4f</b> .....	96
<b>4 CHEMICAL POLYMERIZATION.....</b>	<b>99</b>
Introduction .....	99
Motivation for Research .....	99
Molecular Weight Determination.....	99
Oxidative Polymerizations.....	103
Background .....	103
Oxidative Polymerization of BEDOT-B(OR) <sub>2</sub> with Ferric Chloride.....	103
Oxidative Polymerization of BEDOT-B(OC <sub>16</sub> H <sub>33</sub> ) <sub>2</sub> with Various Oxidants .....	106
Non-Oxidative Coupling Polymerizations .....	109
Homocoupling polymerizations.....	111
Heterocoupling polymerizations .....	117
Comparison of Polymer Properties.....	121
Experimental.....	124
Materials .....	124
Characterization.....	125
Synthesis.....	126
<b>5 CONCLUDING REMARKS.....</b>	<b>133</b>
Monomer Synthesis .....	133
Electrochemistry .....	134

Chemical Polymerizations.....	137
APPENDIX .....	138
REFERENCES .....	144
BIOGRAPHICAL SKETCH.....	158

## LIST OF TABLES

<u>Table</u>	<u>page</u>
1.1 BisEDOT arylene and vinylene .....	20
2.1 Properties of compounds <b>2a–f</b> and BEDOT–B(OR) <sub>2</sub> .....	30
3.1 Oxidation and reduction potentials for monomers and polymers.....	51
3.2 Comparative solid state bandgaps.....	73
4.1 Molecular weights of polymers prepared by ferric chloride–induced oxidative polymerization.....	105
4.2 Effect of oxidant choice on molecular weight of PBEDOT–B(OC <sub>16</sub> H <sub>33</sub> ) <sub>2</sub> .....	109
4.3 Molecular weights of polymers derived from BEDOT–B(OC <sub>16</sub> H <sub>33</sub> ) <sub>2</sub> .....	123
4.4 Concentrations used in oxidative polymerization of BEDOT–B(OC <sub>16</sub> H <sub>33</sub> ) <sub>2</sub> with various oxidants.....	128
A-1 Crystal data and structure refinement for BEDOT–B(OG) <sub>2</sub> .....	138
A-2 Atomic coordinates and equivalent isotropic displacement parameters for BEDOT–B(OG) <sub>2</sub> .....	139
A-3 BEDOT–B(OG) <sub>2</sub> bond lengths.....	140
A-4 BEDOT–B(OG) <sub>2</sub> bond angles.....	141
A-5 Anisotropic displacement paramenters for BEDOT–B(OG) <sub>2</sub> .....	142
A-6 Hydrogen coordinates and isotropic displacement parameters for BEDOT–B(OG) <sub>2</sub> .....	143

## LIST OF FIGURES

<u>Figure</u>	<u>page</u>
1.1 Common conducting polymers.....	2
1.2 Mechanism of oxidative polymerization of thiophene.....	4
1.3 Coupling pathways during polymerization of thiophene.....	6
1.4 Coupling pathways during polymerization of EDOT.....	7
1.5 Regioirregular poly(3-alkyl)thiophene .....	8
1.6 Precursor routes to conducting polymers.....	9
1.7 Effect of conjugation on molecular energetics .....	11
1.8 Examples of degenerate and non-degenerate resonance structures .....	13
1.9 Interconversion between neutral, polaron, and bipolaron in polythiophene .....	14
2.1 Synthesis of 1,4-dialkoxy-2,5-dibromobenzenes.....	24
2.2 Synthesis of 3,6-dioxaoctyl <i>p</i> -toluenesulfonate.....	25
2.3 Modified synthesis of 1,4-dibromo-2,5-dihydroxybenzene .....	25
2.4 General aryl-aryl coupling mechanism .....	26
2.5 Negishi synthesis of BEDOT-B(OR) <sub>2</sub> .....	31
2.6 X-ray crystal structure of BEDOT-B(OG) <sub>2</sub> .....	33
3.1 Standard three-electrode electrochemical cell.....	48
3.2 Electrochemical polymerization of BEDOT-B(OR) <sub>2</sub> .....	49
3.3 Cyclic voltammetric polymerization of BEDOT-B(OC <sub>12</sub> H <sub>25</sub> ) <sub>2</sub> .....	50

3.4	Cyclic voltammograms of PBEDOT-B(OC <sub>12</sub> H <sub>25</sub> ) <sub>2</sub> .....	53
3.5	Cyclic voltammograms of PBEDOT-B(OCH <sub>3</sub> ) <sub>2</sub> .....	54
3.6	Cyclic voltammograms of PBEDOT-B(OG) <sub>2</sub> .....	55
3.7	Electrolyte dependence of PBEDOT-B(OG) <sub>2</sub> cyclic voltammetry.....	57
3.8	Cyclic voltammetry of PBEDOT-B(OG) <sub>2</sub> to higher potentials.....	58
3.9	Cyclic voltammograms of PBEDOT-B(OC <sub>12</sub> H <sub>25</sub> ) <sub>2</sub> in 2:3 CH <sub>3</sub> CN:CH <sub>2</sub> Cl <sub>2</sub> .....	59
3.10	Cyclic voltammograms of PBEDOT-B(OC <sub>12</sub> H <sub>25</sub> ) <sub>2</sub> in CH <sub>3</sub> CN .....	60
3.11	Cyclic voltammograms of PBEDOT-B(OC <sub>12</sub> H <sub>25</sub> ) <sub>2</sub> to subsequently higher switching potentials .....	61
3.12	Electronic transitions available to a conducting polymer.....	63
3.13	Optoelectrochemical analysis of PBEDOT-B(OC <sub>7</sub> H <sub>15</sub> ) <sub>2</sub> .....	66
3.14	Optoelectrochemical analysis of PBEDOT-B(OCH <sub>3</sub> ) <sub>2</sub> .....	67
3.15	Optoelectrochemical analysis of PBEDOT-B(OG) <sub>2</sub> .....	68
3.16	Solution UV–Vis–nIR spectra of PBEDOT-B(OG) <sub>2</sub> in CHCl <sub>3</sub> .....	71
3.17	Solid-state vs. solution UV–Vis–nIR spectra of PBEDOT-B(OEtHex) <sub>2</sub> ....	71
3.18	Ferrocene switching on a platinum button electrode on which PBEDOT-B(OC <sub>12</sub> H <sub>25</sub> ) <sub>2</sub> has been deposited.....	76
3.19	Effect of ferrocene concentration on current response.....	78
3.20	Interconversion between neutral, polaron, and bipolaron in PBEDOT-B(OR) <sub>2</sub> .....	80
3.21	In-situ EPR–electrochemistry cell .....	82
3.22	Evolution of EPR signal for PBEDOT-B(OCH <sub>3</sub> ) <sub>2</sub> upon oxidation.....	84
3.23	Current and EPR signal intensity as functions of potential for PBEDOT-B(OCH <sub>3</sub> ) <sub>2</sub> .....	86
3.24	Current and EPR signal intensity as functions of potential for	

PBEDOT-B(OC <sub>12</sub> H <sub>25</sub> ) <sub>2</sub> in CH <sub>3</sub> CN .....	87
3.25 Current and EPR signal intensity as functions of potential for PBEDOT-B(OC <sub>7</sub> H <sub>15</sub> ) <sub>2</sub> in 1:1 CH <sub>3</sub> CN:CH <sub>2</sub> Cl <sub>2</sub> .....	88
3.26 Current and EPR signal intensity as functions of potential for PBEDOT-B(OC <sub>7</sub> H <sub>14</sub> ) <sub>2</sub> in CH <sub>3</sub> CN .....	89
3.27 Large gap lateral growth electrode for in-situ conductivity measurements.....	94
3.28 Offset potential scan of PBEDOT-B(OC <sub>7</sub> H <sub>15</sub> ) <sub>2</sub> on LG-LGE .....	95
3.29 Structures of PBEDOT-B(OC <sub>7</sub> H <sub>15</sub> ) <sub>2</sub> and its thiophene analog PBT-B(OC <sub>7</sub> H <sub>14</sub> ) <sub>2</sub> .....	97
3.30 Comparative in-situ conductivities.....	97
4.1 Ratio of internal to external aromatic H can be used to determine molecular weight.....	101
4.2 Oxidative polymerization of BEDOT-B(OR) <sub>2</sub> monomers .....	106
4.3 Monomer bromination.....	110
4.4 General Ullmann coupling polymerization.....	111
4.5 Pathway of the Ullmann coupling reaction.....	112
4.6 Ullmann coupling polymerization of <b>5d</b> .....	113
4.7 Attempts at modified Ullmann coupling polymerization of <b>3c,d</b> .....	115
4.8 Lithiation of <b>3d</b> and subsequent deuterium exchange .....	116
4.9 Attempted Stille coupling polymerization using dibrominated phenylene <b>2d</b> .....	118
4.10 Stille coupling polymerization using dibrominated compound <b>5d</b> .....	118
4.11 Suzuki model reaction .....	120
4.12 Suzuki polymerization of <b>5d</b> .....	120
4.13 Effect of structural modification on bandgap.....	124

Abstract of Dissertation Presented to the Graduate School  
of the University of Florida in Partial Fulfillment of the  
Requirements for the Degree of Doctor of Philosophy

LOW OXIDATION POTENTIAL ELECTROACTIVE POLYMERS

By

Jennifer Allison Ash Irvin

December, 1998

Chairman: Professor John R. Reynolds

Major Department: Chemistry

Palladium-catalyzed coupling techniques have been used to prepare a series of 1,4-bis[2-(3,4-ethylenedioxy)thienyl]-2,5-dialkoxybenzenes which can be polymerized chemically or electrochemically. The highly electron rich nature of these materials leads to extremely low oxidation potentials of the monomers and their polymers ( $E_{1/2,p} = -0.15$  to  $-0.35V$  vs.  $\text{Ag}/\text{Ag}^+$ ). Mild oxidation conditions can be used during polymerization and redox switching, resulting in fewer side reactions and more stable polymers; less than 30% loss in electroactivity occurs over 3100 redox cycles.

These polymers are stable over a broad potential range, allowing them to be used as modified electrode materials. For example, ferrocene can be repeatedly oxidized and reduced at the polymer surface. In-situ EPR electrochemistry was used to better understand the polymer redox processes, which are solvent-dependent. Stable polarons are observed in acetonitrile

but not in the presence of methylene chloride. In-situ conductivity measurements reveal that these polymers become conductive at much lower potentials than the analogous thiophene polymers. The polymers are electrochromic, reversibly switching from red to blue upon oxidation with electronic bandgaps at *ca.* 1.9 eV.

A variety of chemical reactions have been used for polymer synthesis. Highest molecular weight (16 repeat units, or 48 rings) and solubility are obtained from oxidative polymerization using ferric perchlorate as the oxidant. Monomers have also been dibrominated to produce materials that can be polymerized using transition metal-mediated coupling reactions. Polymers prepared in this fashion are partially soluble, with molecular weights of the soluble fractions similar to those found in ferric chloride polymerizations (3 to 5 repeat units, or 9 to 15 rings). Heterocoupling polymerizations have been used to incorporate additional EDOT or phenylene rings into the polymer backbone, changing the electron density of the polymers and resulting in significant differences in band gaps (1.7 and 2.4eV, respectively).

## CHAPTER 1

### INTRODUCTION

#### 1.1 Brief History of Conducting Polymers

Polyacetylene was first prepared as an intractible, poorly characterized powder in 1958 by Natta and coworkers.<sup>1</sup> Very little interest was taken in this polymer, however, until Shirakawa and coworkers prepared strong, flexible, free-standing films of polyacetylene.<sup>2</sup> Research in the area of conjugated polymers soon increased dramatically with the discovery in 1977<sup>3,4</sup> that doping the polymer dramatically increased its conductivity from the semiconducting to the metallic regime.

While polyacetylene was found to be highly conductive,<sup>5</sup> it was also found to be of little practical use due to its poor environmental stability.<sup>6</sup> The idea that any conjugated polymer might be capable of conduction led to interest in other conjugated polymers (Figure 1.1), such as poly(*p*-phenylene)s, polyheterocycles, poly(arylenevinylene)s, and polyanilines.

The polyheterocycles have received considerable attention for their electron-rich nature, which leads to materials that are easily oxidized and therefore more stable in the oxidized state. Additionally, the increased

structural complexity of polyheterocycles, relative to polyacetylenes, makes structural modifications possible for improved processability.

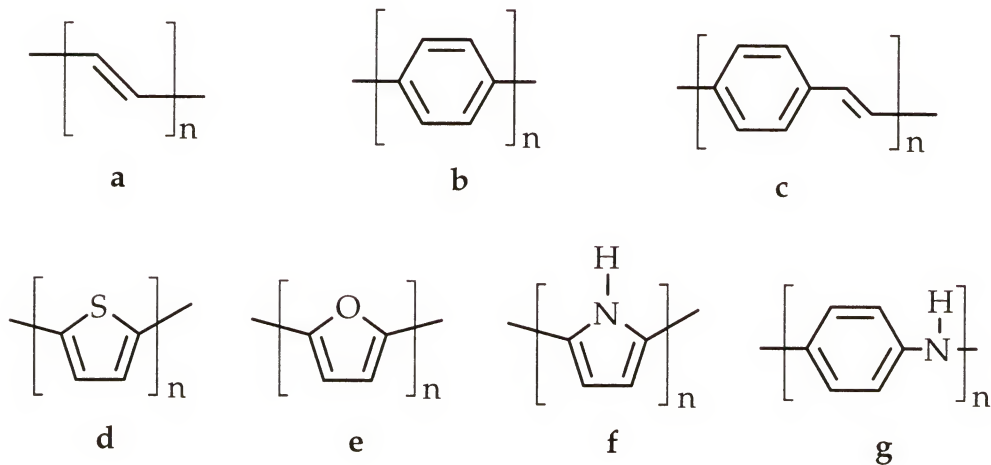


**Figure 1.1:** Common conducting polymers: a) polyacetylene b) poly(*p*-phenylene) c) poly(phenylene vinylene) d) polythiophene e) polyfuran f) polypyrrole g) polyaniline

## 1.2 Oxidative Polymerization Mechanism

Most polyheterocycles can be prepared oxidatively, using chemical or electrochemical oxidation. Chemical oxidative polymerization is advantageous in that the reactions are fast and simple, using relatively mild conditions,<sup>7</sup> and polymers could presumably be mass produced at a reasonable cost.<sup>8</sup> Oxidation potentials depend upon the electron density of the monomers; the more electron-rich a monomer is, the easier it is to oxidize. The polymerization of thiophene is shown in Figure 1.2; this mechanism is equally applicable to other heterocycles. The mechanism is thought to

involve a one-electron oxidation of the monomer to form a resonance-stabilized radical cation. This can couple with a molecule of starting material to form a radical cation dimer which loses another electron to form the dicationic dimer, or the radical cation can couple with another radical cation to form the dicationic dimer. The dicationic dimer then loses two protons to form the neutral dimer, and the entire process is repeated to form polymer. The polymerization can be accomplished either chemically or electrochemically. The fundamental polymerization mechanism is the same for both processes, though there are many other factors that must be considered for electrochemical polymerization. These will be discussed in greater detail in Chapter 3.

In a chemical oxidative polymerization, stoichiometric quantities of oxidant are needed, and the polymer formed initially is in its oxidized state, with cations delocalized along the polymer chain. One of the more common oxidants used to effect polymerization is ferric chloride, which works well with a large variety of heterocycles;<sup>8</sup> however, a large variety of oxidants have been used successfully.<sup>8</sup> The oxidative preparation of poly(*p*-phenylene)s has been most successfully achieved using CuCl<sub>2</sub> as an oxidant with AlCl<sub>3</sub> as a catalyst,<sup>8,9</sup> though other oxidants have been explored.<sup>7,10</sup> In the oxidized state, the cationic polymers are resonance-stabilized and compensated by counterions. Reduction to the neutral polymer is typically accomplished by the addition of a strong base such as ammonium hydroxide or hydrazine.

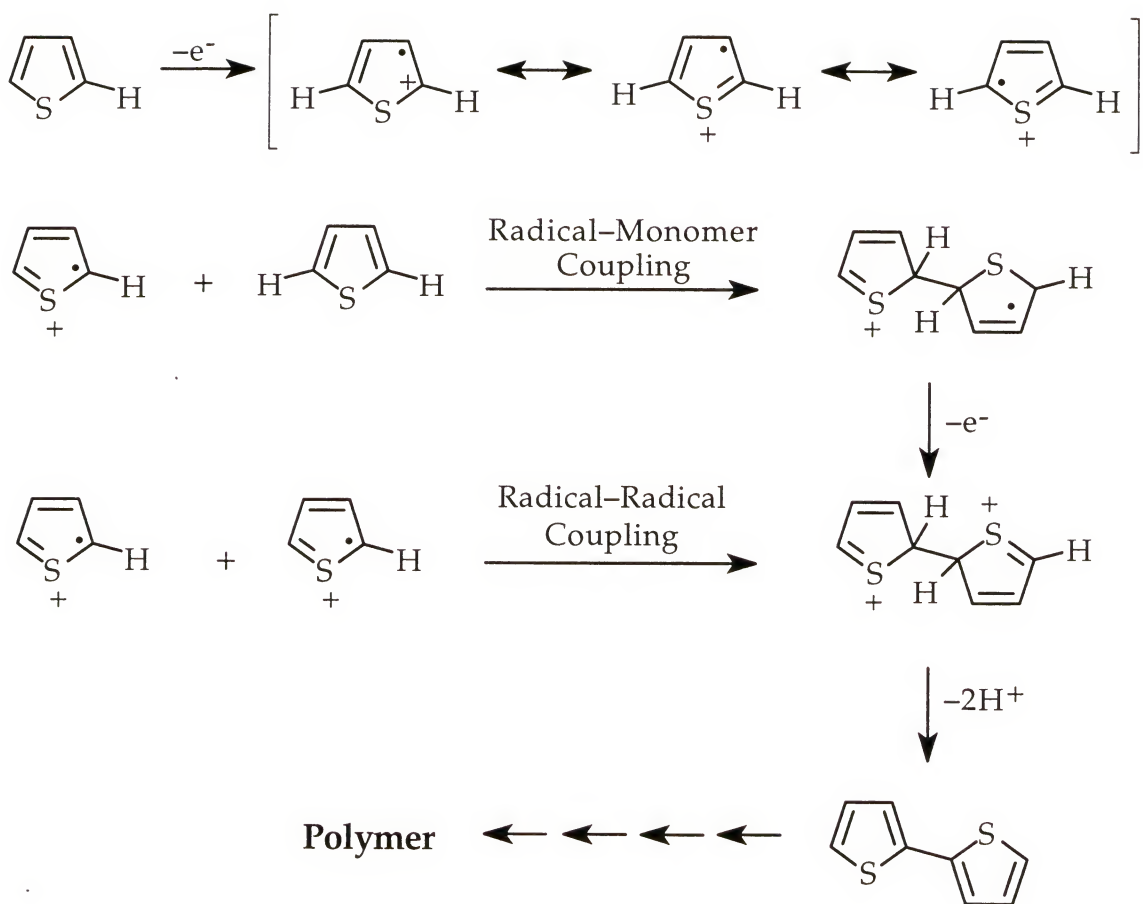


**Figure 1.2:** Mechanism of oxidative polymerization of thiophene

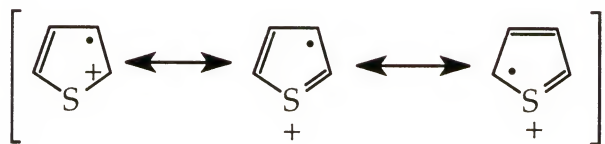
One problem associated with chemical oxidative polymerizations is that the polymer is initially formed in the oxidized state, which requires segments of increased rigidity.<sup>11</sup> The polymers are typically less soluble in the oxidized state than they are in the reduced state, where increased rigidity is not required, and the degree of polymerization is therefore limited by precipitation of the insoluble oxidized polymers. Solubility has been improved considerably through the use of long alkyl substituents, i.e. in the synthesis of poly(3-alkylthiophene)s,<sup>12,13,14,15</sup> but oxidative polymerization of 3-

alkylthiophenes yields regioirregular polymers, i.e. polymers with a mixture of 2, 2'-, 2, 5'-, and 5, 5'-couplings (see below) with disrupted conjugation due to  $\alpha$ ,  $\beta$ -coupling.<sup>16,17</sup>

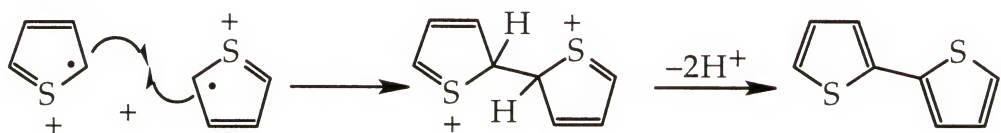
Among the problems associated with oxidative polymerization is the abundance of possible side reactions. Oxidative polymerization of the simple, unsubstituted heterocycles results in poorly soluble, poorly processable materials that are of little use, so structural modifications are typically used to improve polymer properties.<sup>18,19,20</sup> Often the strong oxidizing agents required to effect polymerization cause overoxidation and decomposition. While coupling at a carbon adjacent to the heteroatom is favored, as it is the most electron-rich site, coupling is also possible at other unsubstituted carbons, and irregular polymer backbones can be formed as shown in Figure 1.3 for oxidative polymerization of thiophene (using the radical-radical coupling route discussed earlier). Coupling of thiophenes occurs predominantly through the 2- and 5-positions ( $\alpha$ ,  $\alpha$  coupling), but some coupling also occurs at the 3- and 4-positions to give a small amount of  $\alpha$ ,  $\beta$  and  $\beta$ ,  $\beta$  couplings. The result is an ill-defined polymer backbone, which yields poor electronic properties.<sup>20</sup> Multiple couplings on the same heterocyclic molecule can also occur, resulting in crosslinked polymers.

Coupling at  $\beta$ -positions during polymerization can be avoided by blocking the 3- and 4-positions of the heterocycle. If symmetrical substitution is used, problems associated with regioirregularity can be avoided. For

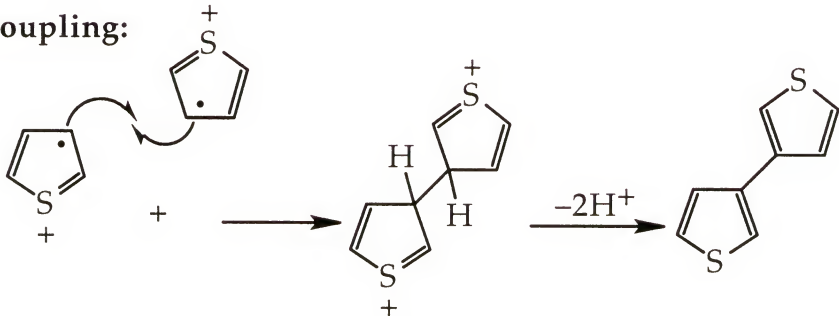
instance, in the polymerization of 3, 4-ethylenedioxythiophene (EDOT) shown below (Figure 1.4), the ethylenedioxy bridge effectively prevents  $\beta$ -coupling to yield a linear polymer. The benefits of the ethylenedioxy bridge are discussed in greater detail in section 1.6.



$\alpha, \alpha$ -coupling:



$\beta, \beta$ -coupling:



$\alpha, \beta$ -coupling:

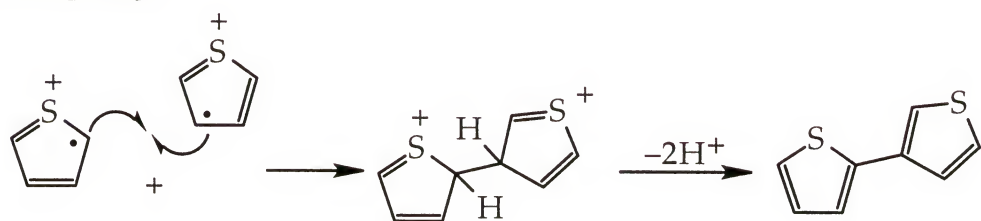
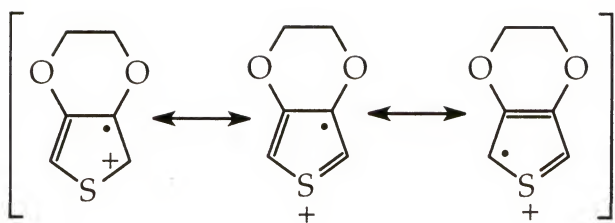
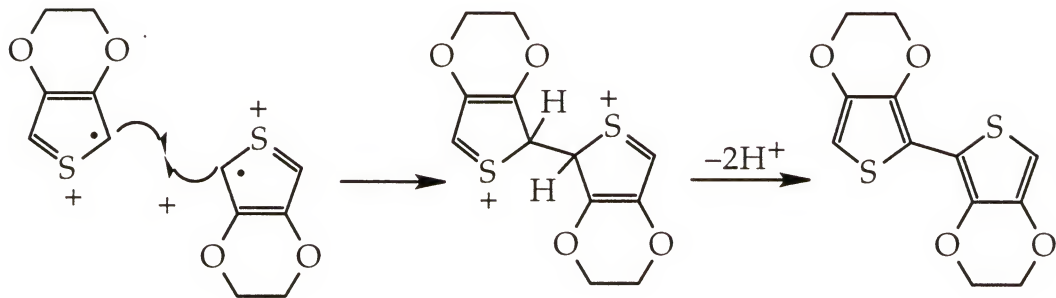


Figure 1.3: Coupling pathways during polymerization of thiophene



**only  $\alpha, \alpha$ -coupling is possible:**



**Figure 1.4:** Coupling pathways during polymerization of EDOT

An unsymmetrical monomer, such as a 3-alkylthiophene (3AT), is said to have a “head” (i.e. the 2 position of the thiophene ring) and a “tail” (i.e. the 5 position of the thiophene ring). Oxidative homopolymerization of 3ATs yields poly(3-alkylthiophene)s (P3ATs) that have “head-to-head” (2, 2', or H-H), “head-to-tail” (2, 5', or H-T) and “tail-to-tail” (5, 5', or T-T) bonds (Figure 1.5). Polymers having this type of bonding are said to be regioirregular, while polymers possessing purely H-T bonds are regioregular. Regioirregular P3ATs are poorly conjugated, because the mixture of linkages leads to unfavorable interaction of side chains, resulting in a sterically driven twist of the polymer backbone.<sup>21</sup> Polymer morphology is also affected by regiochemistry; regioregular polymers are typically crystalline, while regioirregular polymers are amorphous.<sup>22,23</sup> Regioregular P3ATs have been

prepared using non-oxidative coupling polymerizations;<sup>24,25</sup> modified oxidative polymerization techniques have also been used to promote regioregularity.<sup>26,27</sup>

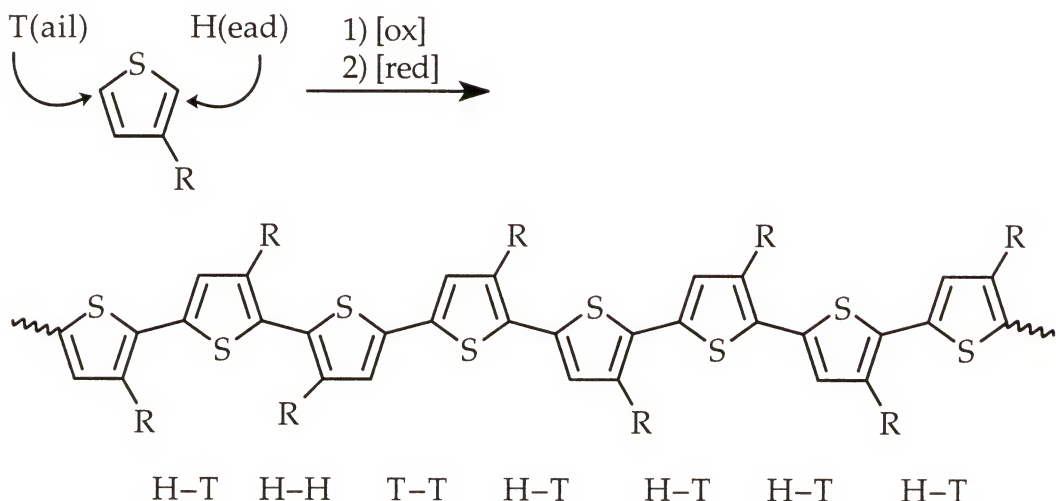


**Figure 1.5:** Regioirregular poly(3-alkyl)thiophene

### 1.3 Non-Oxidative Polymerizations

While oxidative polymerizations are advantageous for their relatively simple and rapid reactions, research into other, non-oxidative polymerizations has been plentiful. Non-oxidative polymerizations are used to avoid problems with regioirregularity and overoxidation, yielding well-defined polymers. These reactions also form the polymers in their more soluble, fully reduced state rather than in the less-soluble, oxidized state obtained initially in oxidative polymerizations. Thus higher molecular

weight polymers can be formed using non-oxidative polymerizations, as long as the reactions proceed in high conversion.

Among the non-oxidative polymerizations, precursor routes (Figure 1.6) have been particularly effective. These involve the initial synthesis of a soluble polymer that can be purified and fully characterized before conversion to the conjugated polymer through further reactions which typically involve chemical or thermal elimination. This technique is commonly used in the synthesis of polyacetylene<sup>28,29,30,31</sup> and poly(arylene vinylene)s,<sup>32,33,34</sup> and it has been investigated for the synthesis of poly(*p*-phenylene)s.<sup>35,36,37</sup>

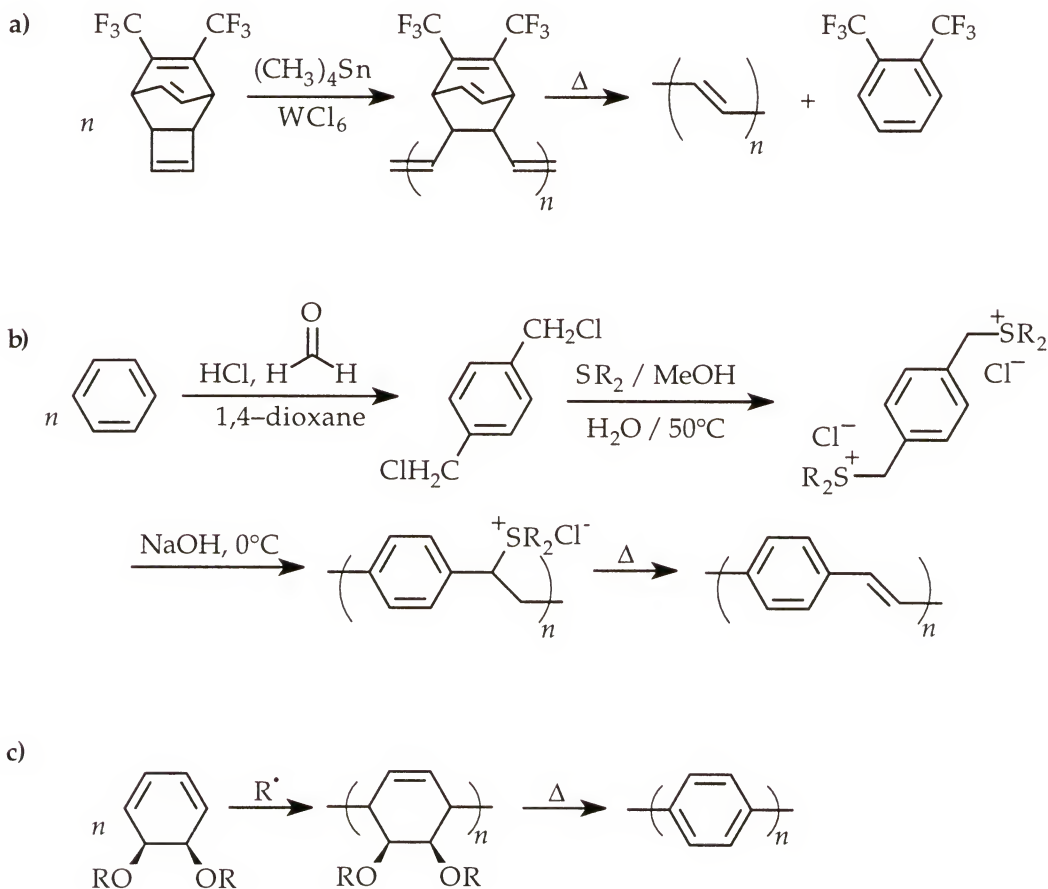


**Figure 1.6:** Precursor routes to conducting polymers: a) polyacetylene b) poly(phenylene vinylene) and c) poly(*p*-phenylene)

In addition to precursor routes, non-oxidative coupling techniques have also been explored extensively for the preparation of conjugated polymers. In recent years, coupling reactions have received considerable interest for the formation of polyheterocycles,<sup>23,38,39,40,41</sup> which are difficult to form via precursor routes. These coupling reactions are typically transition metal-mediated reactions which form neutral polymers in a step-wise fashion. The non-oxidative coupling routes tend to reduce side reactions such as over-oxidation and produce well-defined, soluble polymers.

Most of the coupling reactions used to effect polymerization of heterocycles involve oxidative addition of a heterocycle to a transition metal center, followed by transmetalation of a second, metalated heterocycle to the same transition metal center. Reductive elimination from the transition metal forms a new heterocycle-heterocycle bond and returns the transition metal to its original form for further couplings. In this way, transition metals can be used in catalytic amounts to produce polymers.

Among the non-oxidative coupling polymerizations, it is possible to produce polymers from homocoupling and heterocoupling routes. Homocoupling polymerizations are advantageous in that correct stoichiometry is inherent in pure monomers, but structural versatility is limited. Exact stoichiometry of both monomers is required in heterocoupling polymerizations, but it is possible to produce many different polymers from only a few monomers.

#### 1.4 Conjugation and Conduction in Electroactive Polymers

As conjugation length increases, as with the progression from ethylene to 1,3-butadiene to 1,3,5,7,9,11-dodecahexene to polyacetylene (Figure 1.7), it becomes increasingly easy to promote electrons from the highest occupied molecular orbital (HOMO) to the lowest unoccupied molecular orbital (LUMO). This energy is a simple  $\pi$  to  $\pi^*$  transition in discrete molecules and a band gap for polymers.<sup>42</sup> It can be determined for a neutral species from the onset of absorption in the UV-Vis spectrum.

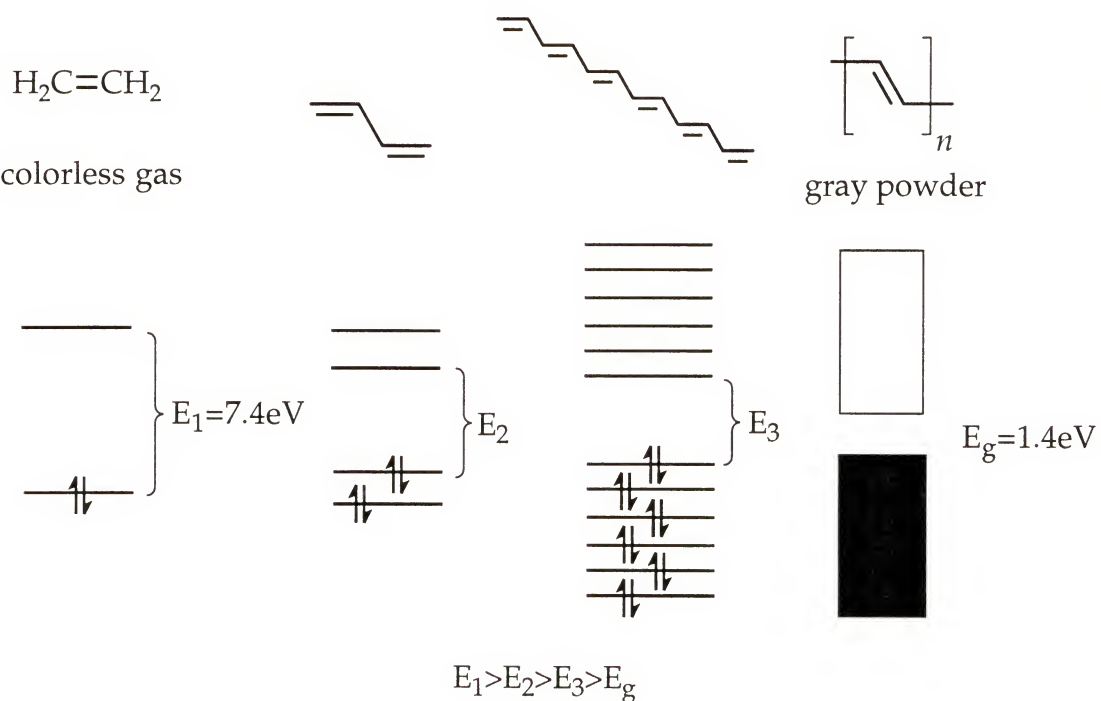


**Figure 1.7:** Effect of conjugation on molecular energetics

Just as increasing conjugation length from ethylene to polyacetylene decreases the  $\pi$  to  $\pi^*$  transition, it also lowers oxidation potential. This is due to the high HOMO and increased resonance stabilization of the radical cation formed in the process. Similarly, polyheterocycles have lower oxidation potentials than their single-ring heterocycle precursors. Increasing conjugation in monomers also lowers monomer oxidation potentials;<sup>43</sup> the oxidation potential of thiophene (2.07V vs. SCE) is much higher than that of terthiophene (1.05V vs. SCE), which is higher than that of polythiophene (0.7V vs. SCE).<sup>44</sup> Extended conjugation monomers have therefore received considerable interest, because lower oxidation potentials lead to fewer side reactions and fewer defects.<sup>45,46</sup> Among the defects minimized through the use of extended conjugation monomers are those caused by  $\alpha, \beta$  coupling, since several  $\alpha, \alpha$  linkages are pre-determined in these materials.

The simplest conducting polymer is trans-polyacetylene; the conjugated nature of the polymer chain allows it to have two possible electronically extreme states (Figure 1.8). Unlike all the other conducting polymers, the two resonance forms of trans-polyacetylene are degenerate, i.e. their ground states are thermodynamically equivalent.<sup>47,48</sup> All other organic conducting polymers reported to date possess non-degenerate ground states;<sup>49</sup> for example, poly(*p*-phenylene) has both benzenoid and quinoid configurations (Figure 1.8), of which the latter is the higher energy configuration.<sup>42</sup> As the polymers discussed in this dissertation all have non-degenerate ground states, trans-polyacetylene will not be discussed further.

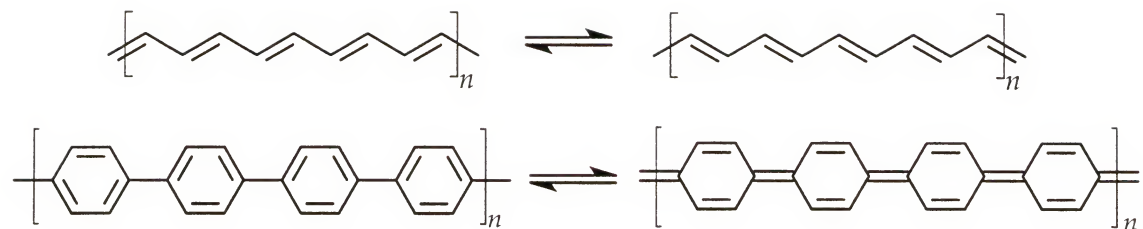


**Figure 1.8:** Examples of degenerate (polyacetylene, top) and nondegenerate (poly(*p*-phenylene), bottom) resonance structures

The mechanism of conduction in non-degenerate ground state conjugated polymers has been the subject of considerable research. The most widely accepted mechanism, illustrated in Figure 1.9 for polythiophene, was proposed simultaneously by Brédas and coworkers<sup>50</sup> and Bishop and coworkers<sup>51</sup> in 1981. This mechanism involves a one-electron oxidation to form a radical cation, which is called a polaron. This radical cation is resonance-stabilized over several rings. Removal of a second electron gives a dicationic species with no unpaired electrons, called a bipolaron. The two ions in a bipolaron electrostatically repel one another to minimize unfavorable interactions; recent work suggests that at least five rings are needed to stabilize a dicationic species.<sup>52</sup> The conversion between neutral, polaronic, and bipolaronic species is reversible, using either chemical or electrochemical means to oxidize or reduce the polymer.

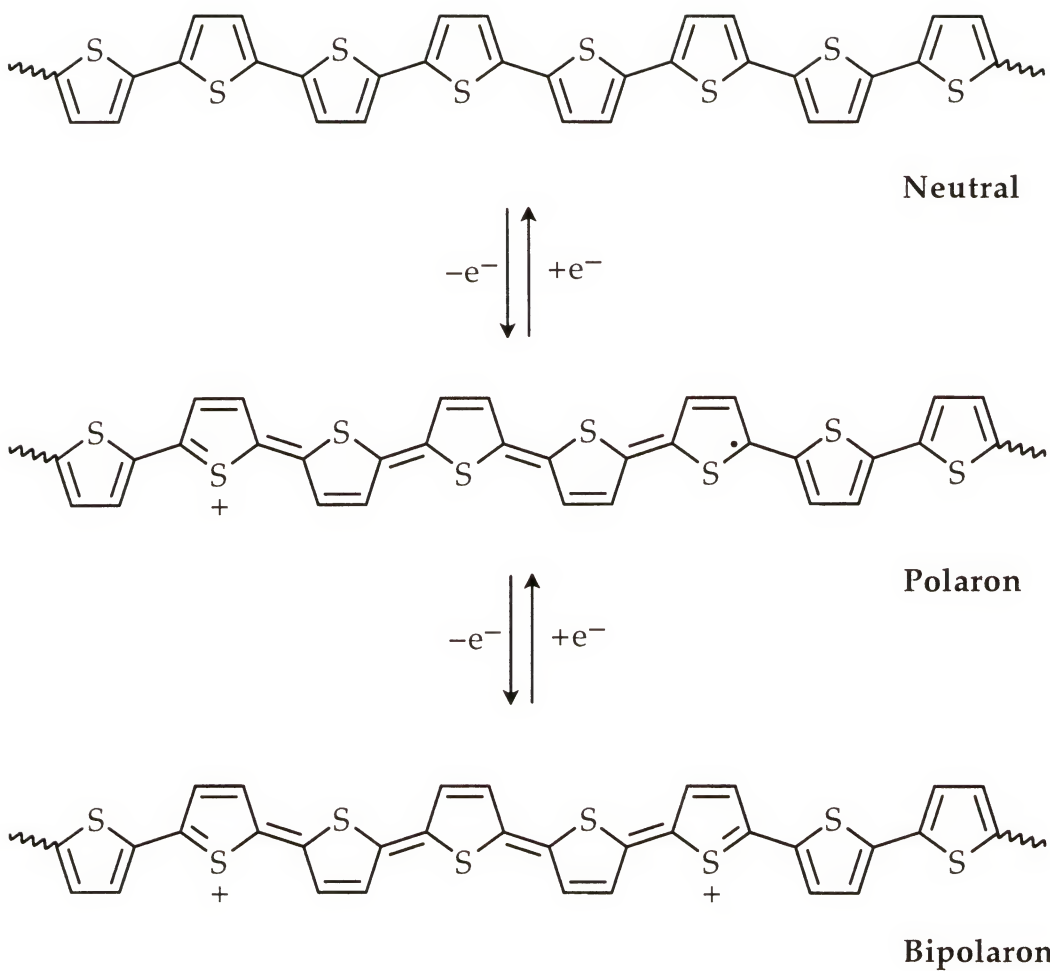


**Figure 1.9:** Interconversion between neutral, polaron, and bipolaron in polythiophene

### 1.5 Substituent Effects

Introduction of long alkyl or alkoxy substituents improves polymer solubility,<sup>15,53</sup> and alkoxy substituents lower the band gap by raising the energy of the valence band electrons (HOMO destabilization) along the conjugated chain.<sup>54,55,56,57,58</sup> These alkoxy substituents also decrease the oxidation potential of both the monomers and their polymers, allowing milder

oxidative polymerization conditions, which results in fewer side reactions and increased polymer stability.

While linear alkoxy substituents improve solubility, additional solubility can be attained by modifying the alkoxy substituents slightly; the beneficial electronic effects of the alkoxy group are maintained. For instance, use of branched rather than linear alkoxy substituents has been shown to improve solubility even further,<sup>59,60</sup> presumably due to increased disorder induced by the side chain relative to a linear chain of similar molecular weight.

Oligomeric ether substituents have been used extensively to improve solubility.<sup>61,62,63</sup> An alkoxy linkage to the main chain can still be used to maintain the beneficial electronic effects, and the additional electron-rich moieties may improve electronic properties further. Improved solubility in this case is thought to be due to better interaction with solvent and decreased enthalpy of solvation.<sup>64</sup>

### 1.6 Polymers Derived from 3,4-Ethylenedioxythiophene

While substitution at the 3- and 4-positions of thiophene monomers prevents  $\beta$  coupling during polymerization, dialkyl substitution results in severe steric hindrance, decreasing conjugation.<sup>65</sup> While alkoxy substituents were expected to decrease steric hindrance and thus lower bandgaps, long alkoxy substituents were found to lower conductivity due to repulsive

interactions between adjacent side chains.<sup>66,67</sup> Monomers containing 3,4-dialkoxy substituents are also poorly reactive toward oxidative polymerization due to stabilization caused by conjugation with thiophene.<sup>67</sup> To eliminate these problems, an ethylenedioxy group can be attached at the 3- and 4-positions of the thiophene; in this manner, the electron donating benefits are maintained, and the steric effects are eliminated. Cyclic alkylatedioxy substituents are also too strained for a high level of conjugation with the thiophene ring,<sup>67</sup> allowing the thiophene rings to polymerize easily.

The polymerization of 3,4-ethylenedioxythiophene (EDOT) as a route to a useful, highly conducting, and quite stable material has been the focus of considerable recent research efforts.<sup>68,69,70</sup> EDOT oxidizes around 1.1V, and the polymer oxidation peaks at -0.20V (vs. Ag/Ag<sup>+</sup>).<sup>71</sup> The polymer (PEDOT) exhibits a low band gap of 1.6 eV, allowing it to be used as a cathodically coloring electrochromic and a highly transmissive conductor.

For improved polymer solubility and processability, EDOT can be modified by incorporating alkyl groups onto the carbons of the ethylenedioxy bridge. These groups are far enough away from the main chain of the resultant polymer that steric repulsion is not a significant problem. While the polymers prepared from alkyl-substituted EDOTs exhibit similar redox properties, solubility is improved significantly; alkyl-EDOT polymers can be solution cast to yield electrochromic films.<sup>72,73</sup> Additionally, the alkyl-

substituted polymers exhibit significantly faster redox switching rates and a higher degree of electrochromic contrast than unsubstituted PEDOT.<sup>73</sup>

### 1.7 Extended Conjugation Monomers

While fully conjugated polyheterocycles and poly(*p*-phenylene)s have attracted significant attention for their electrical and optical properties,<sup>74,75,76,77,78,79,80</sup> their fairly high monomer oxidation potentials make side reactions problematic, and very few structural modifications are possible without disrupting aromaticity. For added structural variability and lower oxidation potentials, researchers have turned toward extended conjugation monomers. In these compounds, aromatic rings are linked together to form new monomers with conjugation extended over several rings.

Extended conjugation monomers have been used to reduce side reactions and regioirregularity in poly(3-alkyl)thiophenes.<sup>81,82,83,84</sup> By preparing symmetrical alkyl thiophene oligomers through a series of controlled coupling reactions, many of the thiophene-thiophene linkages are pre-defined as  $\alpha$ ,  $\alpha$  linkages, reducing the amount of  $\beta$ -coupling possible during oxidative polymerization. Additionally, these oligomers exhibit considerably lower oxidation potentials than the 3-alkyl thiophenes from which they are derived.

Similarly, a series of pyrrole-based oligomers has been prepared<sup>44</sup> by Diaz and coworkers. The researchers found that the oxidation potentials of the oligomers decreased linearly with an increase in the number of pyrrole units. The authors attribute this effect to increased stability of the radical cations.

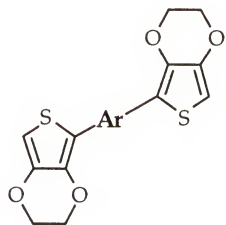
Polymers based on 3, 4-ethylenedioxythiophene (EDOT) can also be prepared from extended conjugation monomers. While EDOT polymerizes at *ca.* 1.1V vs. Ag/Ag<sup>+</sup>,<sup>71</sup> BiEDOT (two EDOT rings connected via a 2,2'-thiophene linkage) polymerizes at 0.51V,<sup>71</sup> and TerEDOT (three EDOT rings) polymerizes at 0.20V.<sup>85</sup> While it would seem that minimizing oxidation potentials would be highly beneficial, there are limits. While TerEDOT has a significantly lower oxidation potential than EDOT and BiEDOT, the oxidation potential is so low that TerEDOT is difficult to handle and store.<sup>85</sup> Oxidation potentials around 0.5V seem optimal to prevent side reactions during polymerization while limiting premature oxidation, allowing for monomers that are easy to handle.

Pelter and coworkers have recently reported the synthesis and polymerization of a large variety of extended conjugation monomers using several types of transition metal-mediated coupling reactions, further demonstrating the versatility of this technique.<sup>39</sup> By using a combination of heterocycles, phenylenes, and/or vinylenes in extended conjugation monomers, it is possible to finely tune the optical and electronic properties of the resultant polymers. Copolymerization of two or more different

monomers, either chemically or electrochemically, produces polymers with ill-defined linkages, so that properties are widely varied from sample to sample, and the desired properties are not typically obtained. While mixed dimers can be prepared, they typically yield regioirregular polymers, so symmetrical oligomers (trimers, tetramers, etc.) are more desireable.

Polymers incorporating both thiophene and phenylene moieties in the backbone have been developed in order to finely control optoelectronic properties on easily functionalized systems.<sup>54,55,56,86,87,88</sup> For example, poly[1,4-bis(2-thienyl)benzene] exhibits a band gap of 2.2eV,<sup>54</sup> intermediate to the bandgaps of polythiophene (2.0eV)<sup>89</sup> and poly(*p*-phenylene) (3.0eV).<sup>90</sup>

By analogy with the thiophene based systems, incorporation of EDOT into similar phenylene containing polymers is expected to yield lower gap materials that will form stable oxidized and conducting states. Indeed, a series of very electron-rich, low oxidation potential bis(EDOT) arylene has been reported recently (Table 1.1) <sup>85,91,92,93</sup> Poly{1,4-bis[2-(3,4-ethylenedioxy)-thienyl]benzene} exhibits a band gap of 1.8eV,<sup>91</sup> intermediate to the bandgaps of poly(3,4-ethylenedioxy)thiophene (1.6eV)<sup>67</sup> and poly(*p*-phenylene). By incorporating a vinylene group into the polymer backbone, it is possible to lower the band gap of the resultant polymer, poly[*trans*-bis(3,4-ethylenedioxythienyl)vinylenes], to 1.4eV. <sup>91,94</sup>

**Table 1.1:** BisEDOT arylens and vinylenes

Ar=	Acronym	$E_g$ (eV)	$E_{p,m}^*$	$E_{1/2,p}^*$	Reference
	BEDOT-V	1.4	0.45	0.02	<sup>85,91</sup>
	BEDOT-CNV	1.2	0.72	0.40, -0.16	<sup>95</sup>
	BEDOT-B	1.8	0.65	0.23	<sup>91</sup>
	BEDOT-BP	2.3	0.75	0.30	<sup>91</sup>
	BEDOT-F	1.7	0.37	-0.09	<sup>91</sup>
	BEDOT-T	1.7	0.40	-0.50	<sup>91</sup>
	TerEDOT	1.6	0.20	-0.27	<sup>91</sup>
	BEDOT-NMC	2.4	0.36	0.19, 0.46	<sup>92,96</sup>
	BEDOT-BF <sub>2</sub>	1.9	0.92	0.61, -0.03	<sup>97</sup>

<sup>\*</sup> V vs. Ag/Ag<sup>+</sup>

### 1.8 Applications

While the polymers discussed herein are typically referred to as "conducting polymers," it is perhaps better to characterize them as "electroactive," because the majority of applications take advantage of properties of these materials resulting from electroactivity. Conductivity in these polymers is typically poor relative to metal conductivities (though if densities are compared, copper and polyacetylene exhibit comparable conductivities<sup>98</sup>), so it is unlikely that they will be used as replacement for metal wires. However, changes in redox state are accompanied by changes in other physical properties in the polymers, and many applications have emerged to capitalize on these changes. Among the properties that vary with oxidation state are conductivity, solubility, reactivity, color, and volume. Electroactive polymers have applications in the areas of antistatic coatings,<sup>99</sup> charge storage batteries,<sup>100</sup> corrosion resistant paints,<sup>101</sup> conductive textiles,<sup>102,103,104,105</sup> chemical/biochemical sensors,<sup>106,107</sup> mechanical actuators,<sup>108</sup> and controlled release/drug delivery.<sup>109,110</sup>

Interconversion between oxidized and reduced states in conducting polymers is accompanied by a significant change in conjugation (i.e. from an aromatic to a quinoidal state in poly(*p*-phenylene)s). As oxidation state changes, so does the absorbance spectrum of the polymer, and often significant color changes occur. These materials are said to be electrochromic; that is, they change colors when a potential is applied. Polymer structures can

be tailored to tune electrochromic properties; the full spectrum of colors can be found in the conducting polymers. Polymers with significant color changes in the visible spectrum are being explored for use in display technologies and “smart” windows.

### 1.9 Thesis of This Work

The major emphasis of this research is the synthesis of soluble, low oxidation potential electrochromic polymers. Alkoxy-substituted bis(EDOT)benzenes were synthesized to produce low oxidation potential monomers and polymers. The alkoxy substituents were varied for improved solubility (and thus higher molecular weight); short and long straight chain alkoxy groups were used, as were branched alkoxy groups and oligomeric ether groups. Both chemical and electrochemical oxidative polymerization techniques were employed. Non-oxidative chemical polymerizations were also used to avoid over-oxidation and produce well-defined, soluble polymers. Polymers prepared by different methods were compared with regard to molecular weight and optical properties. Polymer electrochemistry and optoelectrochemistry were investigated, including in-situ conductivity and use of polymers in modified electrodes. In-situ EPR electrochemistry was used to investigate the polymer redox process.

## CHAPTER 2 MONOMER SYNTHESIS

### 2.1 Motivation for Research

To take advantage of the benefits of 3,4-ethylenedioxythiophene (EDOT) in a series of extended conjugation monomers, a series of 1,4-bis[2-(3,4-ethylenedioxy)thienyl]-2,5-dialkoxybenzenes (BEDOT-B(OR)<sub>2</sub>) was synthesized and polymerized. Alkoxy-substituted phenyl groups were chosen as the central portions of the molecules for their relatively high electron density, as well as for the ability to easily vary the substituent length for improved solubility. The synthesis of these molecules is outlined below.

### 2.2 Synthetic Method

#### 2.2.1 Synthesis of 1,4-Dialkoxy-2,5-dibromobenzenes (2a-f)

1,4-Dialkoxy-2,5-dibromobenzenes (**2a-f**) were prepared by the etherification reaction of 1,4-dibromo-2,5-dihydroxybenzene (**1**) with the corresponding 1-haloalkanes (Figure 2.1). In the case of the oligomeric ether

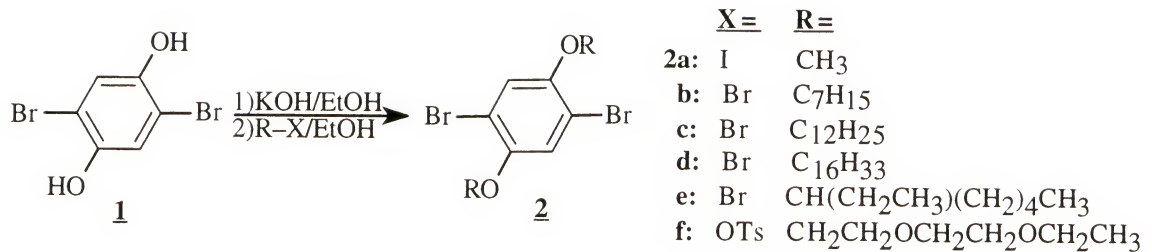


**Figure 2.1:** Synthesis of 1,4-dialkoxy-2,5-dibromobenzenes

**2f**, an oligomeric ether alcohol was converted to the tosylate (Figure 2.2), which was reacted with **1** to produce **2f**. The etherifications gave reasonable yields (Table 2.1) for compounds **2a-d** (77 to 94%) but relatively low yields for **2e** and **2f** (34% and 53%, respectively). Not surprisingly, compound **2e** is a liquid, and the reduced yield is probably due to difficulties during isolation and distillation. The reduced yield for **2f** appears to be due to slight solubility in water, resulting in loss during extraction.

With the exception of **2e**, all 1,4-dialkoxy-2,5-dibromobenzenes had all been previously reported;<sup>55,111,112</sup> however, compounds **2a-d** were originally prepared by reaction of hydroquinone with 1-haloalkanes followed by bromination. The synthetic method reported here requires fewer synthetic steps and milder bromination conditions that eliminate the need for carbon tetrachloride. This improved technique is made possible by a modified synthesis (Figure 2.3) of **1** which takes advantage of differences in solubility of starting material (insoluble), mono-brominated (soluble), and dibrominated (insoluble) products. Previous methods of synthesizing **1** resulted in a product mixture that was difficult to purify. Compound **2f** had been prepared

previously from **1** and 3,6-dioxaoctyl *p*-toluenesulfonate, using  $\text{K}_2\text{CO}_3$  as a base;<sup>112</sup> switching to KOH/EtOH gave the product in the same yield but in 18 hours instead of 48. The previously-prepared 1,4-dialkoxy-2,5-dibromobenzenes were characterized by  $^1\text{H}$  NMR and melting point, while compounds **2e** and **2f** were additionally characterized by  $^{13}\text{C}$  NMR, elemental analysis and HRMS.

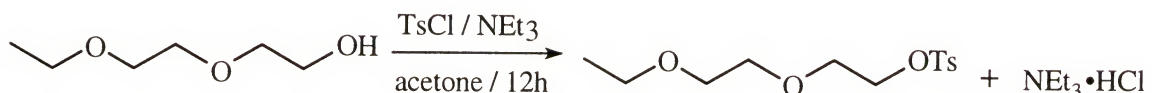


**Figure 2.2:** Synthesis of 3,6-dioxaoctyl *p*-toluenesulfonate

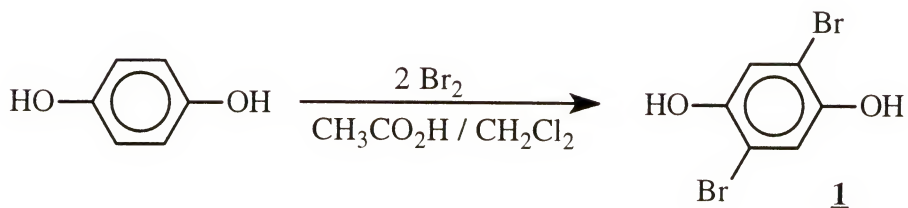


**Figure 2.3:** Modified synthesis of 1,4-dibromo-2,5-dihydroxybenzene

## 2.2.2 Transition Metal-Mediated Coupling Reactions

Carbon–carbon bond formation is typically accomplished through metal-mediated coupling reactions.<sup>113</sup> While many different reactions can be used to affect this coupling, one of the more widely used routes involves the

metal-mediated coupling of an aryl halide with an organometallic species.<sup>38,80,114,115,116,117,118,119</sup> Regardless of the metal or organometallic used, these aryl–aryl (or aryl–heteroaryl) couplings are all thought to follow the same general reaction pathway (Figure 2.4).<sup>115</sup> In this process, oxidative addition of the metal is accompanied by the loss of two ligands from the metal. The aryl group of the organometallic species is then bonded to the same metal atom in a transmetalation step, which involves the formation of a metal halide as a biproduct. The result is that both aryl groups are now bound to the same metal catalyst atom.

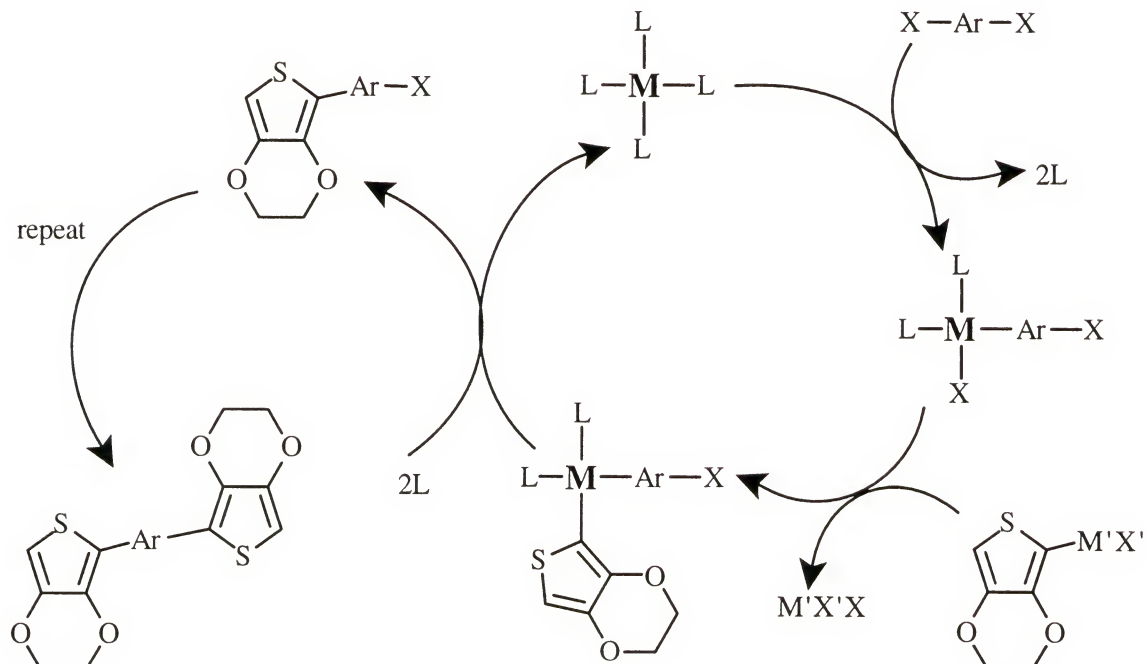


**Figure 2.4:** General aryl–aryl coupling mechanism

Reductive elimination then results in aryl–aryl coupling and reformation of the original catalyst as the two ligand molecules return to the metal.

Aryl–aryl coupling reactions are classified by the catalyst and type of organometallic used; for ease of reference, these different classifications have been given names based on the researchers who did the fundamental work in each classification. If the catalyst is a palladium (0) compound and the organometallic is an aryl zinc halide, the reaction is called a Negishi coupling.<sup>113,120,121</sup> If the catalyst is a nickel (II) compound and the organometallic is an aryl magnesium halide, the reaction is called a Yamamoto coupling,<sup>114,122,123</sup> though sometimes it is referred to as a Grignard coupling,<sup>113</sup> since Grignard reagents are used. If the catalyst is a palladium (0) compound, but the organometallic species is an aryl trialkyl tin compound, the reaction is called a Stille coupling.<sup>41,115,124,125</sup> Finally, if the active form of the catalyst is an aryl boronic acid (or for better stability, an aryl boronate), the reaction is called a Suzuki coupling.<sup>113,126,127</sup> While many other types of coupling reactions are possible, only these few are applicable here.

The type of reaction used is determined by the electronics of both aryl species as well as the desired yield and type of compound sought (i.e. monomer or polymer). Yamamoto reactions are quite fast but are not tolerant of highly electron rich species. Negishi couplings are much slower, but are more tolerant of electron rich species;<sup>38,116</sup> however, they are not tolerant of certain functional groups, such as benzyl, nitrile, and ester groups. Stille couplings are fairly fast and are tolerant of a wide variety of functional

groups, including those above;<sup>115</sup> however, the high toxicity of organotin compounds<sup>128</sup> makes these reactions undesirable except as a last resort. Suzuki reactions are not tolerant of a wide variety of functional groups, including highly electron rich species.<sup>118</sup> The advantage of the Suzuki reaction lies in the fact that aryl boronates (with the exception of electron rich aryl boronates) are stable relative to many other organometallics; similarly, aryl trialkyltin compounds are relatively stable.<sup>115</sup> On the other hand, aryl magnesium halides and aryl zinc halides are not stable, and they must be prepared *in situ* during the course of an aryl–aryl coupling and used without further purification. This is not a problem except in the case of multiple couplings, i.e. polymer synthesis, when it is crucial that stoichiometric quantities of organometallic are present.

### 2.2.3 Synthesis of BEDOT–B(OR)<sub>2</sub>, (3a–f)

Initial attempts to synthesize 1,4-bis[2-(3,4-ethylenedioxy)thienyl]-2,5-dialkoxybenzenes (BEDOT–B(OR)<sub>2</sub>, **3a–f**) utilized Yamamoto coupling techniques with EDOT and **2a**. These reactions, which can be used to couple thiophenes<sup>54</sup> or EDOTs<sup>85</sup> to benzenes or alkyl benzenes, were unsuccessful in the coupling of EDOTs to dialkoxybenzenes. After several attempts to prepare BEDOT–B(OR)<sub>2</sub> (**3a**) in this fashion, all the monomers (**3a–f**) were successfully prepared utilizing Negishi coupling techniques (Figure 2.5), as discussed below. We assume that while the aryl organometallic species may be electron rich (as in the successful cases described above), electron rich aryl halides are

not tolerated by the nickel catalyst. Steric hindrance in the aryl halide can not be the cause, since 1,4-dialkyl-2,5-dibromobenzenes couple under Yamamoto conditions.<sup>54</sup>

Monomers were prepared by Negishi coupling of 1,4-dialkoxy-2,5-dibromobenzenes **2a-f** with EDOT which was first monolithiated with *n*-butyl lithium and transmetalated by reaction with anhydrous zinc chloride (Figure 2.5). Initially, zinc chloride was made anhydrous by fusing with a bunsen burner under vacuum; while this produced monomers in good yield, the drying procedure was tedious, somewhat dangerous, and difficult to monitor for dryness. Instead, anhydrous zinc chloride was purchased in 1.0M ethyl ether solutions from Aldrich (Sure-Seal bottles) and cannula-transferred to the lithiated EDOT solutions, avoiding any exposure to moisture (to do this with the flame-dried solids, ZnCl<sub>2</sub> was weighed in a dry box, sealed into the flask with a septum, dissolved in freshly distilled THF, and cannula-transferred to the reaction mixture.) The resulting BEDOT-B(OR)<sub>2</sub> (**3a-e**) were obtained in 79 to 94% yields (Table 2.1). BEDOT-B(OG)<sub>2</sub> (**3f**) was isolated in lower yield (52%), presumably due to partial solubility of **3f** in water resulting in loss during workup. The compounds were characterized by melting point, <sup>1</sup>H NMR, <sup>13</sup>C NMR, HRMS, and elemental analysis and gave results as required for proper analysis.

**Table 2.1:** Properties of compounds **2a–f** and BEDOT–B(OR)<sub>2</sub> (**3a–f**)

Compound	mp (°C)	% Yield	<sup>1</sup> H NMR (ppm)	<sup>13</sup> C NMR (ppm)
<b>2a</b>	144–147	86	7.10 (s), 3.85 (s) <sup>a</sup>	c
<b>2b</b>	65–67	90	6.98 (s), 3.37 (t), 1.54 (m), 1.25 (m), 0.90 (t) <sup>b</sup>	c
<b>2c</b>	75–77	57	7.18 (s), 4.00 (t), 1.88 (p), 1.53 (p), 1.32 (m), 0.98 (t) <sup>a</sup>	c
<b>2d</b>	87–89	88	6.99 (s), 3.38 (t), 1.55 (q), 1.30 (m), 0.92 (t) <sup>b</sup>	c
<b>2e</b>	210–212 <sup>d</sup>	34	7.01 (s), 3.4 (d), 1.35 (m), 0.9 (m) <sup>b</sup>	150.69, 118.42, 111.53, 72.17, 39.80, 30.87, 29.42, 24.26, 23.42, 14.33, 11.40 <sup>b</sup>
<b>2f</b>	42–44	48	7.13 (s), 4.11 (t), 3.85 (t), 3.73 (t), 3.58 (t), 3.51 (q), 1.18 (t) <sup>a</sup>	150.39, 119.25, 111.43, 71.20, 70.29, 69.96, 69.62, 66.73, 15.22 <sup>b</sup>
<b>3a</b>	197–200	82	7.97 (s), 6.34 (s), 3.63 (s), 3.48 (s) <sup>b</sup>	149.95, 141.31, 138.73, 121.13, 113.28, 95.57, 97.58, 64.90, 64.37, 56.68 <sup>a</sup>
<b>3b</b>	85–87	83	8.10 (s), 6.36 (s), 4.0 (t), 3.5 (m), 1.85 (p), 1.46 (p), 1.23 (m), 0.87 (t) <sup>b</sup>	148.79, 141.05, 138.41, 120.73, 113.30, 99.36, 99.24, 69.72, 64.73, 64.20, 31.71, 29.31, 29.03, 26.14, 22.55, 14.03 <sup>a</sup>
<b>3c</b>	92–95	79	8.11 (s), 6.37 (s), 4.06 (t), 3.5 (m), 1.86 (p), 1.51 (p), 1.28 (m), 0.93 (t) <sup>b</sup>	149.04, 141.20, 138.50, 121.04, 113.60, 99.35, 69.91, 64.82, 64.28, 31.91, 29.68, 29.65, 29.43, 29.34, 26.26, 22.67, 14.06 <sup>a</sup>
<b>3d</b>	92–94	79	8.11 (s), 6.37 (s), 4.06 (t), 3.52 (m), 1.88 (p), 1.52 (m), 1.31 (m), 0.91 (t) <sup>b</sup>	149.04, 141.19, 138.54, 121.02, 113.62, 99.44, 69.93, 64.87, 64.37, 31.96, 29.74, 29.70, 29.65, 29.50, 29.45, 29.39, 26.31, 22.72, 14.14 <sup>a</sup>
<b>3e</b>	121–123	94	8.03 (s), 6.33 (s), 4.01 (d), 3.52 (m), 1.83 (p), 1.6 (m), 1.28 (m), 0.91 (m) <sup>b</sup>	150.0, 141.9, 139.1, 121.9, 114.4, 99.7, 72.2, 64.7, 64.1, 40.1, 31.1, 29.5, 24.4, 23.5, 14.3, 11.4 <sup>a</sup>
<b>3f</b>	100–102	53	7.68 (s), 6.34 (s), 4.27 (t), 4.20 (p), 3.93 (t), 3.71 (t), 3.59 (t), 3.50 (q), 1.20 (t) <sup>a</sup>	148.8, 141.1, 138.7, 121.1, 113.2, 99.5, 70.9, 69.9, 69.7, 69.1, 66.6, 64.8, 64.3, 15.1 <sup>a</sup>

<sup>a</sup> CDCl<sub>3</sub><sup>b</sup> C<sub>6</sub>D<sub>6</sub><sup>c</sup> Not determined (known compound)<sup>d</sup> bp at 0.65Torr

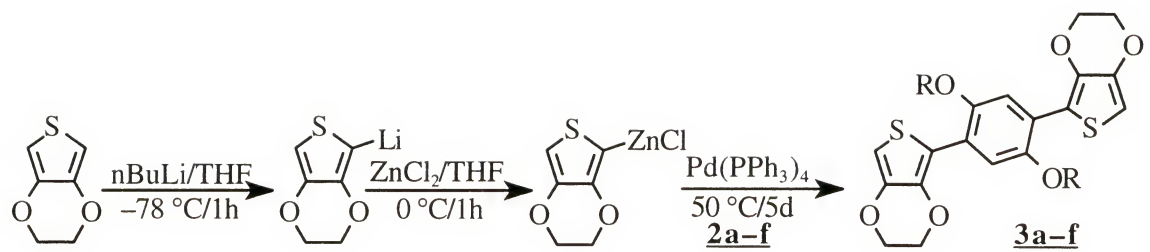


**Figure 2.5:** Negishi synthesis of BEDOT–B(OR)<sub>2</sub>

### 2.3 X-Ray Crystal Structure of BEDOT–B(OG)<sub>2</sub>

To better understand the structure of the monomers described above, the X-ray crystal structure of one of these monomers, BEDOT–B(OG)<sub>2</sub> (**3f**), was examined. With the exception of methoxy–substituted monomer **3a**, the other monomers did not crystallize; monomer **3f** readily crystallized from a variety of solvents. Best crystals were obtained from acetonitrile, to yield the crystal structure given in Figure 2.6.

The structure resembles the previously–reported structure of 1,4-bis[2–(3,4–ethylenedioxy)thienyl]benzene (BEDOT–B),<sup>85</sup> with the exception of the torsion angle between the plane of the benzene ring and the plane of the thiophene ring. In the case of BEDOT–B, the molecule deviates significantly from planarity, with the central benzene being inclined to the plane of the attached thiophene rings at an angle (torsion angle) of 27.5°. BEDOT–B(OG)<sub>2</sub>, on the other hand, is nearly planar in the three ring system; the same torsion angle is only 6.8°. which indicates a very low barrier to planarity of the three ring system. Tables of crystal structure data can be found in the Appendix.

The solid state structure of the monomer can be related to the structure of the repeat unit of the polymer. The small torsion angle found in BEDOT-B(OG)<sub>2</sub> suggests that the resultant polymer, PBEDOT-B(OG)<sub>2</sub>, should have increased conjugation compared to the polymer (PBEDOT-B) derived from BEDOT-B. As the ability of a neutral conjugated polymer to attain a planar conformation increases, less energy is needed to stabilize the bipolaron state upon polymer oxidation. Additionally, increased planarity in the polymer increases the possibility of interchain transport, lowering the  $\pi$  to  $\pi^*$  transition in the neutral polymer.

The phenylene ring in BEDOT-B(OG)<sub>2</sub> is rotated so that the alkoxy side chains are closest to the sulfur of the EDOT rings rather than the oxygens of the EDOT rings; the distance between the sulfur atom on EDOT and the first oxygen of the side chain is 2.626 Å (the sum of the van der Waals radii of the two atoms is 3.2 Å<sup>129</sup>). It is possible that there is an electrostatic attraction between the sulfur and the oxygen, pulling them closer together and therefore making the rings of the molecule nearly coplanar.<sup>130</sup>

The halves of the oligomeric ether side chains closest to the phenylene ring in the crystal are arranged in a transoid configuration, with a cisoid configuration beginning after O5. There is a fair amount of free rotation at the ends of the ether side chains, but the degree of order close to the phenylene rings may be responsible for the high degree of crystallinity in the monomer.

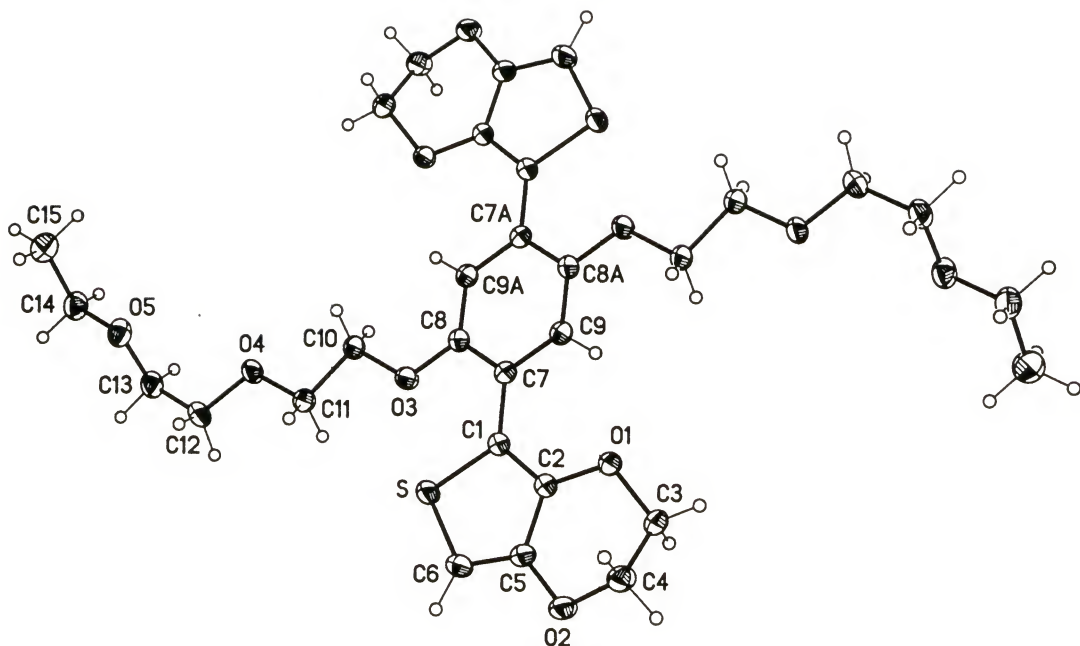


**Figure 2.6:** X-ray crystal structure of BEDOT-B(OG)<sub>2</sub> (3f)

## 2.4 Experimental

### 2.4.1 Materials

Hydroquinone, potassium hydroxide, iodomethane, 1-bromoheptane, 1-bromododecane, 1-bromohexadecane, 1-bromo-2-ethylhexane, bromine, *p*-toluenesulfonyl chloride, di(ethylene glycol) ethyl ether, triethylamine, *n*-butyl lithium (2.5M in hexanes), magnesium bromide diethyl etherate, nickel (II) di(phenylphosphino) propane dichloride, anhydrous zinc chloride (1.0M in ethyl ether) and tetrakis(triphenylphosphine) palladium (0) were obtained

from Aldrich Chemicals and used as received. Solid zinc chloride was obtained from Aldrich Chemicals and flame dried under vacuum prior to use. Concentrated hydrochloric acid, glacial acetic acid, ethyl ether, acetone, methanol, ethanol, and benzene were acquired from Fisher Scientific and used as received. THF, acetonitrile, chloroform and methylene chloride were purchased from Fisher Scientific and dried and distilled prior to use.

3,4-Ethylenedioxythiophene (EDOT) was obtained from AG Bayer. As received, EDOT has as much as 10% quinoline contamination by volume (<sup>1</sup>H NMR and GC), making purification necessary. EDOT was dissolved in methylene chloride, extracted with 0.1M HCl, washed with saturated sodium bicarbonate until neutral, dried over magnesium sulfate, and filtered through neutral alumina. Methylene chloride was removed under reduced pressure, and EDOT was then distilled under vacuum (85°C at 0.65 Torr). The resultant colorless liquid was then stored as a solid in the dark at 0°C (mp=10°C) under argon and thawed prior to use.

#### 2.4.2 Structural Identification of Monomers and Polymers

NMR spectra were obtained in solution and recorded on a Gemini 300 FT-NMR or a VXR 300 FT-NMR spectrophotometer. Elemental analyses were obtained from Robertson Microlit Laboratories, Inc., Madison, NJ. High-resolution mass spectra were obtained using a Finnigan MAT 95Q mass spectrometer.

#### 2.4.3 Synthesis

1,4-Dibromo-2,5-dihydroxybenzene (1). Hydroquinone (0.968mol)

was combined with glacial acetic acid (500mL) and methylene chloride. A solution of bromine (1.88mol) in methylene chloride (100mL) was added dropwise over 2h at room temperature. After approximately half the bromine was added, all solids had dissolved. The solution was stirred at room temperature for 15h, at which time a precipitate was collected by filtration and dried under vacuum over NaOH pellets. Recrystallization from isopropanol yielded a white crystalline solid [mp 191–192°C, 42%]. Anal. calcd for C<sub>6</sub>H<sub>4</sub>Br<sub>2</sub>O<sub>2</sub>: C, 26.90; H, 1.51; Br, 59.65; O, 11.94. Found: C, 26.95; H, 1.43; Br, 58.95. <sup>1</sup>H NMR (acetone-d<sub>6</sub>, ppm): 8.62 (br), 7.15 (s). <sup>13</sup>C NMR (acetone-d<sub>6</sub>, ppm): 148.5, 120.63, 109.48. HRMS: calcd for C<sub>6</sub>H<sub>4</sub>Br<sub>2</sub>O<sub>2</sub>: 265.859; found: 265.864.

1,4-Dibromo-2,5-dimethoxybenzene (2a). A solution of KOH (0.077mol) in ethanol (100mL) was added slowly with stirring to a solution of 1 (0.035mol) in THF (200mL) under argon. The solution was stirred at room temperature for 3h, and then a solution of iodomethane (0.077mol) in THF (100mL) was added slowly with stirring. The mixture was stirred at 50°C for 24h, then precipitated into water. The product was collected by filtration and recrystallized from ethanol to give a white crystalline solid [mp 144–147 °C (lit.<sup>111</sup> mp 142–143°C), 86% yield]. <sup>1</sup>H NMR (CDCl<sub>3</sub>, ppm): 7.10 (s), 3.85 (s).

1,4-Dibromo-2,5-diheptoxybenzene (2b). Compound **2b** was synthesized according to the procedure described for **2a** using KOH (0.069mol), **1** (0.033mol), and 1-bromoheptane (0.069mol). Recrystallization from ethanol gave a white clumped solid [mp 65-67 °C (lit.<sup>55</sup> mp 59-60°C), 90% yield]. <sup>1</sup>H NMR (C<sub>6</sub>D<sub>6</sub>, ppm): 6.98 (s), 3.37 (t), 1.54 (m), 1.25 (m), 0.90 (t).

1,4-Dibromo-2,5-didodecyloxybenzene (2c). Compound **2c** was prepared according to the procedure described for **2a** using KOH (0.032mol), **1** (0.016mol), and 1-bromododecane (0.032mol). Recrystallization from ethanol/benzene (3/1) resulted in a white crystalline solid [mp 75–77°C (lit.<sup>55</sup> mp 77–79°C), 57% yield]. <sup>1</sup>H NMR (CDCl<sub>3</sub>, ppm): 7.18 (s), 4.00 (t), 1.88 (p), 1.53 (p), 1.32 (m), 0.98 (t).

1,4-Dibromo-2,5-dihexadecyloxybenzene (2d). Compound **2d** was prepared according to the procedure described for **2a** using KOH (0.151mol), **1** (0.072mol), and 1-bromohexadecane (0.151mol). Recrystallization from chloroform resulted in a white fluffy solid [mp 87-89°C (lit.<sup>55</sup> mp 88-89°C), 88% yield]. <sup>1</sup>H NMR (C<sub>6</sub>D<sub>6</sub>, ppm): 6.99 (s), 3.38 (t), 1.55 (q), 1.30 (m), 0.92 (t).

1,4-Dibromo-2,5-di(2-ethylhexyl)oxybenzene (2e). Compound **2d** was prepared according to the procedure described for **2a** using KOH (0.113mol), **1** (0.05mol), and 1-bromo-2-ethylhexane (0.12mol). The product was extracted into methylene chloride, dried over magnesium sulfate, filtered through silica gel, and concentrated under reduced pressure to yield a pale yellow

liquid. Vacuum distillation (0.65 Torr) yielded fractions boiling at 190, 200, and 210°C. The fraction boiling at 210°C was found by NMR to be the desired product [bp 210–212°C at 0.65 Torr, 34% yield]. Anal. calcd for C<sub>22</sub>H<sub>36</sub>Br<sub>2</sub>O<sub>2</sub>: C, 53.67; H, 7.37; Br, 32.46; O, 6.50. Found: C, 53.65; H, 7.51; Br, 32.61. <sup>1</sup>H NMR (C<sub>6</sub>D<sub>6</sub>, ppm): 7.01 (s), 3.4 (d), 1.35 (m), 0.9 (m). <sup>13</sup>C NMR (C<sub>6</sub>D<sub>6</sub>, ppm): 150.69, 118.42, 111.53, 72.17, 39.80, 30.87, 29.42, 24.26, 23.42, 14.33, 11.40. HRMS: calcd for C<sub>22</sub>H<sub>36</sub>Br<sub>2</sub>O<sub>2</sub>: 490.1082; found: 490.1089.

3,6-Dioxaoctyl p-toluenesulfonate.<sup>112</sup> Di(ethyleneglycol) ethyl ether (1.25mol) and *p*-toluenesulfonyl chloride (1.04mol) were dissolved in acetone (600mL) with stirring in a 250mL Erlenmeyer flask to yield a pale yellow solution. Triethylamine (1.87mol) was added dropwise to the flask over 4 hours, taking care to add slowly enough to prevent the reaction mixture from heating up; white precipitate began to form after one hour of addition. After stirring 18h at room temperature in air, the reaction mixture was poured into ice (1.5L) and concentrated HCl (200mL). After stirring for 3h, the mixture was extracted with methylene chloride, which was evaporated from the organic layer under reduced pressure at room temperature to give a pale yellow liquid. This was washed with water until neutral, dilute NaOH to pH10, and water until neutral. The product was dried over magnesium sulfate and gravity-filtered; the resultant pale yellow liquid was stirred under reduced pressure for 8h. One peak was observed by GC [85% yield]. Anal. calcd for C<sub>13</sub>H<sub>20</sub>O<sub>5</sub>S: C, 54.15; H, 6.99; O, 27.74; S, 11.12. Found: C, 53.94; H, 6.77. <sup>1</sup>H NMR

(C<sub>6</sub>D<sub>6</sub>, ppm): 7.73 (d), 6.79 (d), 3.91 (t), 3.25 (m), 1.91 (s), 1.03 (t). <sup>13</sup>C NMR (CDCl<sub>3</sub>, ppm): 144.84, 129.84, 128.00, 70.85, 69.75, 69.31, 68.70, 66.67, 21.65, 15.16.

**1,4-Dibromo-2,5-bis(1, 4, 7-trioxanonyl)benzene (2f).** Compound **2f** was prepared according to the procedure described for **2a** using KOH (0.1734mol), **1** (0.07882mol), and 3,6-dioxaoctyl *p*-toluenesulfonate (0.1734mol). The reaction mixture was poured into aqueous sodium chloride and extracted with ethyl ether. Drying over magnesium sulfate followed by concentration under reduced pressure gave a yellow solid. This was recrystallized twice from ethyl ether at -78°C to give a white microcrystalline solid [mp 42–44°C, 48% yield]. Anal. calcd for C<sub>18</sub>H<sub>28</sub>Br<sub>2</sub>O<sub>6</sub>: C, 43.22; H, 5.64; O, 19.19; Br, 31.95. Found: C, 43.25; H, 5.50; Br, 31.81. <sup>1</sup>H NMR (CDCl<sub>3</sub>, ppm): 7.13 (s), 4.11 (t), 3.85 (t), 3.73 (t), 3.58 (t), 3.51 (q), 1.18 (t). <sup>13</sup>C NMR (C<sub>6</sub>D<sub>6</sub>, ppm): 150.39, 119.25, 111.43, 71.20, 70.29, 69.96, 69.62, 66.73, 15.22. HRMS: calcd for C<sub>18</sub>H<sub>28</sub>Br<sub>2</sub>O<sub>6</sub>: 498.0253; found: 498.0247.

**1,4-Bis[2-(3,4-ethylenedioxy)thienyl]-2,5-dimethoxybenzene (3a).**

*n*-Butyl lithium (6.69×10<sup>-2</sup>mol) was slowly added to a stirred solution of EDOT (6.69×10<sup>-2</sup>mol) in THF (75mL) at -78°C under argon. The yellow solution was allowed to stir for 1h. The lithiated EDOT was transferred using a cannula into a stirring solution of ZnCl<sub>2</sub> (6.39×10<sup>-2</sup>mol) in THF (75mL) over a 15min period. The mixture was stirred under argon for 1h. The resulting EDOT-ZnCl was then slowly added to a solution of **2a** (1.67×10<sup>-2</sup>mol) and Pd(PPh<sub>3</sub>)<sub>4</sub> (8.65×10<sup>-5</sup> mol) in THF (50mL). The bright yellow solution was

stirred at 50°C under argon for 5d. It was then cooled to ambient temperature and quenched by pouring the mixture into 1N HCl. A large amount of tan solid precipitated upon contact with the acid. This was collected and washed with saturated NaHCO<sub>3</sub>, then dried under vacuum. The product was purified by recrystallization from ethanol/benzene (3/1) followed by column chromatography (ethyl acetate/pentane, 1/1) to yield a pale green solid [mp 197–200°C, 82%]. Anal. calcd for C<sub>20</sub>H<sub>18</sub>O<sub>6</sub>S<sub>2</sub>: C, 57.40; H, 4.34; O, 22.94; S, 15.32. Found: C, 57.21; H, 4.29; S, 15.44. <sup>1</sup>H NMR (C<sub>6</sub>D<sub>6</sub>, ppm): 7.97 (s), 6.34 (s), 3.63 (s), 3.48 (s). <sup>13</sup>C NMR (CDCl<sub>3</sub>, ppm): 149.95, 141.31, 138.73, 121.13, 113.28, 95.57, 97.58, 64.90, 64.37, 56.68. HRMS: calcd for C<sub>20</sub>H<sub>18</sub>O<sub>6</sub>S<sub>2</sub>: 418.054; found: 418.048.

**1,4-Bis[2-(3,4-ethylenedioxy)thienyl]-2,5-diheptoxybenzene (3b).**

Compound **3b** was prepared according to the procedure described for **3a** using EDOT (3.52×10<sup>-2</sup>mol), *n*-butyl lithium (3.52×10<sup>-2</sup>mol), zinc chloride (3.52×10<sup>-2</sup>mol), Pd(PPh<sub>3</sub>)<sub>4</sub> (4.16×10<sup>-5</sup> mol), and **2b** (8.79×10<sup>-3</sup>mol), resulting in a pale yellow, crystalline solid after recrystallization from ethanol/benzene (3/1) [mp 85–87°C, 83% yield]. Anal. calcd for C<sub>32</sub>H<sub>42</sub>O<sub>6</sub>S<sub>2</sub>: C, 65.50; H, 7.21; O, 16.36; S, 10.93. Found: C, 65.24; H, 7.18; S, 11.09. <sup>1</sup>H NMR (C<sub>6</sub>D<sub>6</sub>, ppm): 8.10 (s), 6.36 (s), 4.0 (t), 3.5 (m), 1.85 (p), 1.46 (p), 1.23 (m), 0.87 (t). <sup>13</sup>C NMR (CDCl<sub>3</sub>, ppm): 148.79, 141.05, 138.41, 120.73, 113.30, 99.36, 99.24, 69.72, 64.73, 64.20, 31.71, 29.31, 29.03, 26.14, 22.55, 14.03. HRMS: calcd for C<sub>32</sub>H<sub>42</sub>O<sub>6</sub>S<sub>2</sub>: 586.24; found: 586.24.

1,4-Bis[2-(3,4-ethylenedioxy)thienyl]-2,5-didodecyloxybenzene (3c).

Compound **3c** was prepared according to the procedure described for **3a** using EDOT ( $3.31 \times 10^{-2}$  mol), *n*-butyl lithium ( $3.31 \times 10^{-2}$  mol), zinc chloride ( $3.31 \times 10^{-2}$  mol), Pd(PPh<sub>3</sub>)<sub>4</sub> ( $3.91 \times 10^{-5}$  mol), and **3b** ( $8.27 \times 10^{-3}$  mol), resulting in a bright green, crystalline solid after recrystallization from ethanol/benzene (3/1) [mp 92–95°C, 80% yield]. Anal. calcd for C<sub>42</sub>H<sub>62</sub>O<sub>6</sub>S<sub>2</sub>: C, 69.38; H, 8.59; O, 13.20; S, 8.82. Found: C, 69.65; H, 8.68; S, 8.57. <sup>1</sup>H NMR (C<sub>6</sub>D<sub>6</sub>, ppm): 8.11 (s), 6.37 (s), 4.06 (t), 3.5 (m), 1.86 (p), 1.51 (p), 1.28 (m), 0.93 (t). <sup>13</sup>C NMR (CDCl<sub>3</sub>, ppm): 149.04, 141.20, 138.50, 121.04, 113.60, 99.35, 69.91, 64.82, 64.28, 31.91, 29.68, 29.65, 29.43, 29.34, 26.26, 22.67, 14.06. HRMS: calcd for C<sub>42</sub>H<sub>62</sub>O<sub>6</sub>S<sub>2</sub>: 726.399; found: 726.398.

1,4-Bis[2-(3,4-ethylenedioxy)thienyl]-2,5-dihexadecyloxybenzene (3d).

Compound **3d** was prepared according to the procedure described for **3a** using EDOT ( $3.52 \times 10^{-2}$  mol), *n*-butyl lithium ( $3.52 \times 10^{-2}$  mol), zinc chloride ( $3.52 \times 10^{-2}$  mol), Pd(PPh<sub>3</sub>)<sub>4</sub> ( $4.16 \times 10^{-5}$  mol), and **2d** ( $8.79 \times 10^{-3}$  mol), resulting in a bright yellow solid after recrystallization from chloroform and column chromatography (ethyl acetate/pentane, 1/1) [mp 92–94°C, 79% yield]. Anal. calcd for C<sub>50</sub>H<sub>78</sub>O<sub>6</sub>S<sub>2</sub>: C, 71.55; H, 9.37; O, 11.44; S, 7.64. Found: C, 71.46; H, 9.29; S, 7.53. <sup>1</sup>H NMR (C<sub>6</sub>D<sub>6</sub>, ppm): 8.11 (s), 6.37 (s), 4.06 (t), 3.52 (m), 1.88 (p), 1.52 (m), 1.31 (m), 0.91 (t). <sup>13</sup>C NMR (CDCl<sub>3</sub>, ppm): 149.04, 141.19, 138.54, 121.02, 113.62, 99.44, 69.93, 64.87, 64.37, 31.96, 29.74, 29.70, 29.65, 29.50, 29.45, 29.39, 26.31, 22.72, 14.14. HRMS: calcd for C<sub>50</sub>H<sub>78</sub>O<sub>6</sub>S<sub>2</sub>: 838.53; found: 838.53.

1,4-Bis[2-(3,4-ethylenedioxy)thienyl]-2,5-di(2-ethylhexyloxy)benzene

(**3e**). Compound **3e** was prepared according to the procedure described for **3a** using EDOT ( $2.76 \times 10^{-2}$  mol), *n*-butyl lithium ( $2.83 \times 10^{-2}$  mol), zinc chloride ( $2.83 \times 10^{-2}$  mol), Pd(PPh<sub>3</sub>)<sub>4</sub> ( $3.58 \times 10^{-5}$  mol), and **2e** ( $6.91 \times 10^{-3}$  mol), resulting in a yellow-green microcrystalline solid after recrystallization from ethanol/toluene [mp 121–123°C, 94% yield]. Anal. calcd for C<sub>34</sub>H<sub>46</sub>O<sub>6</sub>S<sub>2</sub>: C, 66.42; H, 7.54; O, 15.61; S, 10.43. Found: C, 66.24; H, 7.40; S, 10.27. <sup>1</sup>H NMR (C<sub>6</sub>D<sub>6</sub>, ppm): 8.03 (s), 6.33 (s), 4.01 (d), 3.52 (m), 1.83 (p), 1.6 (m), 1.28 (m), 0.91 (m). <sup>13</sup>C NMR (CDCl<sub>3</sub>, ppm): 150.0, 141.9, 139.1, 121.9, 114.4, 99.7, 72.2, 64.7, 64.1, 40.1, 31.1, 29.5, 24.4, 23.5, 14.3, 11.4. HRMS: calcd for C<sub>34</sub>H<sub>46</sub>O<sub>6</sub>S<sub>2</sub>: 614.274; found: 614.274.

1,4-Bis[2-(3,4-ethylenedioxy)thienyl]-2,5-bis (1, 4, 7-trioxanonyl)-benzene (3f). Compound **3f** was prepared according to the procedure described for **3a** using EDOT ( $3.00 \times 10^{-2}$  mol), *n*-butyl lithium ( $3.00 \times 10^{-2}$  mol), zinc chloride ( $3.30 \times 10^{-2}$  mol), Pd(PPh<sub>3</sub>)<sub>4</sub> ( $4.98 \times 10^{-5}$  mol), and **2f** ( $1.00 \times 10^{-2}$  mol), resulting in a bright yellow crystalline solid after recrystallization from methylene chloride [mp 100–102°C, 53% yield]. Anal. calcd for C<sub>30</sub>H<sub>38</sub>O<sub>10</sub>S<sub>2</sub>: C, 57.86; H, 6.15; O, 25.69; S, 10.30. Found: C, 57.53; H, 6.05; S, 10.11. <sup>1</sup>H NMR (CDCl<sub>3</sub>, ppm): 7.68 (s), 6.34 (s), 4.27 (t), 4.20 (p), 3.93 (t), 3.71 (t), 3.59 (t), 3.50 (q), 1.20 (t). <sup>13</sup>C NMR (CDCl<sub>3</sub>, ppm): 148.8, 141.1, 138.7, 121.1, 113.2, 99.5, 70.9, 69.9,

69.7, 69.1, 66.6, 64.8, 64.3, 15.1. HRMS: calcd for C<sub>30</sub>H<sub>38</sub>O<sub>10</sub>S<sub>2</sub>: 622.191; found: 622.192.

## CHAPTER 3 ELECTROCHEMISTRY

### 3.1 Motivation for Research

The extended conjugation monomers described in Chapter 2 are highly electron rich due to the large amount of electron donation from the linear and cyclic alkoxy substituents as well as the electron-rich thiophene rings. The combination of electron-rich thiophene and phenylene rings yields a group of monomers with unique electronic properties. Electrochemical polymerization of the monomers is easily accomplished, yielding regular, electron-rich polymers whose electrochemistry has been studied in combination with a variety of spectroscopic techniques.

### 3.2 Cyclic Voltammetry

#### 3.2.1 Background

Conjugated monomers can be oxidized both chemically (Chapter 4) and electrochemically. Electrochemical polymerization is advantageous in that the oxidation potential can easily be controlled to prevent side reactions;

when a chemical oxidant is used, overoxidation can occur, resulting in disordered materials with poor electronic properties.<sup>131,132,133</sup>

Cyclic voltammetry is a useful tool for understanding a wide range of oxidation and reduction processes, particularly those occurring during the synthesis and redox reactions of conducting polymers. To understand the cyclic voltammetry experiments described in this chapter, it is necessary to have a basic understanding of the fundamentals involved. The electrochemistry of electroactive monomers and their polymers is somewhat complex, so it is best to start with the simple case of reversible redox processes for freely diffusing species.

During cyclic voltammetry (CV), a potential is applied at an electrode, and the current response is measured. A supporting electrolyte must be present to carry current and to balance any charges generated in the electroactive species during the electrochemical process. As the potential at the electrode is increased, any freely diffusing electroactive species near the electrode surface is oxidized, generating a current response. This current response decreases as the concentration of reduced species near the electrode decreases. As the direction of the scan is reversed, the oxidized material is reduced; current response increases as the reduced species is released near the electrode and then decreases as the reduced species diffuses away. The Randles-Sevick equation<sup>134</sup> states that the current at the peak potential is given by:

$$i_p = (2.69 \times 10^5) n^{3/2} A D^{1/2} C^b v^{1/2} \quad (3-1)$$

where  $n$  is the number of electrons transferred,  $A$  is the electrode surface area (in  $\text{cm}^2$ ),  $D$  is the diffusion constant ( $\text{cm}^2\text{s}^{-1}$ ),  $C^b$  is the bulk concentration ( $\text{mol}\text{cm}^{-3}$ ) and  $v$  is the scan rate ( $\text{Vs}^{-1}$ ). Thus, in a diffusion controlled system, peak current is proportional to  $v^{1/2}$ .

In the case of electroactive polymer electrochemistry, the process is somewhat different. Polymerization of electroactive monomers is an irreversible process, with monomer in solution next to the electrode diffusing to the surface when a potential is applied. At the surface, the monomer is irreversibly oxidized, polymerization occurs, and a film of electroactive polymer is formed.

To study electroactive polymer electrochemistry, it is necessary to remove all monomer, since the oxidative polymerization process obscures the polymer electrochemistry. The polymer redox process is quasi-reversible, but because the polymer is immobilized at the electrode surface, the polymer redox process is not diffusion controlled. Thus, the Randles-Sevick equation given above does not apply. Instead, according to the theory for surface immobilized redox centers,<sup>135,136</sup> the peak current is given by

$$i_p = \frac{n^2 F^2 \Gamma v}{4RT} \quad (3-2)$$

where  $\Gamma$  is the total amount of reactant initially present at the electrode surface. From this relationship, it follows that for a surface-immobilized

electroactive species, the peak current will be linearly dependent on the scan rate. Thus, an examination of the peak current dependence on scan rate reveals whether an electrochemical process is diffusion controlled or whether the polymer is well-adhered to the electrode surface.

### 3.2.2 Techniques

Electrochemical polymerization can be accomplished using simple linear potential sweep voltammetry (cyclic voltammetry, CV) with a conventional three electrode cell. Because several cycles are generally needed to deposit a significant amount of polymer at the electrode surface, this technique is often called repeated potential scanning electropolymerization. While this technique is advantageous in that the monomer electrochemistry can be probed, it is also possible to polymerize at a constant potential at or above the monomer oxidation potential. This technique keeps the polymer oxidized until the polymerization is complete, thus limiting morphological changes due to redox switching. Polymerization at constant potential is commonly used when the electrochemistry of polymerization is already known but polymer samples are needed for further studies.

In order for current to flow in the electrochemical cell, it is necessary to have a conducting medium, typically an electrolyte dissolved in a polar solvent. During oxidation, the electrolyte anions balance the cations that

form in the monomer and/or polymer chains, with the electrolyte cations solvated by the polar solvent (which also minimizes resistance in the cell).

The three electrode cell (Figure 3.1) consists of a working electrode, a counter electrode, and a reference electrode. The working electrode consists of a small amount of conductive material such as platinum, gold, or graphite, typically called a button, while the counter electrode is a much larger plate of conductive material (typically platinum) to allow for passage of current. A reference electrode is placed close to the other electrodes to control the electrochemical potential; this electrode contains a solution of ions that undergo an equilibrium reaction at a known potential which can be used to monitor the potential in the electrochemical cell. In organic solutions, the Ag/Ag<sup>+</sup> reference electrode is the most commonly used reference;<sup>137</sup> unless otherwise noted, all electrochemistry described in this dissertation is referenced to Ag/Ag<sup>+</sup> (in CH<sub>3</sub>CN, Ag/Ag<sup>+</sup> = 0.499V + NHE, Ag/Ag<sup>+</sup> = 0.2578V + SCE). During polymerization, monomer is dissolved in the electrolyte solution, and polymerization occurs at the working electrode.

Cyclic voltammetry was carried out with an EG&G Princeton Applied Research model 273 potentiostat/galvanostat employing a platinum button working electrode, a platinum plate counter electrode, and a Ag/Ag<sup>+</sup> reference electrode. The monomer concentration was 10mM in each case, and unless otherwise noted, the electrolyte was 0.1M tetra-*n*-butylammonium perchlorate (TBAP) in acetonitrile or acetonitrile/methylene chloride.

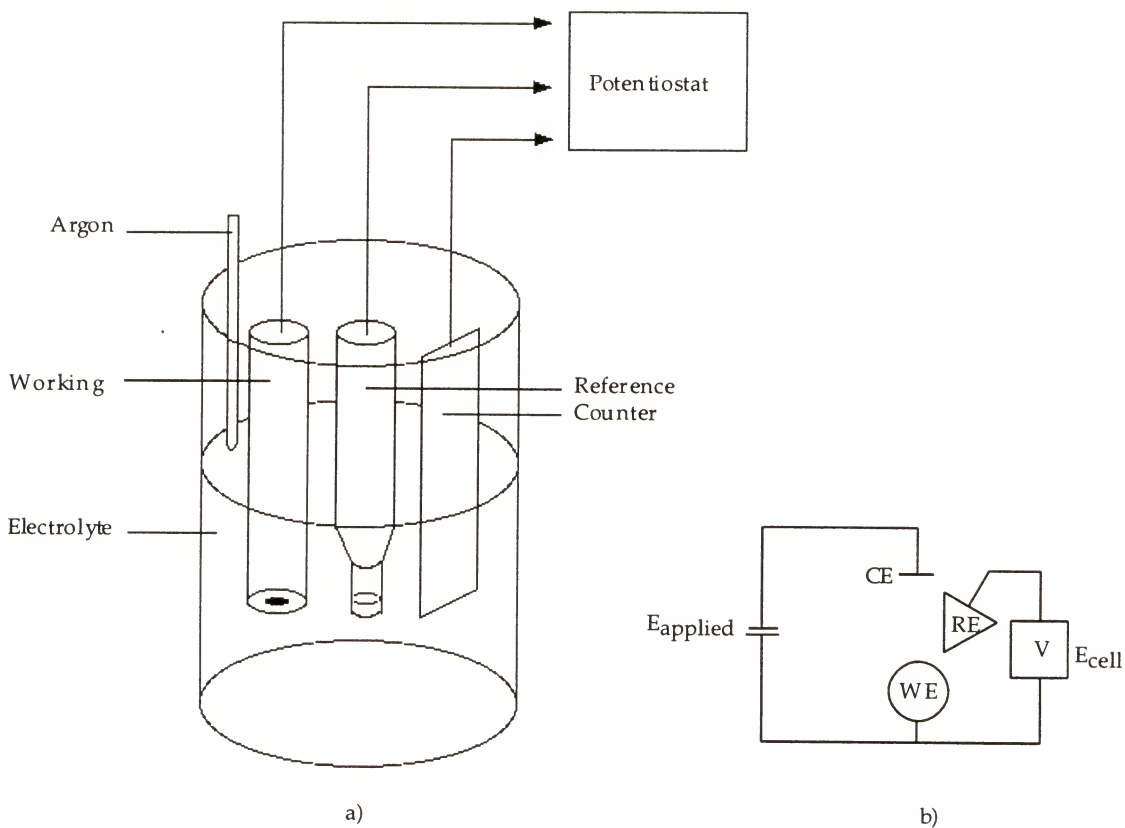


**Figure 3.1:** Standard three-electrode electrochemical cell: a) schematic b) circuit

### 3.2.3 Electropolymerization of BEDOT-B(OR)<sub>2</sub> (3a-f)

All BEDOT-B(OR)<sub>2</sub> (3a-f) were electrochemically polymerized (Figure 3.2) in an argon atmosphere using 0.01M monomer and 0.1M tetrabutylammonium perchlorate (TBAP) in CH<sub>3</sub>CN/CH<sub>2</sub>Cl<sub>2</sub>. The mixture of CH<sub>2</sub>Cl<sub>2</sub> and CH<sub>3</sub>CN was required for electropolymerization, because the monomers were poorly soluble in CH<sub>3</sub>CN. For all monomers, polymer film

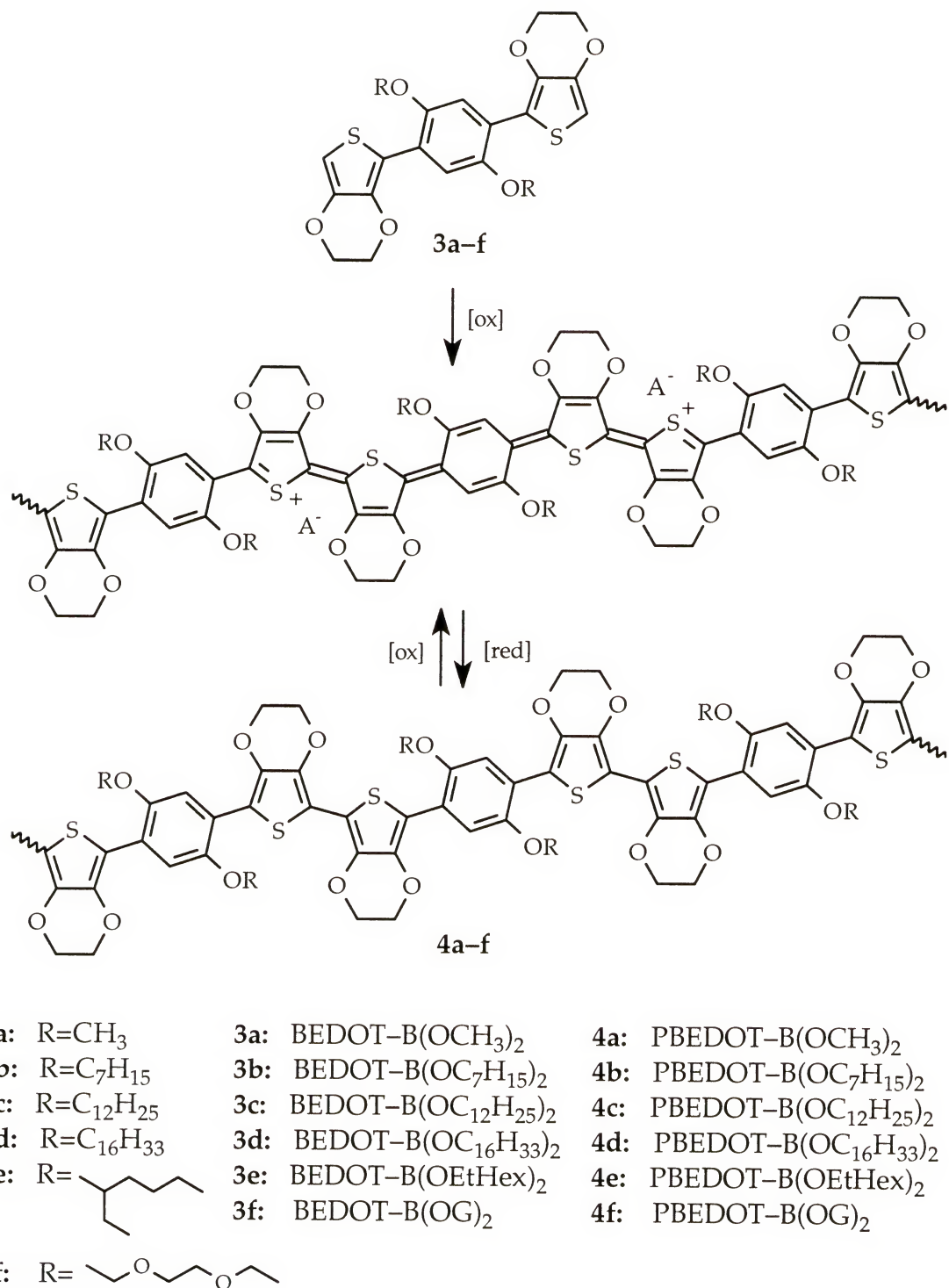


**Figure 3.2:** Electrochemical polymerization of BEDOT-B(OR)<sub>2</sub> (3a-f)

deposition in  $\text{CH}_2\text{Cl}_2$  electrolyte alone was quite slow, likely due to solubility of oligomers. A solubility study was conducted to determine the minimum amount of  $\text{CH}_2\text{Cl}_2$  needed to solubilize the monomers in  $\text{CH}_3\text{CN}$ . As expected, the longer the alkoxy substituent, the more  $\text{CH}_2\text{Cl}_2$  was needed. For R=methyl, heptyl, dodecyl, hexadecyl, 2-ethylhexyl, and glyme, the ratios of  $\text{CH}_2\text{Cl}_2$  to  $\text{CH}_3\text{CN}$  required were, respectively, 2:3, 1:1, 3:2, 7:3, 1:9, and 1:9.

Figure 3.3 shows multiple cyclic voltammograms for the repeated scanning electropolymerization of BEDOT-B( $\text{OC}_{12}\text{H}_{25}$ )<sub>2</sub> (**3c**), which is representative of the polymerizations of **3a-f**. During the first anodic scan, a single peak is observed for all monomers which corresponds to irreversible monomer oxidation at a bare metal electrode. For comparative purposes, BEDOT-B( $\text{OCH}_3$ )<sub>2</sub> (**3a**) exhibits a monomer oxidation onset ( $E_{\text{on,m}}$ ) at +0.30 V, and a peak ( $E_{\text{p,m}}$ ) is observed at +0.46 V vs. Ag/Ag<sup>+</sup>. The  $E_{\text{p,m}}$  values shown in Table 3.1 are low relative to the analogous 1,4-bis(2-thienyl)-2,5-dialkoxybenzene monomers; for example 1,4-bis(2-thienyl)-2,5-dimethoxybenzene exhibits an  $E_{\text{p,m}}$  250 mV higher at +0.71 V.<sup>56</sup> These low oxidation potentials are important as they are indicative of the ease with which the monomers are oxidized, and the electropolymerization can proceed with minimal side reactions.

With repeated potential scanning, thin, insoluble films of the polymers **4a-f** form on the electrode surface. Cathodic redox processes at about +0.2 V and at 0.0 V are observed during reduction of the polymer and evolve in intensity with repeated scanning. On the anodic scans, polymer oxidation is

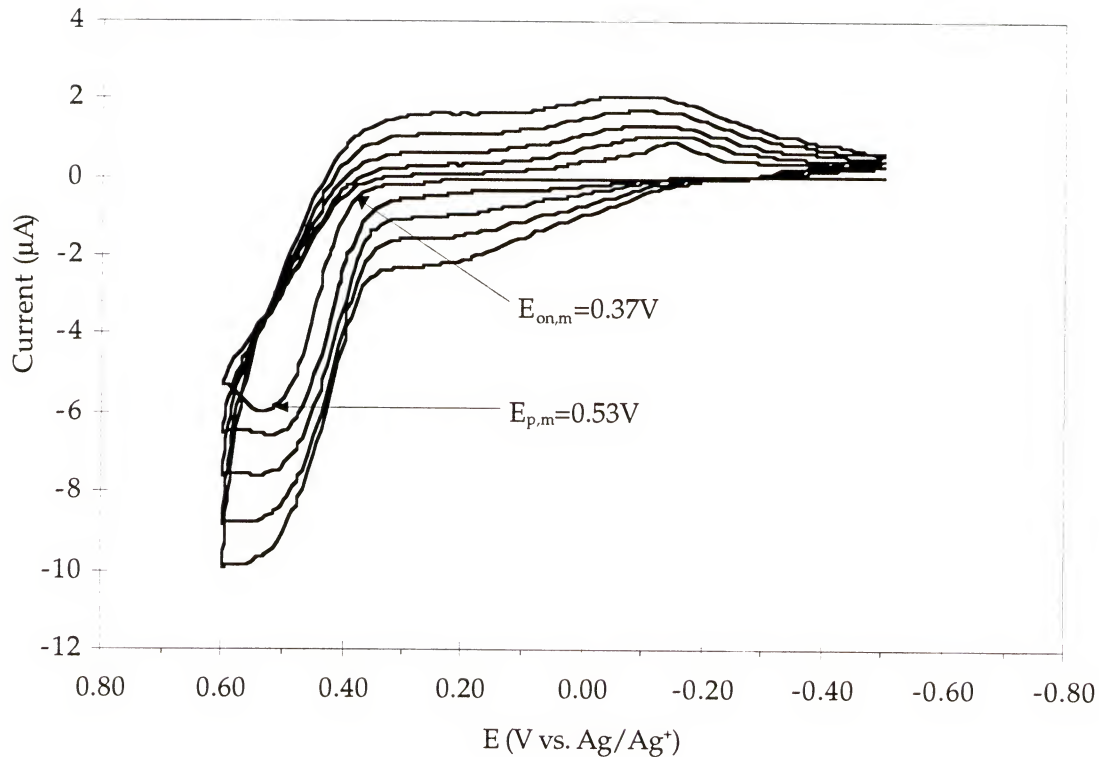


**Figure 3.3:** Cyclic voltammetric polymerization of BEDOT-B(OC<sub>12</sub>H<sub>25</sub>)<sub>2</sub> (**3c**) (0.01M) carried out in 0.1M TBAP in 2:3 CH<sub>3</sub>CN:CH<sub>2</sub>Cl<sub>2</sub> (100mVs<sup>-1</sup>)]

**Table 3.1:** Oxidation and reduction potentials for monomers and polymers

Monomer	$E_{on,m}$ <sup>a</sup>	$E_{p,m}$	$E_{a,p}$	$E_{c,p}$	$E_{1/2,p}$
<b>3a</b> , BEDOT-B(OCH <sub>3</sub> ) <sub>2</sub>	+0.30	+0.46	-0.20	broad	<sup>b</sup>
<b>3b</b> , BEDOT-B(OC <sub>7</sub> H <sub>15</sub> ) <sub>2</sub>	+0.32	+0.46	-0.28	-0.36	-0.32
<b>3c</b> , BEDOT-B(OC <sub>12</sub> H <sub>25</sub> ) <sub>2</sub>	+0.38	+0.41	-0.25	-0.31	-0.28
<b>3d</b> , BEDOT-B(OC <sub>16</sub> H <sub>33</sub> ) <sub>2</sub>	+0.41	+0.66	-0.30	-0.40	-0.35
<b>3e</b> , BEDOT-B(OEtHex) <sub>2</sub>	+0.34	+0.44	+0.01	-0.33	-0.16
<b>3f</b> , BEDOT-B(OG) <sub>2</sub>	+0.30	+0.50	-0.45	-0.55	-0.50

<sup>a</sup> All potentials reported in V vs. Ag/Ag<sup>+</sup>

<sup>b</sup> Could not be determined

seen to evolve at about +0.15 V, prior to further monomer oxidation and polymerization. The increase in current response with each scan indicates that effective electroactive polymer film deposition is occurring.<sup>134</sup>

### 3.2.4 Polymer Cyclic Voltammetry

Films of polymers **4a-d** were washed with electrolyte solution and placed in monomer-free electrolyte solution. Cyclic voltammograms of the polymers were obtained as a function of scan rate between 50 and 350 mVs<sup>-1</sup>. For example, the cyclic voltammograms of PBEDOT-B(OC<sub>12</sub>H<sub>25</sub>)<sub>2</sub> (**4c**), which are representative of **4b-f**, are shown in Figure 3.4. A linear increase in peak current for both the cathodic and anodic redox processes as a function of scan rate is observed and indicates that the film is electrode supported and electroactive.

It is evident that all of these polymers are converted into their doped forms remarkably easily. The half wave potentials ( $E_{1/2,p}$ ) of the polymers are all very low (Table 3.1) as desired for polymers which are highly stable conductors. In fact, these switching potentials are the lowest we have ever observed for a thiophene-based conducting polymer. By comparison, poly[1,4-bis(2-thienyl)-2,5-diheptoxybenzene] exhibits much higher anodic peak potentials at  $E_{a,p} = +0.4$  and  $+0.7$  V.<sup>56</sup> The low oxidation potentials of the EDOT polymers can be attributed to electron donation from the ethylenedioxy

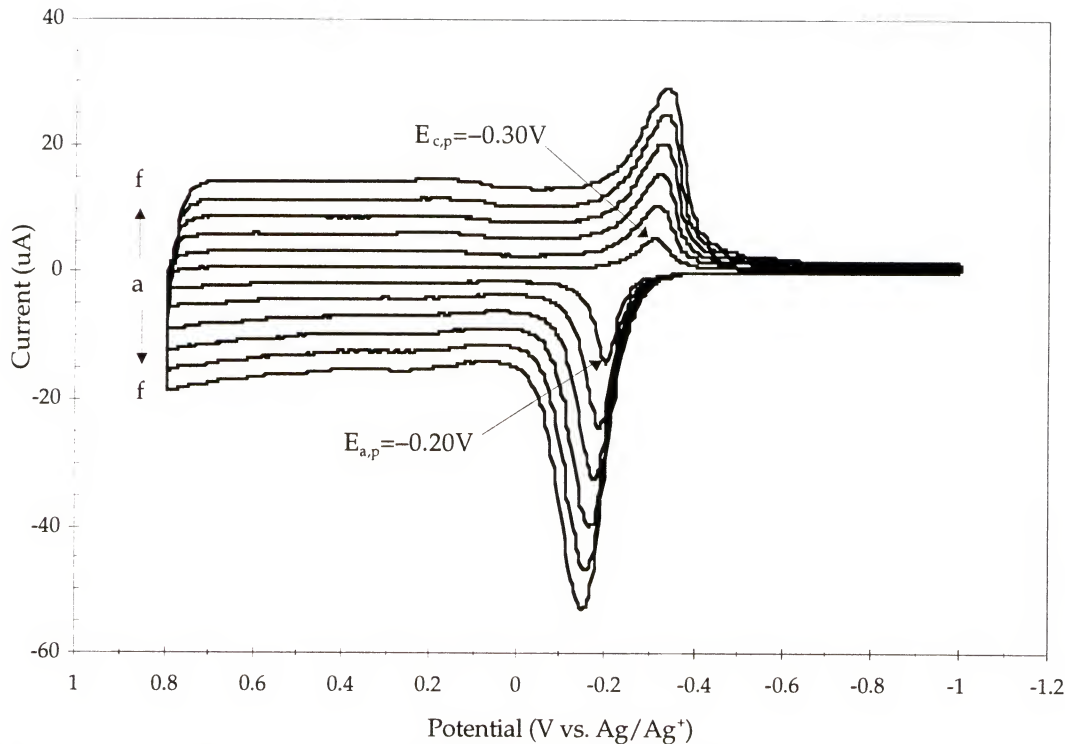


**Figure 3.4:** Cyclic voltammograms of PBEDOT-B(OC<sub>12</sub>H<sub>25</sub>)<sub>2</sub> (**4c**): a) 50, b) 100, c) 150, d) 200, e) 250, and f) 300mVs<sup>-1</sup> in 0.1M TBAP in 2:3 CH<sub>3</sub>CN:CH<sub>2</sub>Cl<sub>2</sub>

substituents along with the low steric requirements of the ethylenedioxy ring appended to the thiophene.

The cyclic voltammograms of PBEDOT-B(OCH<sub>3</sub>)<sub>2</sub> (**4a**) differ somewhat from those of polymers with longer straight chain alkoxy substituents. As shown in Figure 3.5, the redox switching occurs at a slightly higher potential (though still less than 0.0 V) and is significantly broadened; in addition a second oxidative process peaks at about +0.4 V. This cyclic voltammetry is reminiscent of the CV responses for dialkoxy-substituted bis(2-thienyl)benzene polymers, though the redox processes for PBEDOT-B(OCH<sub>3</sub>)<sub>2</sub> occur at lower potentials.<sup>138</sup>

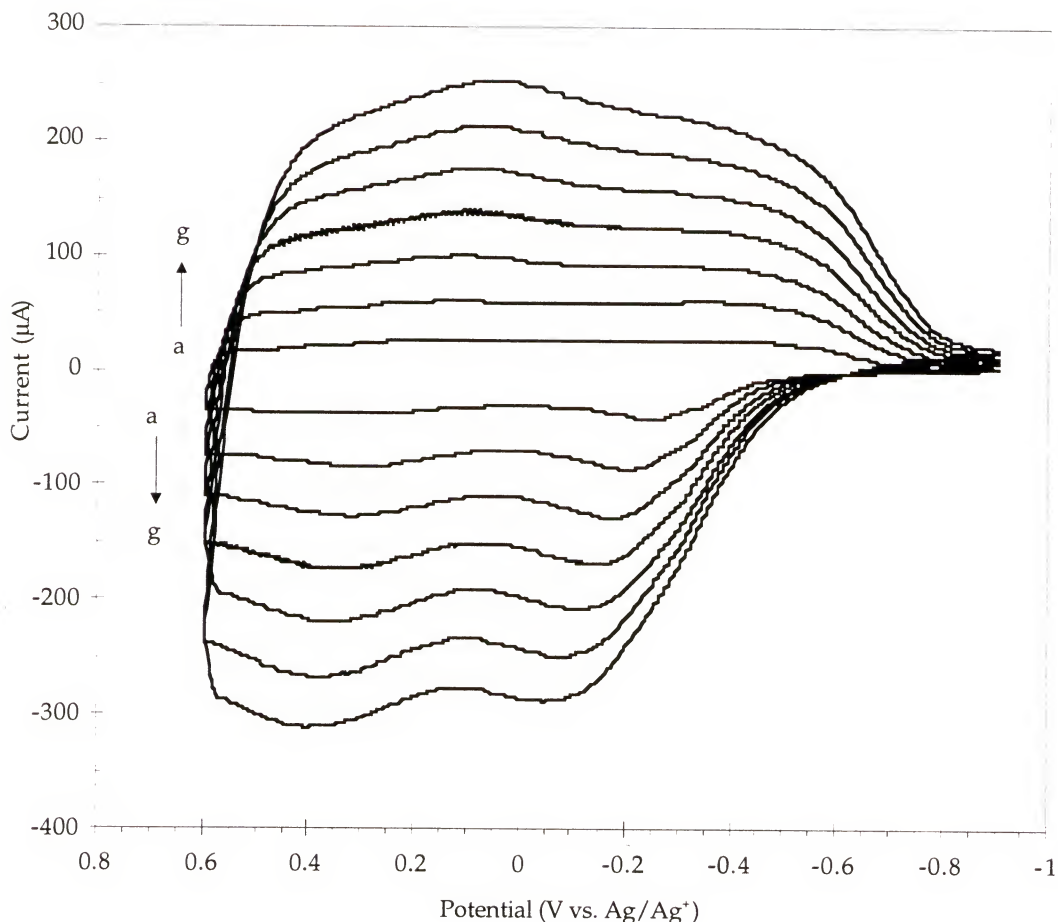


**Figure 3.5:** Cyclic voltammograms of PBEDOT-B(OCH<sub>3</sub>)<sub>2</sub> (**4a**): a) 50, b) 100, c) 150, d) 200, e) 250, f) 300, and g) 350 mVs<sup>-1</sup> in 0.1M TBAP in CH<sub>3</sub>CN

The cyclic voltammetry of the oligomeric ether-substituted polymer PBEDOT-B(OG)<sub>2</sub> (**4f**) in TBAP is also considerably different from that of the other polymers (Figure 3.6). The redox process occurs at a considerably lower potential ( $E_{a,p} = -0.45\text{V}$ ,  $E_{c,p} = -0.55\text{V}$ ,  $E_{1/2,p} = -0.50\text{V}$ ) than for the other polymers. Also, a second, broad redox process occurs almost immediately after the first process; this second process is irreversible and is presumably due to polymer overoxidation and decomposition.

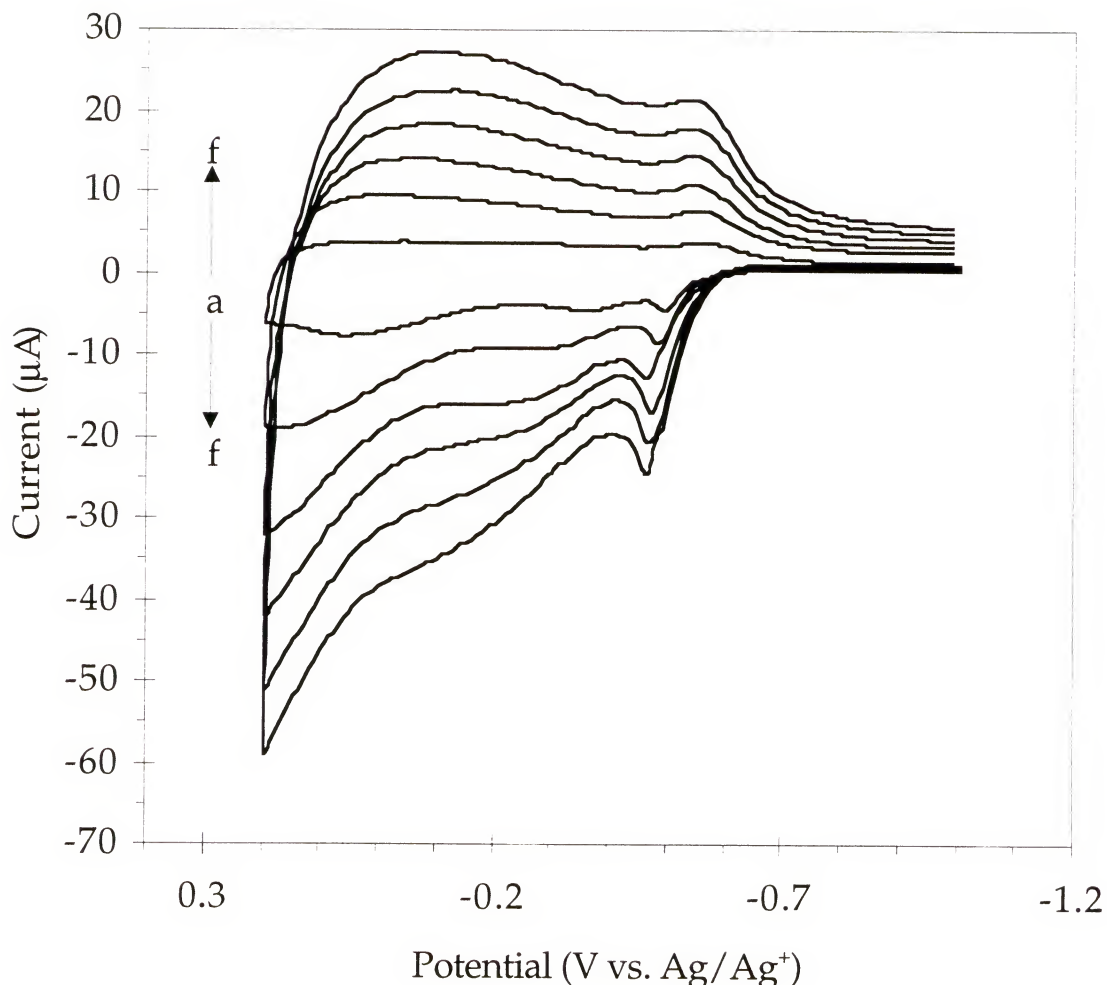


**Figure 3.6:** Cyclic voltammograms of PBEDOT-B(OG)<sub>2</sub> (**4f**): a) 50, b) 100, c) 150, d) 200, e) 250, and f) 300mVs<sup>-1</sup> in 0.1M TBAP in 9:1 CH<sub>3</sub>CN:CH<sub>2</sub>Cl<sub>2</sub>

This interesting electrochemistry in TBAP led to the examination of the electrochemistry of **4f** in different electrolytes. Ion coordination effects have been seen in other conjugated polymers that possess oligomeric- or crown-ether side chains.<sup>139,140,141,142,143</sup> A variety of perchlorates were chosen to study the effect of the cation on PBEDOT-B(OG)<sub>2</sub> electrochemistry. When

the electrolyte was changed to lithium, cesium, barium, or magnesium perchlorate, similar polymer growth was observed by repeated potential scanning electropolymerization, but polymer electrochemistry varied with each electrolyte. The polymer oxidation peak potential varied only slightly in most of the electrolytes (from -0.42V to -0.48V), as seen in Figure 3.7 below. However, when Ba(ClO<sub>4</sub>)<sub>2</sub> was used as the electrolyte, a significant (*ca.* 300mV) anodic shift in the first oxidation peak potential to -0.15V was observed. Other researchers<sup>144</sup> have recently noted a significant anodic shift in oxidation potential of oligomeric-and crown ether-functionalized polythiophenes in the presence of Ba<sup>2+</sup>. The authors attribute the strong shift (130 to 300mV, depending on the polymer structure studied) to electrostatic interactions between the complexed cation and the redox center.

The electrochemistry of PBEDOT-B(OG)<sub>2</sub> in most of the electrolytes exhibits a second, broad, irreversible oxidation below 0.0V similar to that visible in TBAP (Figure 3.6). However, when the polymer is switched in Mg(ClO<sub>4</sub>)<sub>2</sub>, a fairly broad window of stability in the oxidized state is observed similar to those found in polymers **4b-e**, which were all cycled in TBAP (Figure 3.8).

The strong electrolyte dependence of the electrochemistry of conducting polymers possessing oligomeric ether substituents is a complex issue that is not fully understood. The ability of oligomeric and crown ethers to coordinate to cations has lead to applications in catalysis; current research in conducting polymers containing oligomeric and crown ethers seeks to use

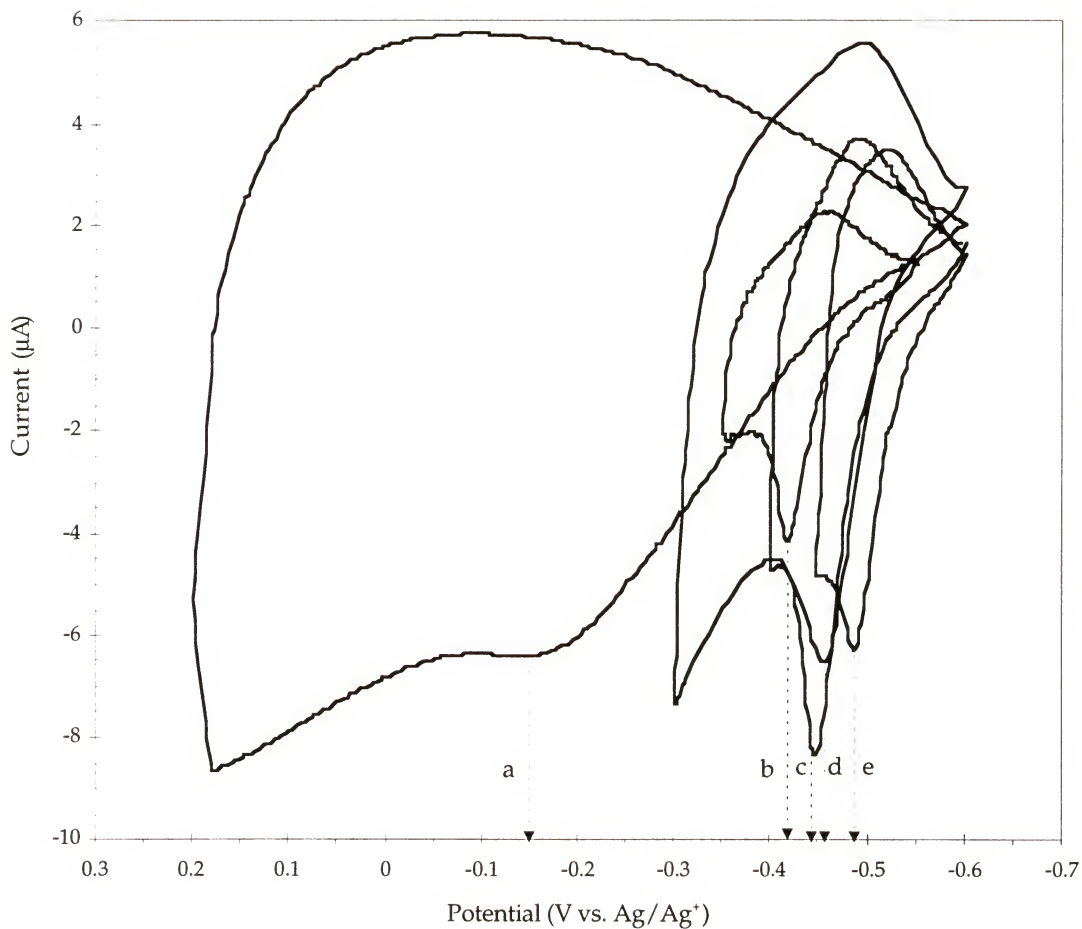


**Figure 3.7:** Electrolyte dependence of PBEDOT-B(OG)<sub>2</sub> (**4f**) cyclic voltammetry: a) Ba(ClO<sub>4</sub>)<sub>2</sub>, b) Mg(ClO<sub>4</sub>)<sub>2</sub>, c) LiClO<sub>4</sub>, d) Bu<sub>4</sub>NClO<sub>4</sub> and e) CsClO<sub>4</sub> (all at 50mVs<sup>-1</sup>, 0.1M electrolyte in CH<sub>3</sub>CN)

the ion sensitivity of these substituents to yield reliable molecular recognition materials.<sup>21,139,144</sup> Efforts continue in the Reynolds research group to understand ion effects in electroactive polymers possessing oligomeric ether side chains (including PBEDOT-B(OG)<sub>2</sub>).

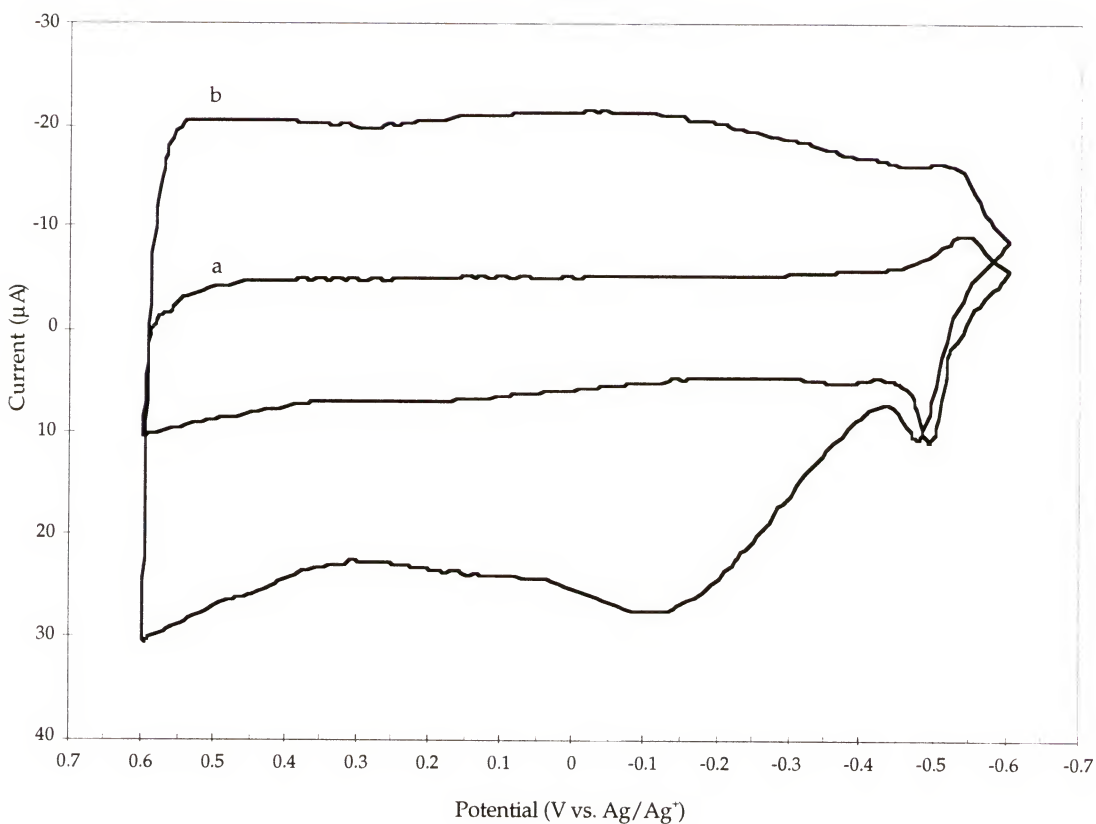


**Figure 3.8:** Cyclic voltammetry of PBEDOT-B(OG)<sub>2</sub> (**4f**) to higher potentials:  
a) in Bu<sub>4</sub>NClO<sub>4</sub> b) in Mg(ClO<sub>4</sub>)<sub>2</sub> (both at 100mVs<sup>-1</sup>, 0.1M electrolyte in CH<sub>3</sub>CN)

### 3.2.5 Electrochemical Stability of Polymers

The low monomer and polymer oxidation potentials lead to fewer side reactions during polymerization and switching; thus more stable polymers are obtained. A relative measure of polymer stability was obtained by monitoring the loss in electroactivity, indicated by a decreased current response with repeated redox cycling.

PBEDOT-B(OC<sub>12</sub>H<sub>25</sub>)<sub>2</sub> (**4c**) was cycled repeatedly between -0.5 and 0.0V in monomer-free electrolyte solution. The loss in electroactivity was found

to be a function of the solvent chosen for switching. When the solvent system was the same as that used for polymer growth (a 60:40 mixture of  $\text{CH}_2\text{Cl}_2:\text{CH}_3\text{CN}$  with 0.1M TBAP), very little loss in current response was observed with repeated scanning; after 3,100 scans, only 27% loss in electroactivity was observed (Figure 3.9).

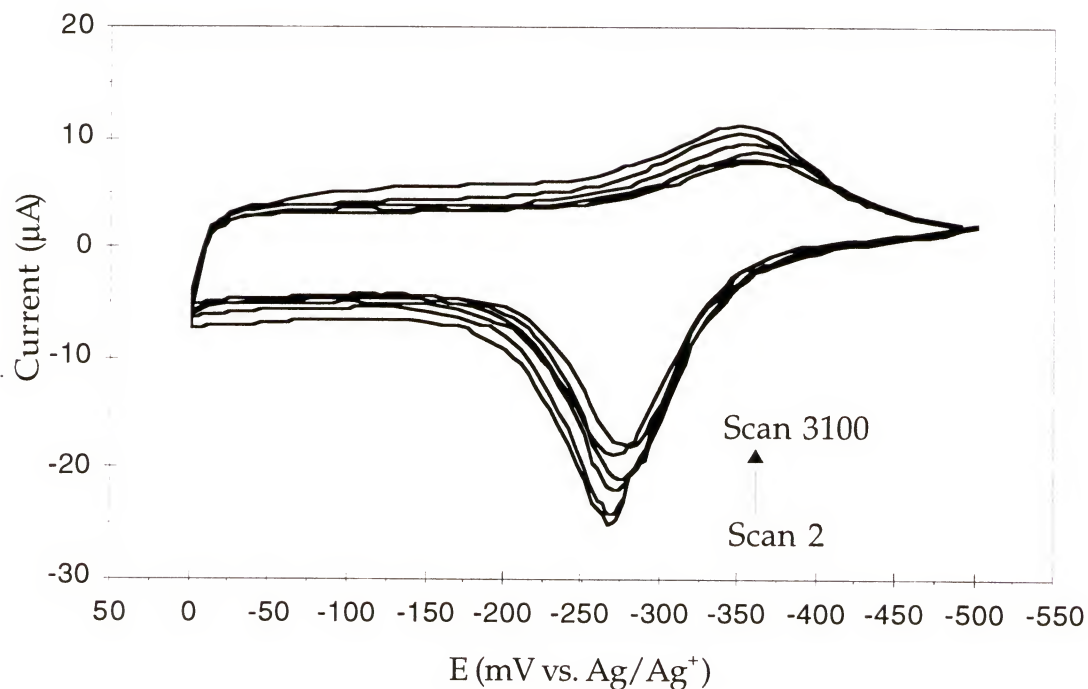


**Figure 3.9:** Cyclic voltammograms of PBEDOT-B( $\text{OC}_{12}\text{H}_{25}\right)_2$  (**4c**) in 2:3  $\text{CH}_3\text{CN}:\text{CH}_2\text{Cl}_2$  (scans 2, 100, 500, 1000, 1900, and 3100 at  $100\text{mVs}^{-1}$  in 0.1M TBAP)

When PBEDOT-B( $\text{OC}_{12}\text{H}_{25}\right)_2$  (**4c**) was switched in 0.1M TBAP/ $\text{CH}_3\text{CN}$ , the same electroactivity loss occurred in only 50 scans (Figure 3.10). This disparity, which has been observed previously for polypyrroles,<sup>145</sup> has been

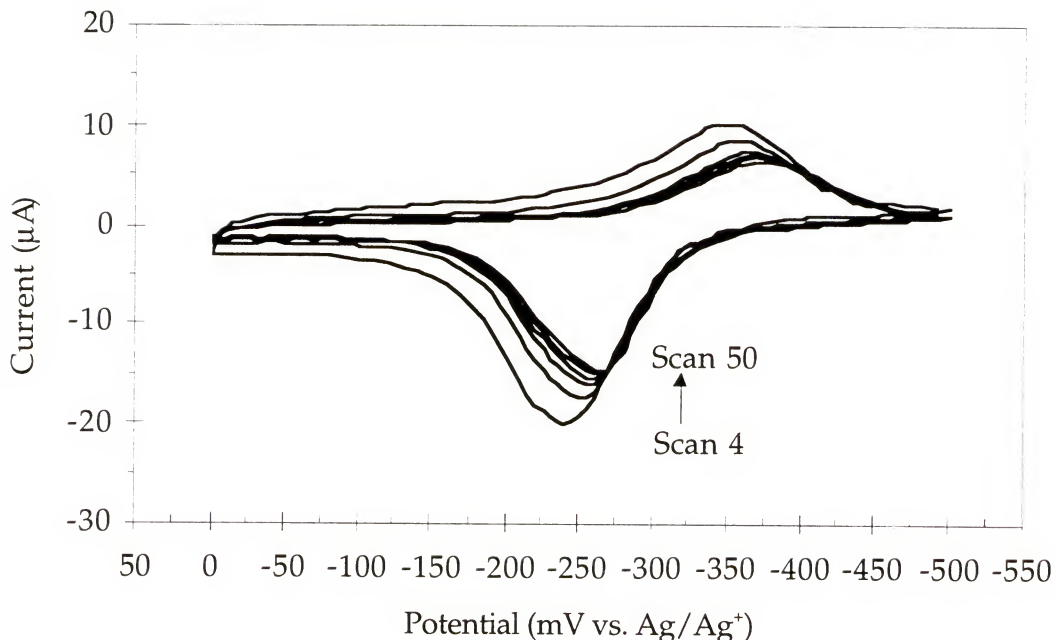


**Figure 3.10:** Cyclic voltammograms of PBEDOT-B(OC<sub>12</sub>H<sub>25</sub>)<sub>2</sub> (**4c**) in CH<sub>3</sub>CN (scans 4, 10, 20, 30, 40, and 50 at 100mVs<sup>-1</sup> in 0.1M TBAP)

attributed to a solvent memory effect in the polymer. These polymers are swollen to some extent by solvent during film growth and switching. Subsequent exposure to a poorer solvent system during switching leads to film collapse (and ultimately delamination from the electrode) and a reduction in electroactivity.

Of special interest in considering these polymers for electrode applications (see Section 3.4) is the flat current response visible in Figure 3.4 which extends to well beyond +0.7 V. This indicates that polymers **4b-d** are stable over a broad potential window where they can be used as conductors. To determine the useful potential window for PBEDOT-B(OC<sub>12</sub>H<sub>25</sub>)<sub>2</sub> (**4c**), films were cycled to sequentially higher potentials while monitoring the current

response in monomer-free 0.1M TBAP/CH<sub>3</sub>CN. As can be seen in Figure 3.11, the flat anodic response extends to *ca.* 1.0V. A second oxidation process, attributed to polymer overoxidation, begins above 1.0V. As the second process occurs, the current response for the low potential reversible redox process decreases. After scanning to +1.4V, greater than 70% loss in the current response of the polymer oxidation peak at -0.20V is observed.

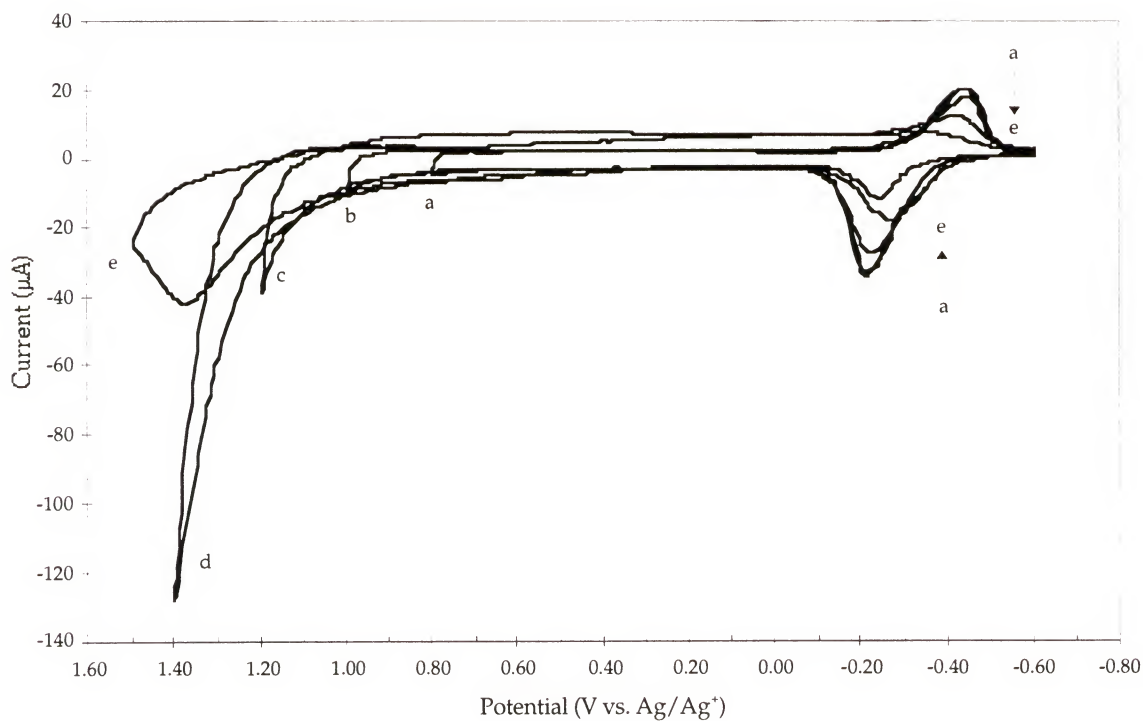


**Figure 3.11:** Cyclic voltammograms of PBEDOT-B(OC<sub>12</sub>H<sub>25</sub>)<sub>2</sub> (**4c**) to subsequently higher switching potentials: a) 0.8, b) 1.0, c) 1.2, d) 1.4, and e) 1.5V (carried out in 0.1M TBAP in CH<sub>3</sub>CN at 100mVs<sup>-1</sup>)

### 3.3 In-Situ Optoelectrochemistry

#### 3.3.1 Background

As mentioned in Chapter 1, changes in charge state of conducting polymers during oxidation and reduction are accompanied by significant changes in the optical spectrum of the polymer. For this reason, many conducting polymers are said to be electrochromic, that is, they change color when subjected to an applied potential. This has led to much research in conducting polymers for use as electrochromic materials, with potential applications in the areas of display technologies and smart windows.

The reason for the change in the optical spectra of the polymers can be more clearly understood with an examination of the change in polymer band structure upon redox doping (Figure 3.12). In the neutral state, electrons can be excited from the valence band to the conduction band (Figure 3.12a); the energy of this transition is the polymer bandgap,  $E_g$ , which is typically determined from the onset of absorption in the reduced polymer. With the first oxidation, one electron is removed from the polymer, leaving an unpaired electron (polaron) which will have a higher energy than any of the degenerate electrons in the valence band, thus yielding two intraband levels (Figure 3.12b). Since the intraband levels are taken from the edges of the bands, the band gap increases. As the polymer is oxidized further, the unpaired electron is removed (Figure 3.12c), yielding a dicationic polymer

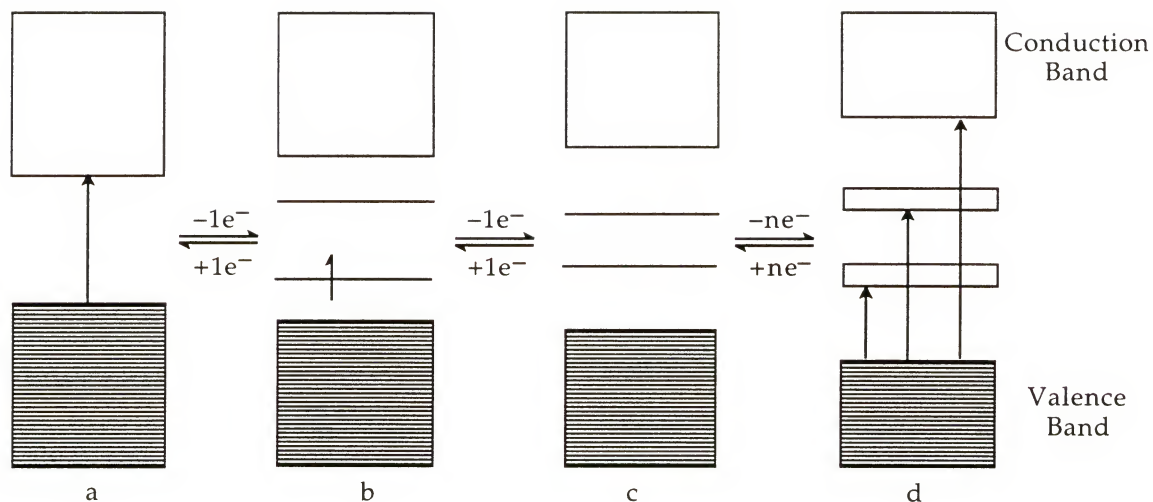


**Figure 3.12:** Electronic transitions available to a conducting polymer: a) neutral polymer b) polaronic polymer c) bipolaronic polymer d) highly oxidized polymer with bipolaronic bands

(bipolaron); further oxidation yields broadened intraband transitions (Figure 3.12d).

The optical transitions in an electroactive polymer can be observed in the UV-Vis-nIR spectrum. When this spectrum is studied as a function of oxidation state of the polymer (i.e. as a function of applied potential), it is possible to see the evolution of bipolaronic bands. This technique, commonly known as optoelectrochemistry or spectroelectrochemistry, is easily accomplished by the construction of an electrochemical cell in the spectrophotometer.

### 3.3.2 Techniques

For optoelectrochemistry, polymers are typically prepared electrochemically using a standard three-electrode cell with slight modifications. The typical platinum button working electrode is replaced with conductive glass, i.e. glass that has been coated with a conductive substrate, typically indium tin oxide (ITO). A polymer film is deposited on the electrode using either repeated potential scanning electropolymerization or constant potential electropolymerization. While either method produces the same polymer, deposition at a constant potential is used more frequently, since the polymer remains in its oxidized form during the entire polymerization, limiting loss of polymer due to solubility in the reduced state or due to changes in morphology causing the polymer to fall away from the electrode.

Once the polymer is deposited on the ITO-coated glass, the electrode is transferred to a quartz cuvette. A three-electrode cell is established; a standard  $\text{Ag}/\text{Ag}^+$  reference electrode can be used, making sure to keep the electrode out of the path of the spectrophotometer beam. For a counter electrode, a clean, large platinum plate is used in standard electrochemistry. To allow the spectrophotometer beam to pass through the cell, either a hole can be cut in the center of the platinum plate or a second ITO-coated glass slide can be used as the counter electrode. When an ITO-coated glass slide is used as a counter electrode, the reference cell for the spectrophotometer is filled with two ITO-coated glass slides and monomer-free electrolyte solution.

Once the optoelectrochemistry cell is filled with monomer-free electrolyte solution (typically 0.1M TBAP in acetonitrile), the polymer can be oxidized in a stepwise fashion, and its UV-Vis-nIR spectrum can be obtained at each potential step. During this stepwise oxidation, the polymers studied here switch from a red reduced state to a deep blue oxidized state.

Spectra were obtained using a Varian Cary 5E ultraviolet-visible-near infrared (UV-Vis-nIR) spectrophotometer in the range of 0.5 to 4.0eV. Polymers were prepared by electrochemical polymerization at a constant potential approximately 0.1V above the onset of monomer oxidation potentials listed in section 3.2. Polymer growth and electrochemistry were controlled using the EG&G Princeton Applied Research model 273 potentiostat/galvanostat as described in section 3.2. Cell designs discussed above were used.

### 3.3.3 Optoelectrochemistry for polymers **4a-f**

Solid state spectra. A series of optoelectrochemical spectra for PBEDOT-B(OC<sub>7</sub>H<sub>15</sub>)<sub>2</sub> (**4b**) is shown in Figure 3.13. At low potential (-0.4 V) the polymer is in its reduced (insulating) form, and the electronic bandgap ( $E_g$ , Table 3.2) can be determined from the onset of the  $\pi$  to  $\pi^*$  transition. In this state,

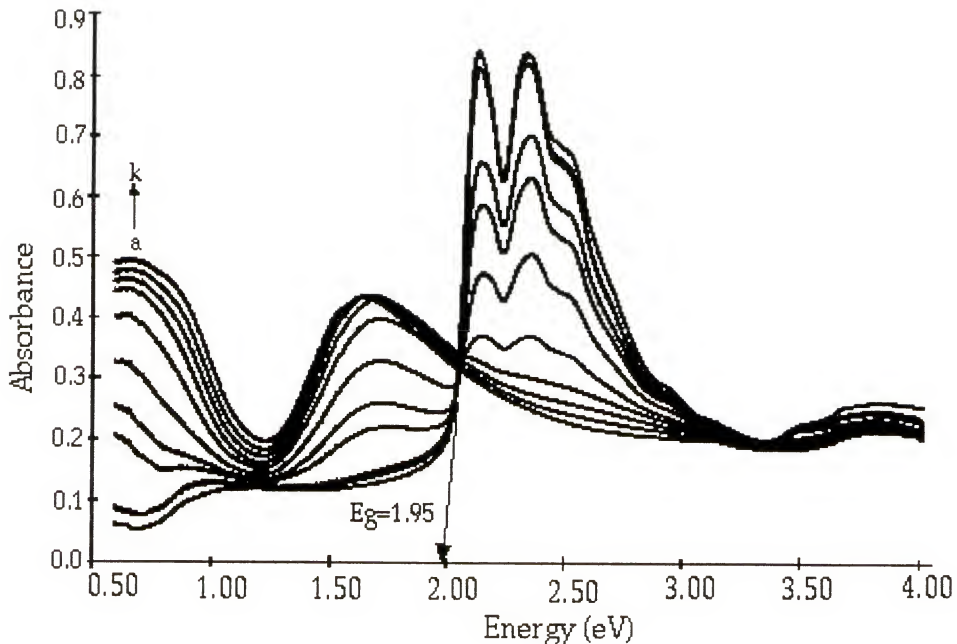


**Figure 3.13:** Optoelectrochemical analysis of PBEDOT-B(OC<sub>7</sub>H<sub>15</sub>)<sub>2</sub> (**4b**): UV-Vis-nIR spectra taken at potentials of a) -0.40, b) -0.30, c) -0.20, d) -0.10, e) -0.08, f) -0.04, g) 0.0, h) 0.10, i) 0.20, j) 0.30, and k) 0.40V vs. Ag/Ag<sup>+</sup>.

the only significant absorption is due to the excitation of electrons from the valence band to the conduction band. The onset of the transition occurs at 1.95 eV for **4b**, with peaks at 2.10 eV and 2.35 eV and a shoulder at 2.45 eV. The splitting of the  $\pi$  to  $\pi^*$  absorption is a solid state effect commonly attributed to vibronic coupling of the  $\pi$  electrons of the polymer backbone.<sup>119</sup> In this instance, the splitting is 1600cm<sup>-1</sup> and can be attributed to coupling of the lattice to the thiophene C=C vibrational mode. Interestingly, the strong coupling is observed only in the polymers (**4b-f**) with longer alkoxy substituents and becomes more pronounced as the chain length is increased; coupling in the dimethoxy polymer is much less intense (Figure 3.14), yet the polymer has a similar band gap. As the potential is increased, the polymer

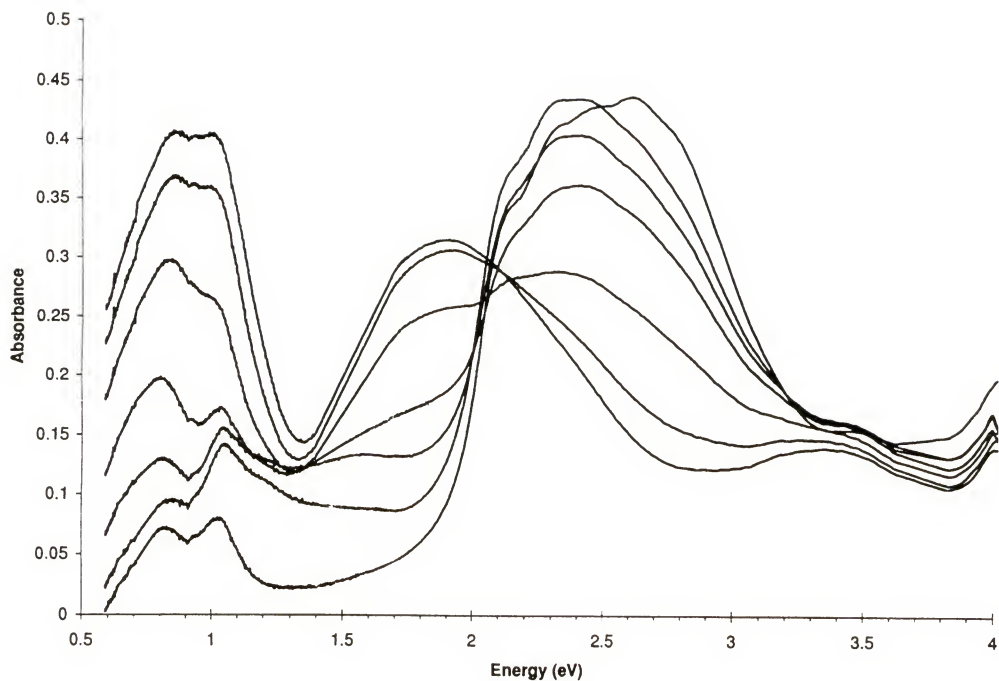


**Figure 3.14:** Optoelectrochemical analysis of PBEDOT-B(OCH<sub>3</sub>)<sub>2</sub> (**4a**): -0.50, -0.3, -0.2, -0.1, 0.0, 0.2, and 0.4V

oxidatively dopes. The interband transition decreases in intensity, and two absorbances evolve at lower energies due to formation of bipolaronic species.<sup>138</sup> This behavior is consistent with the many thiophene based conducting polymers that have been studied to date.

The optoelectrochemistry of PBEDOT-B(OG)<sub>2</sub> (**4f**) (Figure 3.15) differs from that of **4a-e**. While polymers **4b-e** exhibit well-defined vibronic coupling in the reduced state, the peaks disappear as the polymers are oxidized. In the case of the glyme-substituted polymer, two absorptions are present in the reduced state, each split by vibronic coupling; only one of the

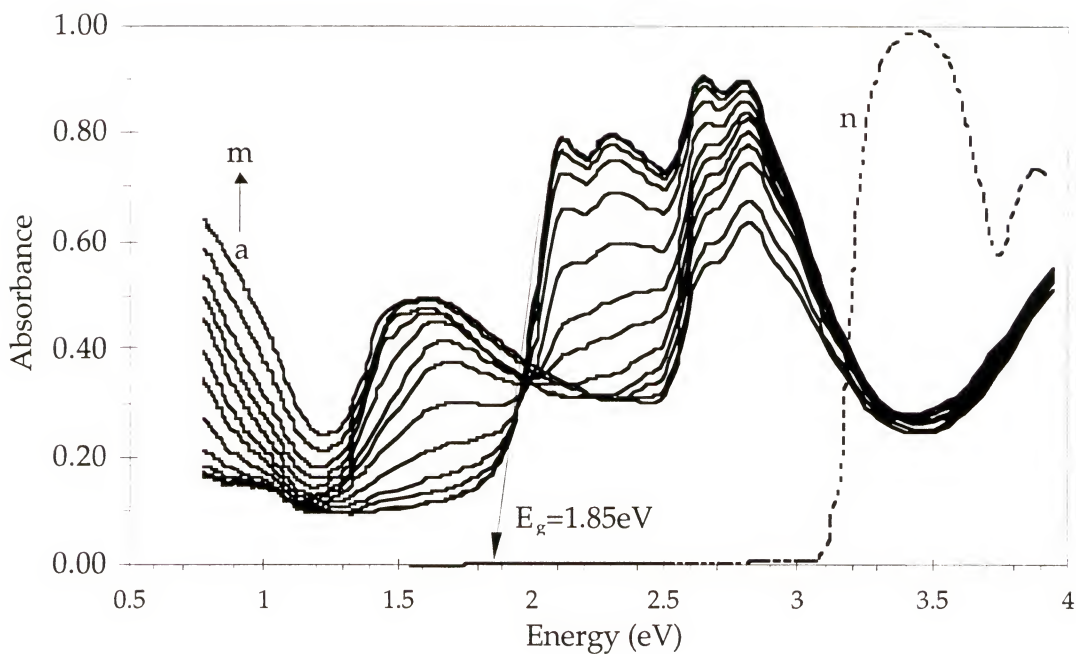


**Figure 3.15:** Optoelectrochemical analysis of BEDOT-B(OG)<sub>2</sub> (**4f**): UV-Vis-nIR spectra taken at potentials of a) -0.40, b) -0.20, c) -0.15, d) -0.10, e) -0.05, f) 0.00, g) 0.05, h) 0.10, i) 0.20, j) 0.30, k) 0.40, l) 0.50 and m) 0.60V vs. Ag/Ag<sup>+</sup>. The solution spectrum (n) of monomer **3f** is shown for comparison.

peaks disappears as the polymer is oxidized. That absorption has an onset of 1.85eV, which is consistent with  $E_g$  values of the other polymers studied here.

The second absorption onset in the spectrum of the reduced polymer occurs at approximately 2.4eV, intermediate to the lower energy peak believed to be due to the polymer and the high-energy (onset *ca.* 3.1eV) peak of the monomer (shown for comparison in Figure 3.15). This second absorption may correspond to dimer, which was trapped in the film and therefore not removed by rinsing with monomer-free electrolyte solution; changes in film morphology during the optoelectrochemistry experiment would then release the dimer. In fact, examination of the electrolyte solution in the cell after the

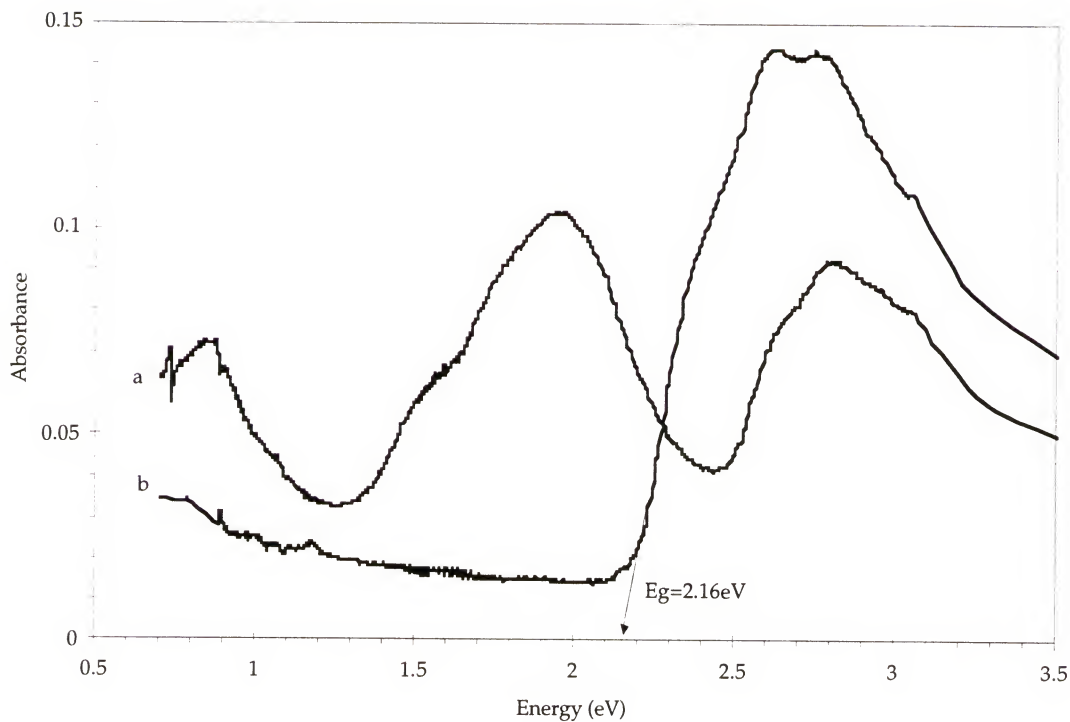
experiment reveals that the solution is typically a vivid green color. The UV-Vis-nIR spectrum of this solution reveals a single absorption with an onset at *ca.* 2.4eV. The slight decrease in intensity of the higher energy absorption as oxidation potential is increased may be due to polymerization.

As conjugation length is increased from monomer to polymer, resonance stabilization makes it easier to excite an electron from the HOMO to the LUMO, so the  $\pi$  to  $\pi^*$  transition occurs at lower energy. Thus, the  $\lambda_{\max}$  in glyme monomer **3f** (monomers **3a-f** all have  $\lambda_{\max} \approx 3.4\text{eV}$ ) is considerably higher than the 2.2eV  $\lambda_{\max}$  of the glyme polymer **4f** (Figure 3.15), and dimer absorption would be expected to occur at intermediate energy. As will be discussed in Chapter 4, the absorption spectrum of a trimer derived from BEDOT-B(OC<sub>16</sub>H<sub>33</sub>)<sub>2</sub> (**3d**) is identical to the spectrum of a much higher molecular weight PBEDOT-B(OC<sub>16</sub>H<sub>33</sub>)<sub>2</sub>. It appears that maximum resonance stabilization is reached within three repeat units (9 rings), with intermediate stabilization occurring in the dimer (6 rings).

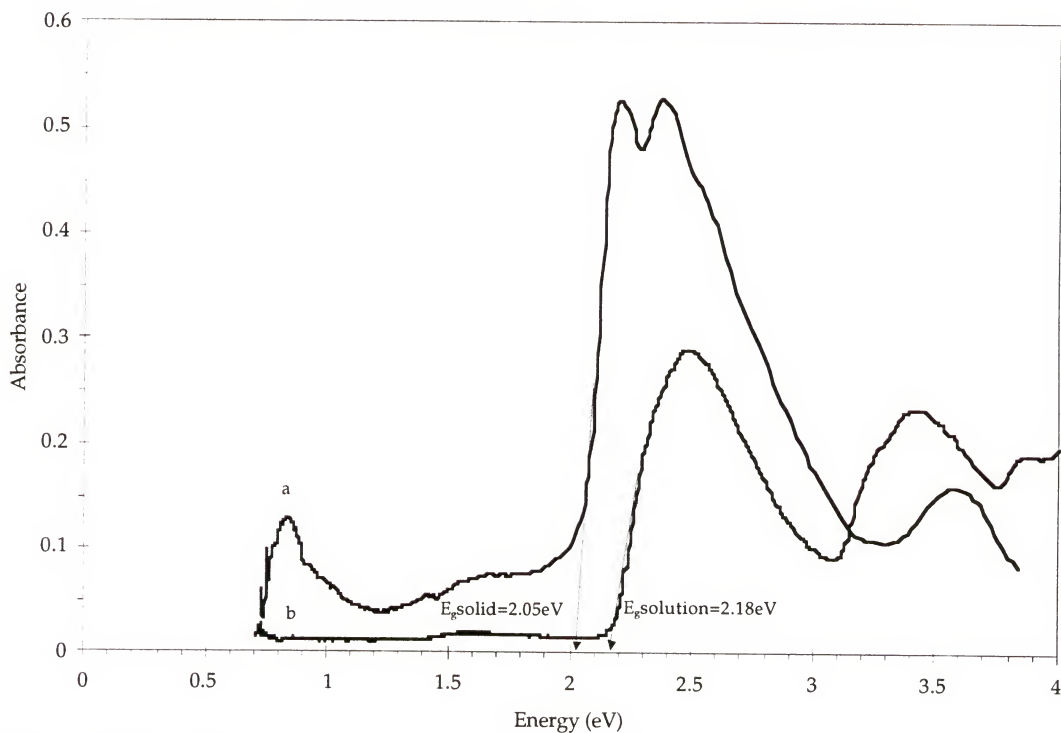
Solution spectra Significant changes between solution and solid state spectra have been reported in the literature.<sup>119,146,147,148</sup> The  $\pi$  to  $\pi^*$  transitions of solid state spectra are typically shifted to higher energy when compared to their solution spectra; this has been attributed to an intrachain coil-to-rod conformational change going from solution to the solid state, resulting in extended delocalization and a shift to lower energy.<sup>148</sup>

To investigate the solution spectra of CHCl<sub>3</sub>-soluble polymers **4d-f**, films of **4d-f** were prepared by electrochemical polymerization of **3d-f** onto ITO glass electrodes using the standard polymerization conditions described earlier. The reduced films were rinsed with acetonitrile to remove the monomer/electrolyte solution. The films were then dissolved in CHCl<sub>3</sub> to give light brown solutions, the UV-Vis-nIR spectra of which were then examined. The polymers appeared slightly oxidized, as evidenced in the case of PBEDOT-B(OG)<sub>2</sub> (**4f**, Figure 3.16) by the appearance of two small broad absorptions with  $\lambda_{\text{max}}$  values of 0.85 and 1.95eV. Addition of 1d. hydrazine monohydrate caused the solutions to become bright pink, and the spectra of the solutions (as shown for PBEDOT-B(OG)<sub>2</sub> in Figure 3.16) revealed that the two peaks attributed to oxidized polymer were gone.

The spectra of the polymers in solution differ considerably from those of the polymer films. The vibronic coupling apparent in the spectra of the films (see Figures 3.13 and 3.15) is instead a broad absorption in solution, and the onset of the  $\pi$  to  $\pi^*$  transition is increased from 1.85eV to 2.16eV in the case of polymer **4f**. Similarly, comparison of the solid state spectrum of PBEDOT-B(OEtHex)<sub>2</sub> (**4e**) to its solution spectrum (Figure 3.17) reveals that the vibronic coupling is gone and that the onset of the  $\pi$  to  $\pi^*$  transition is shifted from 2.05eV to 2.18eV; the same occurs with polymer **4d**, with the bandgap shifting from 2.0 to 2.4eV in solution.



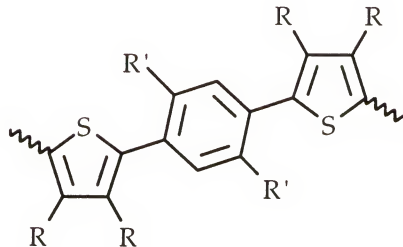
**Figure 3.16:** Solution UV-Vis-nIR spectra of PBEDOT-B(OG)<sub>2</sub> (**4f**) in CHCl<sub>3</sub>: before (a) and after (b) addition of hydrazine



**Figure 3.17:** Solid state (a) vs. solution (b) UV-Vis-nIR spectra of PBEDOT-B(OEtHex)<sub>2</sub> (**4e**)

Effect of structural changes on bandgap. With the availability of the PBEDOT-B(OR)<sub>2</sub> (**4a-f**) series of polymers, it is now possible to determine the steric and electronic effects of substituent groups on the electronic properties. Table 3.2 compares E<sub>g</sub> values for the polymers described here with a series of related polymers. For poly[1,4-bis(2-thienyl)benzene], (PBTB) a bandgap of 2.2 eV has been previously reported,<sup>54</sup> which is intermediate to the bandgaps of polythiophene and poly(*p*-phenylene).<sup>90</sup> Derivatization with methyl substituents in the 2- and 5-positions of the phenyl ring increases the bandgap to 2.7 eV.<sup>54</sup> This can be attributed to steric effects; the methyl substituents decrease interaction between adjacent rings, decreasing the extent of conjugation.

When methoxy substituents are used instead of methyl substituents, the bandgap is identical to that of the unsubstituted polymer, 2.2 eV;<sup>54</sup> presumably, the steric effect of ring substitution is counteracted by electron donation from the ether groups. The addition of the ethylenedioxy bridge to the thiophenes in poly{1,4-bis[2-(3,4-ethylenedioxy)thienyl]benzene} (PBEDOT-B) to give four electron donating substituents per monomer repeat unit significantly decreases the bandgap to 1.8 eV.<sup>149</sup> As with the analogous thiophene polymers, addition of methoxy groups to the internal phenylene ring does not have a net effect on the bandgap. This can be attributed to interplay of steric and electronic effects; the additional electron density imparted by the alkoxy substituents, which should lower the bandgap slightly, is counteracted by the increased steric repulsion. Increasing the alkoxy

**Table 3.2:** Comparative solid state bandgaps

Compound	R	R'	$E_g$ (eV)	Reference
polythiophene			2.0	<sup>89</sup>
poly- <i>p</i> -phenylene			3.0	<sup>90</sup>
polyEDOT			1.6	<sup>67</sup>
PBTB-(Me) <sub>2</sub> <sup>a</sup>	H <sub>2</sub>	CH <sub>3</sub>	2.6	<sup>54</sup>
PBTB <sup>b</sup>	H	H	2.3	<sup>54</sup>
PBTB-(OMe) <sub>2</sub> <sup>c</sup>	H	OCH <sub>3</sub>	2.2	<sup>54</sup>
PBEDOT-B <sup>d</sup>	OCH <sub>2</sub> CH <sub>2</sub> O	H	1.8	<sup>149</sup>
<b>4a</b>	OCH <sub>2</sub> CH <sub>2</sub> O	OCH <sub>3</sub>	1.8	this work
<b>4b</b>	OCH <sub>2</sub> CH <sub>2</sub> O	OC <sub>7</sub> H <sub>15</sub>	1.9	this work
<b>4c</b>	OCH <sub>2</sub> CH <sub>2</sub> O	OC <sub>12</sub> H <sub>25</sub>	2.0	this work
<b>4d</b>	OCH <sub>2</sub> CH <sub>2</sub> O	OC <sub>16</sub> H <sub>33</sub>	2.0	this work
<b>4e</b>	OCH <sub>2</sub> CH <sub>2</sub> O	2-ethylhexyloxy	2.1	this work
<b>4f</b>	OCH <sub>2</sub> CH <sub>2</sub> O	OC <sub>2</sub> H <sub>4</sub> OC <sub>2</sub> H <sub>4</sub> OC <sub>2</sub> H <sub>5</sub>	1.8	this work

<sup>a</sup> PBTB-(Me)<sub>2</sub> = poly[1,4-bis(2-thienyl)-2,5-dimethylbenzene]

<sup>b</sup> PBTB = poly[1,4-bis(2-thienyl)benzene]

<sup>c</sup> PBTB-(OMe)<sub>2</sub> = poly[1,4-bis(2-thienyl)-2,5-dimethoxybenzene]

<sup>d</sup> PBEDOT-B = poly{1,4-bis[2-(3,4-ethylenedioxy)thienyl]benzene}

substituent length or adding branching to the alkoxy substituent further increases the steric interactions while maintaining the same degree of electron donation from the alkoxy substituents, and the bandgaps increase slightly (to *ca.* 1.9, 2.0, 2.0, and 2.1 eV for heptoxy, dodecyloxy, hexadecyloxy, and 2-ethylhexyloxy polymers, respectively).

Since all of the polymers exhibit oxidation potentials below 0V, the polymers should be more stable in their oxidized states than in their reduced

states. This is indeed the case with the majority of the PBEDOT-B(OR)<sub>2</sub> films prepared for optoelectrochemistry are typically stored in their oxidized state in 0.1M TBAP/acetonitrile and remain electroactive months later. Films that are stored in their reduced form typically oxidize slowly over time, changing to blue films after only a few days in electrolyte solution. The exception to this is PBEDOT-B(OEtHex)<sub>2</sub> (**4e**), which spontaneously reduces in electrolyte solution within one minute after the applied potential is removed; the polymer returns to its oxidized state upon further electrochemical oxidation. While similar to the other PBEDOT-B(OR)<sub>2</sub> in other ways, PBEDOT-B(OEtHex)<sub>2</sub> has a somewhat higher oxidation potential ( $E_{a,p} = +0.01V$ ) than the other polymers ( $E_{a,p} ca. -0.25V$ ). Presumably, this higher oxidation potential is due to steric effects. Branched substituents have been shown to have significant effects on the properties of polythiophenes,<sup>150</sup> and it seems likely that a similar, though less pronounced, effect might be seen in the PBEDOT-B(OR)<sub>2</sub> polymers. The 2-ethylhexyl group is flexible enough to rotate out of plane as a potential is applied, allowing adjacent rings to become coplanar with a low barrier to planarity. However, when the potential is removed, the side chains may relax back to a position that causes steric repulsion with adjacent rings, resulting in reduction of the polymer to its less planar state.

### 3.4 Polymer Modified Electrodes

The low potential redox process visible in the cyclic voltammograms of polymers **4a-e** (Figure 3.4) is unaccompanied by any other electrochemistry until overoxidation at *ca.* 1.0V vs. Ag/Ag<sup>+</sup> (Figure 3.11). Additionally, these polymers are stable to redox switching over thousands of cycles (section 3.2.5). This leaves a very broad (>1V) potential window where these polymers are stable conductors, making possible the use of these materials in applications involving repeated redox switching, such as polymer modified electrodes.

Polymer films are adhered to electrode surfaces to modify electrode properties for a variety of applications. Modified electrodes are currently being examined for use in such technologies as energy storage, microelectrochemical devices, electrochromic displays, electrocatalysis, and electroanalysis.<sup>151,152,153,154</sup>

To demonstrate the feasibility of using these polymers as polymer modified electrodes, ferrocene was switched on an electrochemically deposited film of PBEDOT-B(OC<sub>12</sub>H<sub>25</sub>)<sub>2</sub> (**4c**). In order to accomplish this, monomer **3c** was electrochemically polymerized as described in section 3.2.3. The polymer modified platinum button electrode was removed from the monomer/electrolyte solution and rinsed free of monomer, then placed in electrolyte solution to determine the polymer electrochemistry (Figure 3.18a).

The polymer modified electrode was then placed in a 0.01M ferrocene/0.1M electrolyte solution, and the ferrocene redox process was

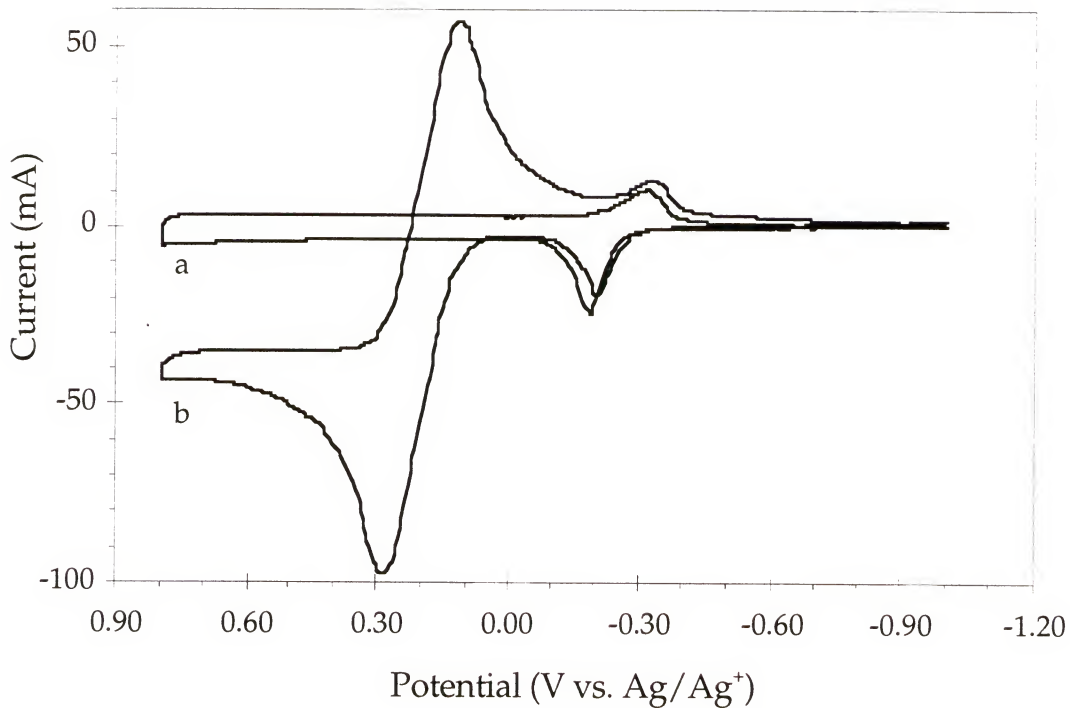


**Figure 3.18:** Ferrocene switching on a platinum button electrode on which PBEDOT-B(OC<sub>12</sub>H<sub>25</sub>)<sub>2</sub> (**4c**) has been deposited: a) polymer **4c** before addition of ferrocene b) ferrocene switching on the electrode modified with polymer **4c** (0.1M TBAP, 3:2 CH<sub>2</sub>Cl<sub>2</sub>:CH<sub>3</sub>CN during polymer growth and polymer and ferrocene switching, 100mVs<sup>-1</sup>)

probed at the electrode (Figure 3.18b). The potential was cycled from -1.0V to +0.6V, a potential window in which both polymer and ferrocene electrochemistry occur. The ferrocene redox process exhibited an  $E_{1/2}$  of +0.20V, the same as on the surface of the Pt button electrode without the polymer.

The effect of scan rate on current response of the ferrocene redox process was examined; both the cathodic and anodic processes exhibited a

direct dependence on the square root of the scan rate, indicating that the ferrocene redox process is diffusion controlled, i.e. that the ferrocene diffuses from solution to the electrode for oxidation to occur, and then diffuses away from the electrode and into solution upon reduction. For the same cyclic voltammograms, the polymer redox process was found to exhibit a linear dependence on the scan rate. This is important in that it indicates that, while the polymer redox process was not diffusion controlled, and that the polymer was adhered to the electrode, the electroactive ferrocene probe remained in solution and was not concentrated or partitioned into the organic polymer.

This was further confirmed by studying the effect of ferrocene concentration on current response at a bare platinum button electrode and at a polymer-modified electrode. A greater than linear correlation between increased ferrocene concentration and increased current response at the polymer modified electrode would be indicative of adsorption of ferrocinium onto/into the polymer film, accelerating the redox process. Ferrocene concentrations of 0.1, 0.5, 1.0, 5.0, and 10mM in 0.1M TBAP were investigated. In all cases, a linear increase in current response occurred with increasing concentration, both at the platinum button electrode and at the polymer modified electrode (Figure 3.19). Additionally, no significant shift in the  $E_{1/2}$  of ferrocene was observed when comparing the redox process at the platinum button electrode and at the polymer modified electrode. Therefore the polymer modified electrode has neither an electrocatalytic effect nor a passivation effect on the redox process.

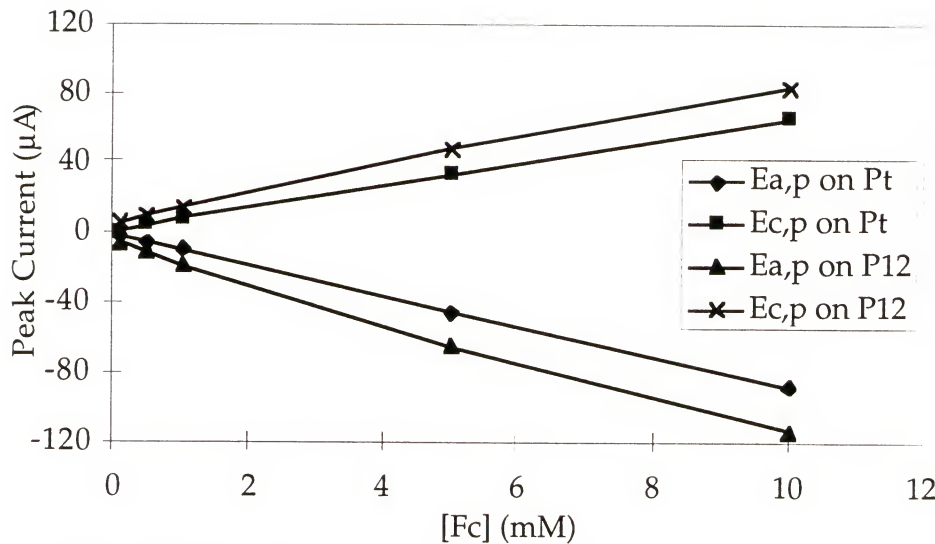


**Figure 3.19:** Effect of ferrocene concentration on current response

### 3.5 In-Situ EPR Electrochemistry

The electrochemistry of PBEDOT-B(OCH<sub>3</sub>)<sub>2</sub> (**4a**) differs considerably from that of polymers **4b-f**, as described in section 3.2.3. The presence of two redox processes in the electrochemistry of polymer **4a** is indicative that partially oxidized forms of the polymer are stable at moderate dopant levels.<sup>155,156</sup> The presence of only one redox couple in the cyclic voltammograms of **4b-f** could be indicative that each of the polymers is converted from the reduced state to the bipolaronic state through a single two-electron processes, or it could be possible that two one-electron processes occur but are too close in energy for the energy difference to be detected voltammetrically.<sup>157</sup>

Electron paramagnetic resonance spectroscopy (EPR) has been used in the past in conjunction with electrochemical methods to detect polarons formed during doping of polythiophene<sup>158</sup> and polypyrrole,<sup>159</sup> both of which reveal only one redox couple voltammetrically. To better understand the oxidative processes occurring in polymers **4a-f**, in-situ EPR electrochemistry has been investigated.

### 3.5.1 Background

Molecules with a net electron magnetic moment, i.e. unpaired electrons, or “spins,” become oriented in a magnetic field. These magnetic dipoles interact with the magnetic component of microwave radiation and, when a material with unpaired electrons is placed in a static magnetic field, absorption due to magnetic dipole transitions may occur at one or more characteristic frequencies.<sup>160</sup> This technique is known as electron paramagnetic resonance (EPR) (or electron spin resonance, ESR) spectroscopy.

As an electroactive polymer is oxidized from the neutral form to the polaronic form, unpaired electrons are formed. Subsequent oxidation to the bipolaronic form in these polymers removes unpaired electrons (Figure 3.20; see also sections 1.4 and 3.3.1). The reversible formation of unpaired electrons in conducting polymers makes EPR a useful tool for probing the redox mechanism.

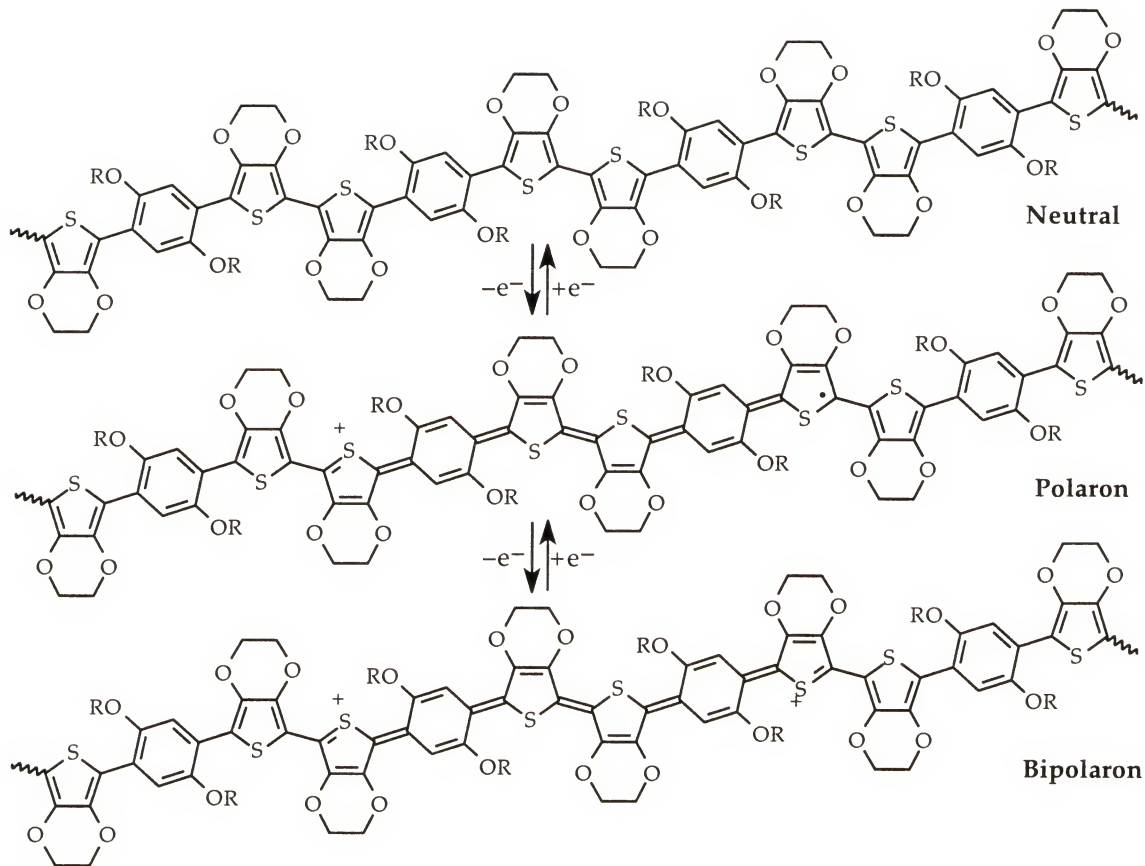


**Figure 3.20:** Interconversion between neutral, polaron, and bipolaron in PBEDOT-B(OR)<sub>2</sub> (**4a-f**)

### 3.5.2 Techniques

Early EPR studies of conducting polymers involved chemical oxidation of the polymers, with EPR spectra being obtained at several different dopant levels.<sup>161,162,163,164,165,166,167</sup> While this method was useful for gaining initial evidence of polaron and bipolaron formation in conducting polymers, it was severely limited by difficulties in the chemical doping process, including time constraints and difficulties removing all the dopant in a stepwise fashion to study the reduction process. To allow electrochemical oxidation and

reduction while minimizing the amount of solvent present in the EPR cavity, a special quartz EPR-electrochemistry cell is necessary (Figure 3.21).<sup>168,169</sup> Using this cell, a polymer film can be reversibly oxidized and reduced in the EPR cavity, and its EPR signal can be monitored throughout the redox process.

### 3.5.3 Experimental

Films were prepared electrochemically using an EG&G Princeton Applied Research Model 273 potentiostat/galvanostat employing a platinum wire working electrode, a platinum wire counter electrode, and a Ag° wire quasi-reference electrode (externally referenced to ferrocene). Polymerization was accomplished by applying a constant potential to a solution of 0.010M monomer in 0.10M TBAP in CH<sub>3</sub>CN or a mixture of CH<sub>3</sub>CN/CH<sub>2</sub>Cl<sub>2</sub> (as discussed below) in a 10mL graduated cylinder under inert atmosphere. Potentials chosen were 0.1-0.2V above the onset of monomer oxidation potential ( $E_{on,m}$ , Table 3.1). The polymers were reduced electrochemically and placed in a 0.10M TBAP solution in the quartz EPR-electrochemistry cell obtained from Wilmad Glass.

Spectra were obtained using a Bruker Model ESP 300 Electron Paramagnetic Resonance Spectrometer operating at X-band with 100kHz magnetic field modulation at room temperature. Microwave powers of

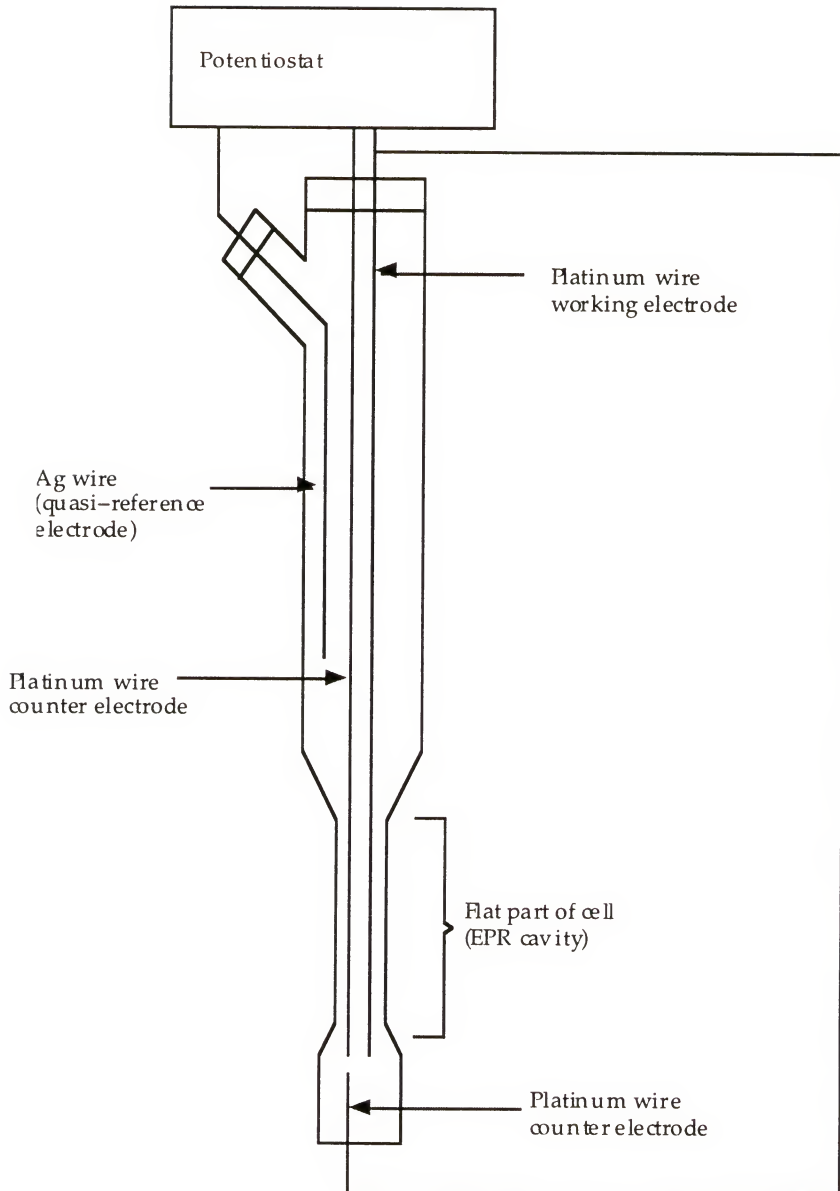


**Figure 3.21:** In-situ EPR-electrochemistry cell

50mW for polymers **4a-c** and 100mW for **4f** were used. Magnetic fields were measured with a Hall field probe, and microwave frequencies in the 9GHz

range were directly measured using a Hewlett Packard 5342A microwave frequency counter. The resulting EPR spectra were analyzed using WinEPR software from Bruker.

Once the cell was placed in the EPR cavity, the polymer was held at a potential significantly negative to cause reduction (values described in Table 3.1), and the EPR spectrum was monitored over time until no more reduction could be seen (as indicated by loss of EPR signal intensity). At this point, the potential was increased in a stepwise manner, and the polymer was held at each potential for 2 minutes before 4 EPR spectra were obtained. An average of the 4 spectra was then used to obtain signal intensity at each potential, which is given by the sum of the absolute values of the maximum and minimum peak intensities of the derivative EPR signal. This procedure was completed at each step of the oxidative process and again during the reductive process.

### 3.5.3 EPR-Electrochemistry of Polymers 4a-c,f

Upon oxidation the of polymer films, an EPR signal is seen to evolve (Figure 3.22). This signal increases in intensity to a certain potential and then begins to decrease. The signal grows in response to evolution of unpaired electrons, i.e. as the neutral form of the polymer is converted to the polaronic form (Figure 3.20). Upon further oxidation, the polarons are converted to bipolarons, and the EPR signal decreases in intensity as oxidation potential continues to increase. Upon reduction, the reverse process is true, with

reduction from the bipolaron to the polaron state evolving an EPR signal which devolves upon conversion of polarons to neutral polymer.

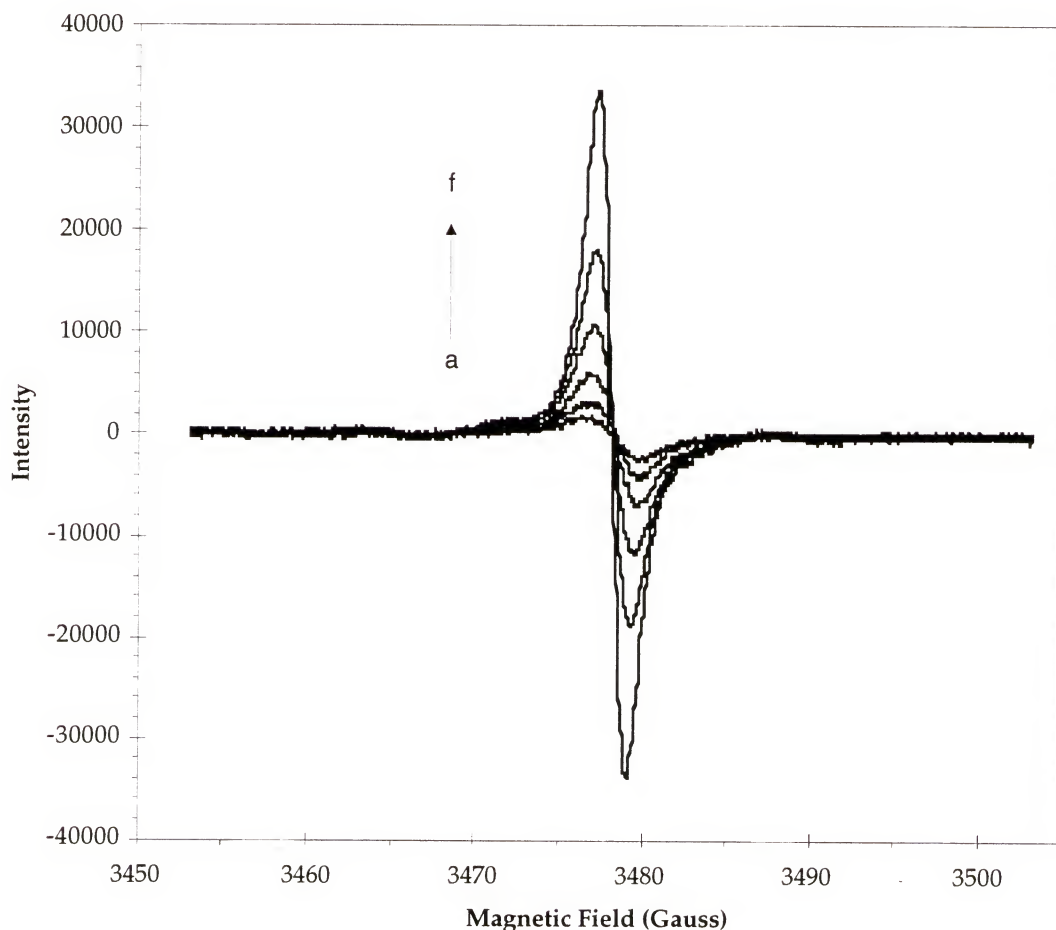


**Figure 3.22:** Evolution of EPR signal for PBEDOT-B(OCH<sub>3</sub>)<sub>2</sub> (**4a**) upon oxidation: a) -1.33 b) -1.0 c) -0.35 d) -0.25 e) -0.20 and f) -0.14V

To more easily understand the relationship between the applied potential during a scan and the EPR signal, it is possible to look only at peak signal intensity as a function of potential, rather than at the entire spectrum at each potential (assuming line width is constant, as is apparent in Figure 3.22). This relationship can then be graphically compared to the relationship

between current response and applied potential, i.e. the cyclic voltammogram of the polymer. To facilitate comparison of the two graphs, the direction of the EPR signal intensity is inverted on the cathodic scan.

The overlaid EPR-electrochemistry and CV for PBEDOT-B(OCH<sub>3</sub>)<sub>2</sub> (**4a**) can be seen in Figure 3.23. As the polymer is oxidized from its reduced state at -1.0V, the EPR signal, i.e. the concentration of polarons, increases to a maximum at 0.0V. As the oxidation potential is increased further, the signal intensity decreases, presumably due to further oxidation of polarons into bipolarons, which have no EPR signal. While most of the signal that evolves during the oxidation disappears as the polymer becomes completely oxidized, the signal intensity (30,000 arb units) at the maximum potential is higher than the initial signal intensity (10,000 arb units), indicating that there are some polarons that are not converted to bipolarons. The signal intensity at the maximum potential is stable for several hours, indicating no further conversion of polarons; increasing the potential further results in a decrease in electroactivity of the film rather than a decrease in polaron concentration. When the potential is reduced from +0.5V, an EPR signal appears again (maximum signal intensity of 75,000 arb units at -0.3V), corresponding to reduction of the bipolaronic polymer to its polaronic state. Further reduction to -1.0V results in the decay of the EPR signal to the initial intensity observed prior to oxidation. This complete decay indicates the high efficiency of the reduction process.

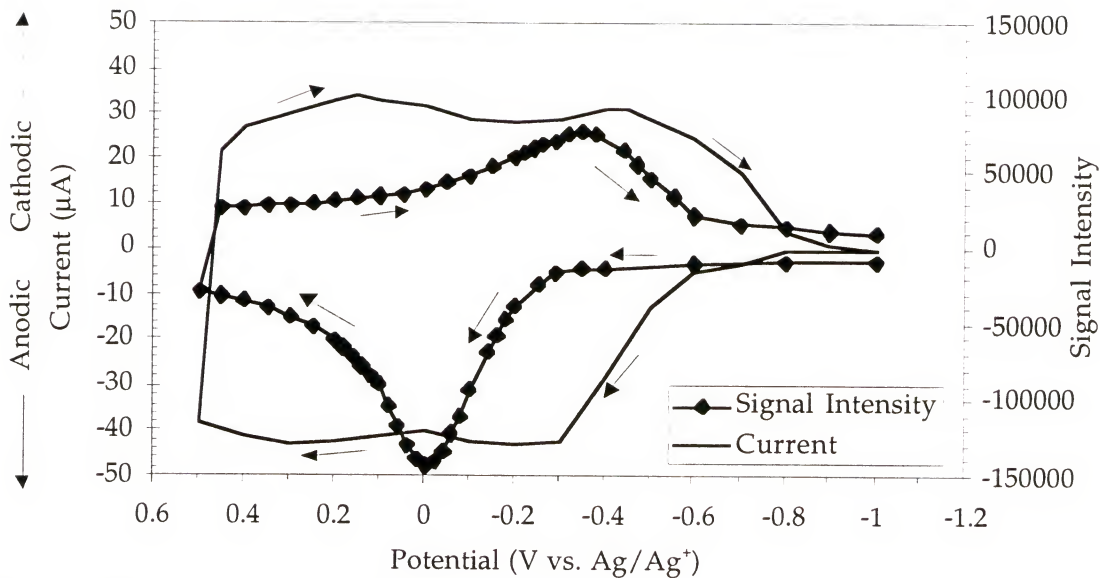


**Figure 3.23:** Current and EPR signal intensity as functions of potential for PBEDOT-B( $\text{OCH}_3$ )<sub>2</sub> (**4a**) (in 0.1M TBAP in 3:2  $\text{CH}_3\text{CN}:\text{CH}_2\text{Cl}_2$ )

The EPR signal response shown in Figure 3.23 for PBEDOT-B( $\text{OCH}_3$ )<sub>2</sub> (**4a**) is characteristic of the responses of PBEDOT-B( $\text{OC}_7\text{H}_{15}$ )<sub>2</sub> (**4b**) and PBEDOT-B(OG)<sub>2</sub> (**4f**) when switched in mixtures of  $\text{CH}_3\text{CN}$  and  $\text{CH}_2\text{Cl}_2$ . However, the EPR-electrochemistry of PBEDOT-B( $\text{OC}_{12}\text{H}_{25}$ )<sub>2</sub> (**4c**) was studied in 0.1M TBAP in  $\text{CH}_3\text{CN}$  alone. Polymer **4c** is somewhat soluble in  $\text{CH}_2\text{Cl}_2$ , so to prevent loss of polymer to solution, **4c** was prepared in 0.1M TBAP/ $\text{CH}_3\text{CN}$  at *ca.* 82°C (heat was needed to dissolve the monomer).

Results for **4c** in  $\text{CH}_3\text{CN}$  were somewhat different (Figure 3.24) from the results obtained from polymers in mixtures of  $\text{CH}_3\text{CN}$  and  $\text{CH}_2\text{Cl}_2$ . While the EPR signal evolves as it does for the other polymers, peaking at -0.15V, the polaron concentration only drops partially upon further oxidation;

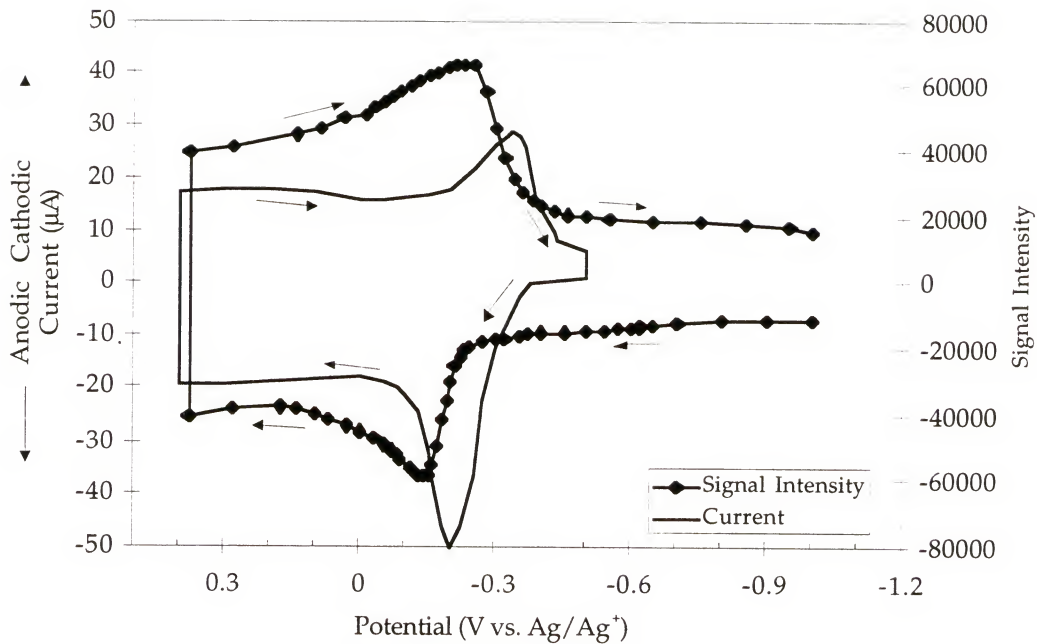


**Figure 3.24:** Current and EPR signal intensity as functions of potential for PBEDOT-B(OC<sub>12</sub>H<sub>25</sub>)<sub>2</sub> (**4c**) in CH<sub>3</sub>CN (in 0.1M TBAP)

reduction regenerates polarons, which are completely reduced to neutral polymer upon further cathodic stepping. While a slight amount (*ca.* 15%) of stable polarons was observed for all of the polymers studied in the CH<sub>3</sub>CN/CH<sub>2</sub>Cl<sub>2</sub> solvent mixture, approximately 60% of the polarons generated during oxidation are not converted to bipolarons in the **4c** EPR-electrochemistry experiment conducted in CH<sub>3</sub>CN.

To determine whether the stabilized polarons seen for **4c** were due to the change in substituent or to the change in solvent, PBEDOT-B(OC<sub>7</sub>H<sub>15</sub>)<sub>2</sub> (**4b**) (prepared by polymerization of **3b** in 0.1M TBAP in CH<sub>3</sub>CN at *ca.* 82°C) was also studied in 0.1M TBAP in CH<sub>3</sub>CN only. For comparative purposes,

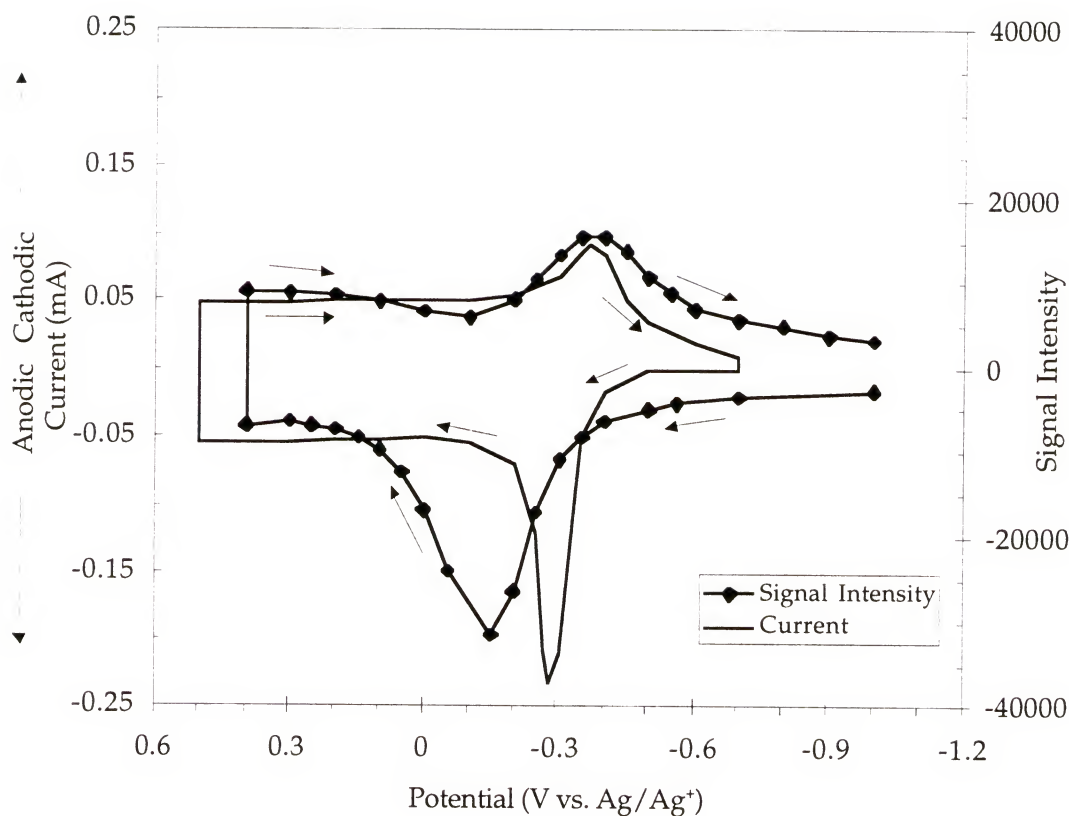


**Figure 3.25:** Current and EPR signal intensity as functions of potential for PBEDOT-B(OC<sub>7</sub>H<sub>15</sub>)<sub>2</sub> (**4b**) in 1:1 CH<sub>3</sub>CN:CH<sub>2</sub>Cl<sub>2</sub> (in 0.1M TBAP)

the results of the study of **4b** in the solvent mixture are given in Figure 3.25, and the results in CH<sub>3</sub>CN are given in Figure 3.26. Notice that in the solvent mixture, almost all of the polarons formed during oxidation are converted to bipolarons by the time the polymer has been oxidized further to +0.3V. Oxidation as high as +0.8V had little further effect on the polymer spectra. While the maximum signal intensity is reached at approximately the same potential in CH<sub>3</sub>CN (-0.10V in Figure 3.26), a large portion of the polarons (*ca.* 65%) remain at +0.20V, at which point a second increase in signal intensity

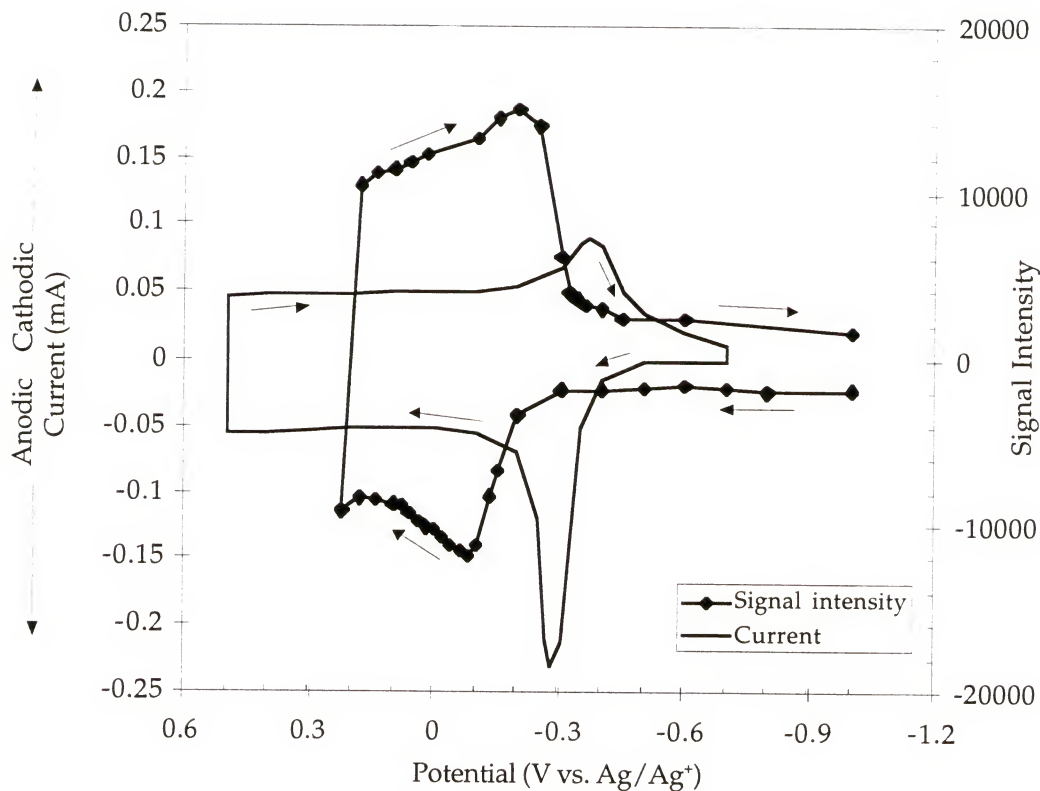


**Figure 3.26:** Current and EPR signal intensity as functions of potential for PBEDOT-B(OC<sub>7</sub>H<sub>15</sub>)<sub>2</sub> (**4b**) in CH<sub>3</sub>CN (in 0.1M TBAP)

becomes apparent. Because this second process was likely the beginning of overoxidation, the polymer was not oxidized further. Upon reduction, nearly all the spins formed in the oxidation process disappeared in both the pure CH<sub>3</sub>CN and the solvent mixture, indicating that all polarons, including any that were not converted to bipolarons during the oxidation (trapped polarons) were reduced to neutral. A similar effect was observed with polymer **4f**.

In general for this family of PBEDOT-B(OR)<sub>2</sub>, whenever CH<sub>2</sub>Cl<sub>2</sub> is included in the electrolyte solution, the majority of the EPR signal disappears upon oxidation. This trend is seen even when CH<sub>2</sub>Cl<sub>2</sub> comprises only 10% of

the total solvent volume (in the case of **4f**, whereas studies on polymers **4a** and **4b** contain 40% and 50% CH<sub>2</sub>Cl<sub>2</sub> by volume, respectively). In all cases studied in electrolyte solution in CH<sub>3</sub>CN alone, the polarons generated during oxidation do not dissipate; in fact, for polymers **4b**, **4c**, and **4f**, 65%, 60%, and 60% of the signal remains, respectively.

A likely explanation for this behavior is that when the polymers are grown in CH<sub>3</sub>CN alone, their morphology is more compact than it is when grown in the presence of CH<sub>2</sub>Cl<sub>2</sub>, because the films are swollen by CH<sub>2</sub>Cl<sub>2</sub>. In the solvent-swollen films it is easier for counterions to move in and out of the film, compensating any charges formed during the redox process. This seems feasible, given that the polymers are much more soluble in CH<sub>2</sub>Cl<sub>2</sub>. While there may be space in CH<sub>3</sub>CN-prepared polymers for an anion to move in to compensate one cation (allowing a polaron to be formed) on a polymer chain, if the polymers are very compactly packed it may be more difficult to fit two counterions near each other to allow formation of a dication (bipolaron).

### 3.6 In-Situ Conductivity

#### 3.6.1 Background

Conductivity in polymers relies largely on the degree of conjugation in the backbone and inter-chain interactions. Overlap of  $\pi$  orbital electrons allows charge to be delocalized along the polymer chain. In their neutral

form, conjugated polymers are insulators or semiconductors; in order for the polymers to become conductive, charge must be introduced chemically or electrochemically in a process known as doping. In the presence of an electric field, the charges are mobile, and the polymer can transport charge.

Conductivity ( $\sigma$ ) is controlled by number of carriers *per* unit volume (n) and the mobility of the carriers ( $\mu$ ) according to equation 3-3:

$$\sigma = ne\mu \quad (3-3)$$

where the carriers in the case of polythiophene-based materials are single electrons, and e is the electronic charge.<sup>170</sup> Conductivity can be determined by measuring the resistance, R, to charge transport through a known volume as given by

$$\sigma = \ell / RA \quad (3-4)$$

where  $\ell$  is the length over which the resistance is measured and A is the cross-sectional area through which the current is passed. Conduction is a complex property determined by structural aspects of the system including main chain structure and  $\pi$  orbital overlap, molecular weight and polydispersity, charge carrier density as determined by redox doping, interchain interactions controlled by main chain and side chain structures,

and chain orientation, which is effected by processing conditions.<sup>98</sup> Charge transport is also highly affected by sample morphology, i.e. crystallinity and density, as well as gross defects such as pinholes and cracks.

While conductivity is crucial to most properties of conductive polymers, conductivity cannot be determined absolutely; rather, conductivity is highly sample dependent. It is interesting, however, to look at the dependence of relative conductivity on the oxidation state of the polymer. In the fully reduced state, most conjugated polymers are insulators; as the polymers are oxidized, however, they become conductive. Therefore, conductivity is directly dependent upon applied potential. In practical applications of conducting polymers, it is desireable to minimize the energy required to make the polymers conduct, i.e. to use polymers with low oxidation potentials.

Several groups have reported potential-dependent conductivities of common conducting polymers.<sup>171,172,173,174</sup> In these cases, polymers were typically deposited across a small ( $20\mu\text{m}$ ) gap across which resistance was measured. The potential dependence of the conductivity of poly(3,4-ethylenedioxythiophene) (PEDOT) has been measured in the Reynolds group on films deposited across large gap ( $200\mu\text{m}$ ) electrodes in both aqueous and organic media.<sup>175</sup> Relatively thick ( $323\mu\text{m}$ ) films of PEDOT can be switched from the reduced state at  $-0.6\text{V}$  to the fully conductive state at  $+0.1\text{V}$  in a variety of solvents and electrolytes. Conductivities are dependent upon growth conditions and vary from  $0.2$  to  $13.0 \text{ Scm}^{-1}$ .

### 3.6.2 Techniques and Instrumentation

Electropolymerization on LG-LGEs and in-situ conductivity measurements were performed on a Pine Instrument Company model AFCBPI bipotnetiostat. Film thicknesses were obtained using a Sloan Dektak II profilometer.

The electrodes used in this experiment were large gap, lateral growth electrodes, or LG-LGEs. These electrodes (Figure 3.27) consist of two gold electrodes parallel to each other on a flat substrate with a  $200\mu\text{m}$  gap between them; the gold is masked so that only the internal edge of the gold is exposed. A graphite bridge was deposited between the gold electrodes using Electrodag<sup>®</sup> until a resistance *ca.*  $1000\Omega$  was reached.

Polymer films were then deposited potentiostatically from 0.01M solutions of monomer in 0.10M  $\text{Li}(\text{CF}_3\text{SO}_2)_2\text{N}$  in a mixture of tetrahydrofuran and propylene carbonate. To deposit the polymers, LG-LGEs were placed in an electrochemical cell with a  $\text{Ag}/\text{Ag}^+$  reference electrode and a copper mesh counter electrode, which was positioned above the LG-LGE (with the large surface parallel to the surface of the LG-LGE). The monomer/electrolyte solutions were added, and the potential at working electrode 1 ( $\text{WE}_1$  in Figure 3.27) was set at a potential 50mV above that of the monomer oxidation potential (determined from the polymer cyclic voltammetry, 510mV in the case of polymer **4b**) while the potential at working electrode 2 ( $\text{WE}_2$  in Figure 3.27) was set at a potential 5mV below that of  $\text{WE}_1$ . The polymers were then

deposited for one hour while the potentials at  $WE_1$  and  $WE_2$  were switched every 10 minutes to ensure even deposition. The polymer coated LG-LGEs were then rinsed with monomer-free electrolyte solution and stored wet until conductivity measurements were taken.

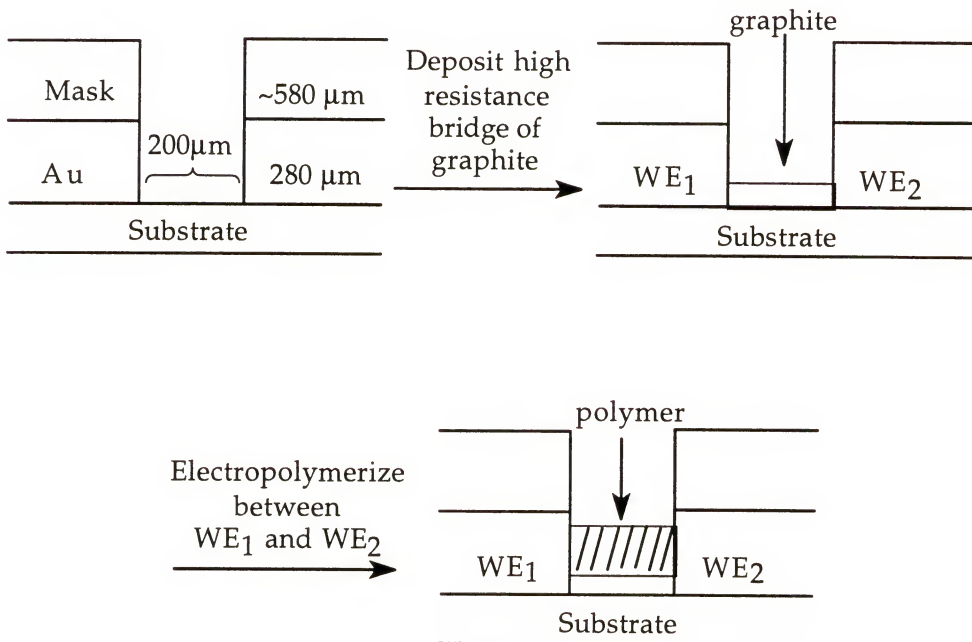


**Figure 3.27:** Large gap lateral growth electrode for in-situ conductivity measurements

Offset potentials of the films were measured to ensure that the polymers were well-connected to the electrodes and to determine the onset potential of conductivity for the polymer devices. The polymer-coated LG-LGEs were placed in monomer-free electrolyte solution in an electrochemical cell with a copper mesh counter electrode and a  $\text{Ag}/\text{Ag}^+$  reference electrode. Offset potential scans were obtained by setting an offset potential of 5, 50, or

180mV between  $WE_1$  and  $WE_2$  on the bipotentiostat. The polymers were then cycled at  $10\text{mVs}^{-1}$  from -1.0V to 1.0V while the drain current ( $i_D$ ) versus potential was recorded, as shown in Figure 3.28. The symmetry between the two CVs indicates that the film is well-connected to the electrodes.

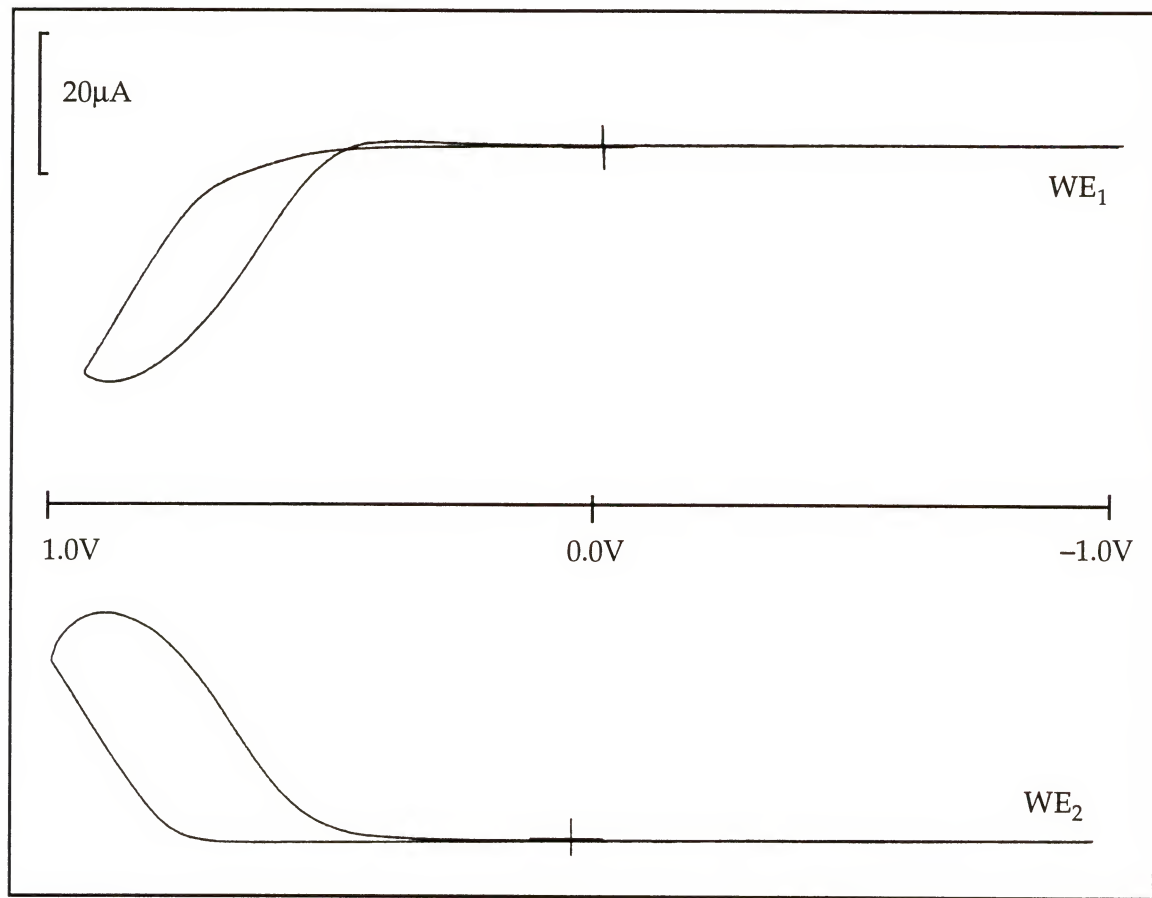


**Figure 3.28:** Offset potential scan of PBEDOT-B( $\text{OC}_7\text{H}_{15}\right)_2$  (**4b**) on LG-LGE: with a  $1,100\Omega$  graphite bridge with working electrode 2 offset by -180mV from working electrode 1 (polymer grown and switched in 0.1M  $\text{Li}(\text{CF}_3\text{SO}_3)_3\text{N}$  in 3:1 propylene carbonate:THF)

In situ conductivity was then determined by setting the potential at  $WE_1$  at a static potential (e.g. 0.0V) while the potential at  $WE_2$  was cycled

$\pm 50\text{mV}$  from WE<sub>1</sub> and the drain current vs. potential was recorded. The process was repeated over the desired potential range to obtain drain currents at each potential. Given drain current and potential, it was then possible to determine resistance of the device. Film thicknesses were measured and used with the resistance at each potential and the area of the sample (simplified with the use of the masked LG-LGE, which limits polymer growth to the area between the electrodes) to calculate conductivity as in Equation 3-4, above. The potential dependence of conductivity could then be determined as shown in Figure 3.29.

### 3.6.2 In situ conductivity of polymers 4a,c,d, and 4f

The benefits of the extremely low oxidation potentials of PBEDOT-B(OR)<sub>2</sub> can be seen in the in-situ conductivity measurements of these polymers. Compare, for example, the in-situ conductivity of heptoxy-substituted EDOT polymer **4b** (PBEDOT-B(OC<sub>7</sub>H<sub>15</sub>)<sub>2</sub>) with its thiophene analog (PBT-B(OC<sub>7</sub>H<sub>15</sub>)<sub>2</sub>), prepared previously by Reynolds and coworkers (Figure 3.29).<sup>55</sup> While PBEDOT-B(OC<sub>7</sub>H<sub>15</sub>)<sub>2</sub> exhibits an oxidation potential peaking at -0.28V, its thiophene analog exhibits a much higher oxidation peak potential of +0.40V;<sup>56</sup> as discussed earlier in this chapter, the lower oxidation potential of PBEDOT-B(OC<sub>7</sub>H<sub>15</sub>)<sub>2</sub> as compared to PBT-B(OC<sub>7</sub>H<sub>15</sub>)<sub>2</sub> is due to the increased electron density imparted by the electron-rich ethylenedioxy bridges of the EDOTs. The effect of these differing oxidation potentials on in-situ conductivity measurements can be clearly seen in Figure 3.30; while

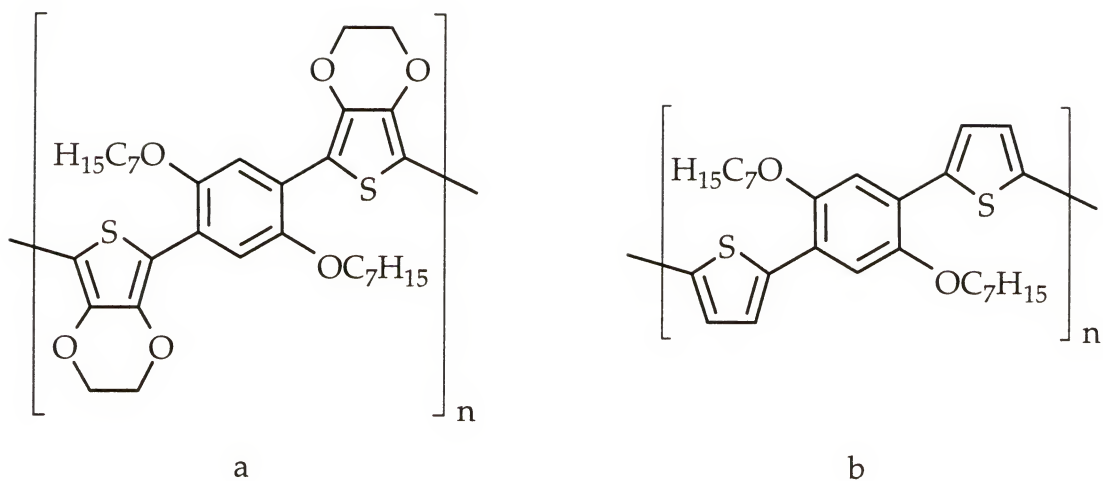


**Figure 3.29:** Structures of PBEDOT-B(OC<sub>7</sub>H<sub>15</sub>)<sub>2</sub> (**4b**) (a) and its thiophene analog PBT-B(OC<sub>7</sub>H<sub>15</sub>)<sub>2</sub> (b)

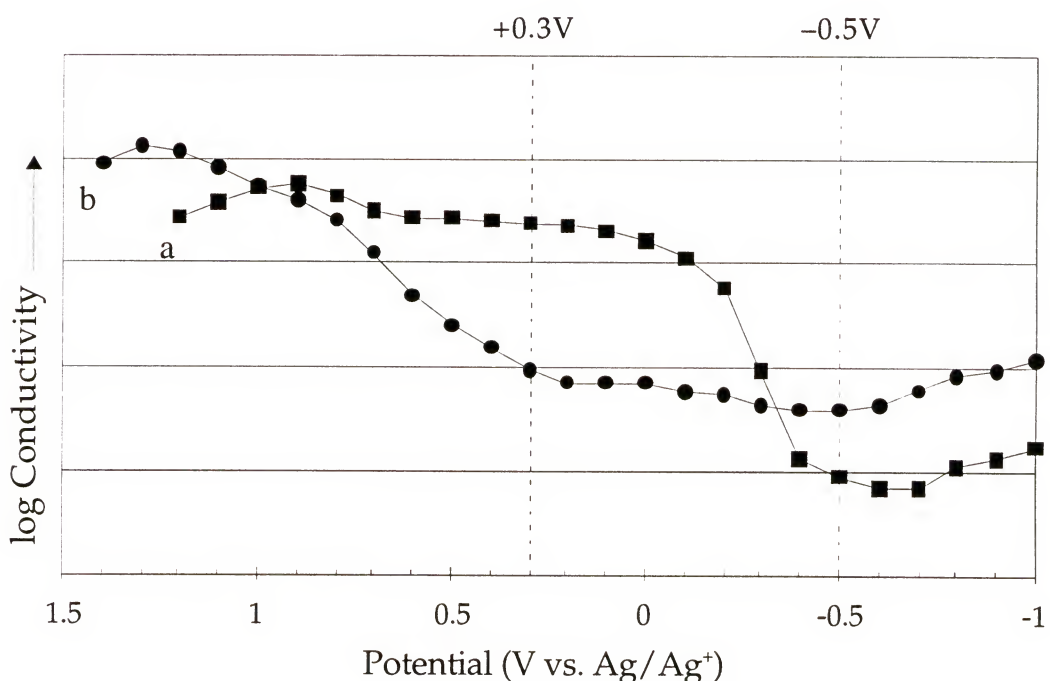


**Figure 3.30:** Comparative in-situ conductivities: a) PBEDOT-B(OC<sub>7</sub>H<sub>15</sub>)<sub>2</sub> (**4b**) and b) PBT-B(OC<sub>7</sub>H<sub>15</sub>)<sub>2</sub>

PBEDOT-B(OC<sub>7</sub>H<sub>15</sub>)<sub>2</sub> (**4b**) begins to become conductive just above -0.50V, the device prepared using PBT-B(OC<sub>7</sub>H<sub>15</sub>)<sub>2</sub> does not begin to conduct until +0.3V. Thus there is a large potential window (0.8V) where PBEDOT-B(OC<sub>7</sub>H<sub>15</sub>)<sub>2</sub> is a useful conductor while the thiophene polymer is not. The same general trend was also observed in polymers **4a,c,d**, and **4f**, with onset of conductivity coinciding with the onset of the polymer oxidation *ca.* -0.5V.

It is important to note that the conductivity values determined using the in-situ method described here yield the conductivity of the device, i.e. the polymer deposited on graphite deposited on the LG-LGE, rather than the true conductivity of the polymers. Large variations in conductivities are found for samples polymerized and examined under very similar conditions at different times. For this reason, quantification of conductivities in Figure 3.30 has been omitted; while the general trends of conductivity increasing as a function of potential are real, the magnitudes of those conductivities are not. This is a problem inherent to electrodeposition of the polymers on the large gap electrodes; the necessity of depositing graphite in the gap to facilitate film formation results in inconsistencies in initial device resistance. These problems are reduced when smaller gap electrodes (10–20μm) are used. Interdigitated electrodes are currently being explored that have small gaps, thus avoiding the need to deposit graphite in the electrodes.

## CHAPTER 4 CHEMICAL POLYMERIZATION

### 4.1 Introduction

#### 4.1.1 Motivation for Research

Many routes are available to prepare polyheterocycles. While the monomers described in Chapter 2 have been successfully polymerized electrochemically (Chapter 3), only small amounts of polymer can be prepared in an electrochemical fashion, and other routes must be used to produce polymers in bulk. Within this chapter, efforts to produce well-defined, soluble electroactive polymers of high molecular weights are described. The monomers described in Chapter 2 have been oxidatively polymerized using several reagents, and polymers having similar repeat units have been prepared using transition metal-mediated coupling methods.

#### 4.1.2 Molecular Weight Determination

End group analysis. For low molecular weight polymers, end group analysis can be used to determine the number of repeat units in a soluble polymer (degree of polymerization,  $X_n$ ). In this analysis, a property

that is characteristic of the end groups, and can be compared to the internal portions of the polymer chain, can be examined and quantified. This value can then be related to sample mass and molecular mass of the repeat unit to determine the average number of repeats for every two end groups, which is  $X_n$ . This ratio approach can be applied using titration,<sup>176</sup> quantitative infrared spectroscopy,<sup>177,178</sup> quantitative ultraviolet spectroscopy,<sup>179</sup> or nuclear magnetic resonance (NMR) spectrometry with a variety of nuclei.<sup>180,181,182</sup> End group analysis is not especially useful for high molecular weight polymers because contributions from the very small fraction of end groups at high molecular weights are insignificant relative to contributions from internal groups. Polymers with molecular weights above 30,000g/mol are often difficult to analyze by end group analysis,<sup>183</sup> but the effects are highly dependent upon polymer composition and the method used.<sup>184</sup>

For most of the polymers studied here, quantitative  $^1\text{H}$  NMR end group analysis can be used to determine an average number of thietyl hydrogens relative to internal phenyl hydrogens. As illustrated below in Figure 4.1, EDOT is especially well-suited for this type of analysis, as the only thietyl hydrogens present in the polymer are the end groups. This is in contrast to thiophene, where the presence of hydrogens in the 3- and 4-positions complicates the spectrum.

In the polymers, the number of phenyl hydrogens is greater than the number of thietyl hydrogens, and the ratio corresponds to the average degree of polymerization,  $X_n$  (n in Figure 4.1b):

$$X_n = 2H_b / 2H_a = H_b / H_a \quad (4-1)$$

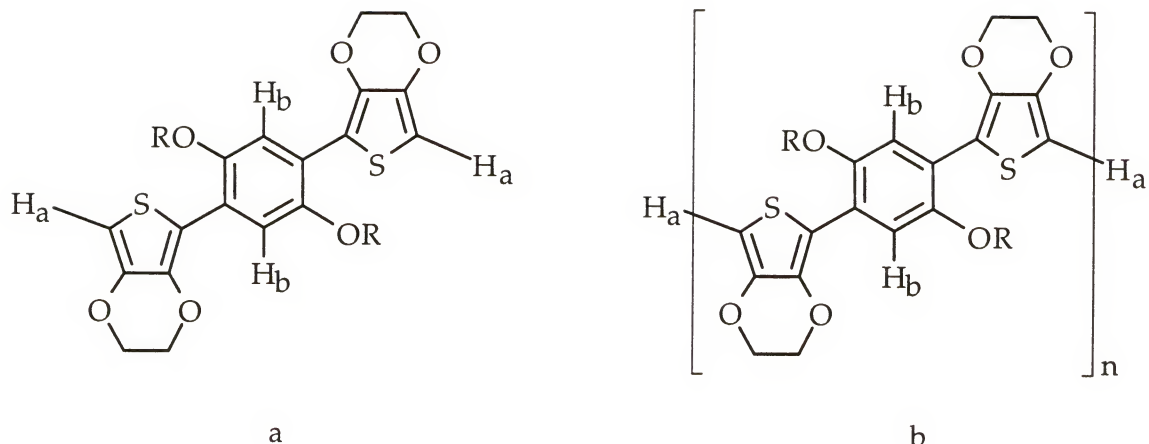


**Figure 4.1:** Ratio of internal to external aromatic H can be used to determine molecular weight: a) Monomer,  $H_a/H_b=1$  b) Polymer,  $H_a/H_b=1/n$

Average degree of polymerization ( $X_n$ ) is related to number average molecular weight ( $M_n$ ) according to Equation 4-2 where  $M_{rep}$  is the molecular weight of the repeat unit in grams per mole. The contribution of the terminal hydrogens to the molecular weight is minimal, so that  $M_n$  is approximately equal to the product of  $X_n$  and  $M_{rep}$ :

$$M_n = (X_n)(M_{rep}) + 2(1.0079 \text{ g/mol}) \approx (X_n)(M_{rep}) \quad (4-2)$$

At very high molecular weights, the magnitude of the terminal  $^1\text{H}$  NMR absorbance would be insignificant relative to the phenyl  $^1\text{H}$  NMR absorbance, and end group analysis would no longer be useful. Molecular weights of thiophene-based polymers are usually well below 30,000g/mol,<sup>12,185,186</sup> although values of  $M_n$  up to 300,000g/mol have been reported for some poly-3-alkylthiophenes.<sup>187</sup> For the thiophene analogs of the EDOT polymers studied here,  $M_n$  values of 2,000 to 4,000g/mol were obtained based on  $^1\text{H}$  NMR end group analysis as well as gel permeation

chromatography.<sup>55</sup> At these relatively low molecular weights, these materials might more accurately be called oligomers, but the trend in the conducting polymers field is to refer to these materials as polymers. In fact, oligomers are of considerable interest in the field of conducting polymers, because precise structure-property relationships can be determined in oligomers, allowing extrapolation of those relationships to polymers.<sup>188</sup>

Gel permeation chromatography (GPC). Also known as size exclusion chromatography (SEC), GPC is a widely used method of determining molecular weight relative to standards of known molecular weight. This technique provides number average ( $M_n$ ) and weight average ( $M_w$ ) molecular weight as well as molecular weight distribution (polydispersity,  $M_w/M_n$ ) and can be used in conjunction with other techniques to obtain quantitative molecular weights.

Rate of elution through GPC columns is determined primarily by hydrodynamic volume of the macromolecules.<sup>189,190</sup> Therefore, two polymers of equal molecular weights will not elute at the same rate unless they both possess the same solution properties. The polymer used as a calibration standard should be structurally similar to the polymer being tested, or the values obtained for molecular weights will be approximate. For this reason, most GPC results are reported as values relative to the calibration standards. Polystyrene standards with molecular weights similar to those of the polymers of interest are often used for calibration, as the cost and limited availability of more appropriate standards (for example in this case, conjugated polymers solubilized by long, flexible side groups, such as a substituted poly-*p*-phenylene) precludes use.

A UV detector is commonly used to determine polymer concentration in the eluent. Previous studies of the UV-visible spectra of the polymers in the reduced state (Chapter 3) reveal broad absorptions, with  $\lambda_{\text{max}}$  at approximately 480 to 525 nm.<sup>20</sup> Monomers studied here exhibit  $\lambda_{\text{max}}$  values *ca.* 365nm. For GPC determination of molecular weights of the polymers described in this chapter, the UV detector was set at 500nm.

## 4.2 Oxidative Polymerizations

### 4.2.1 Background

As discussed in Chapter 1, oxidative polymerization has been used previously to prepare a wide variety of electroactive polymers. Among these reactions, ferric chloride has been used in the synthesis of poly[1,4-bis(2-thienyl)-2,5-dialkoxybenzenes].<sup>54,55</sup> In those instances, chloroform-soluble polymers were obtained with alkoxy substituents  $R=C_{16}H_{33}$  and  $C_{20}H_{41}$ , while  $R=C_{12}H_{25}$  was insoluble. In general, EDOT derivatives typically have lower solubilities than their thienyl counterparts.

### 4.2.2 Oxidative Polymerization of BEDOT-B(OR)<sub>2</sub> (**3a-f**) with Ferric Chloride

Oxidative polymerization of BEDOT-B(OR)<sub>2</sub> monomers **3b-f** (Figure 4.2) was accomplished using FeCl<sub>3</sub> in chloroform followed by reduction in

concentrated NH<sub>4</sub>OH. One to four equivalents of FeCl<sub>3</sub> were used, but broad molecular weight distributions and poor yields were obtained with low oxidant concentration, while high oxidant concentration produced materials that had little or no soluble fraction. An optimal oxidant level of 2.0 to 2.5 equivalents was found to yield products of highest quality. All attempts to polymerize BEDOT-B(OCH<sub>3</sub>)<sub>2</sub> (**3a**) yielded completely insoluble materials that could not be characterized further. This was expected due to the lack of the solublizing long-chain alkoxy side groups; polymerization of BEDOT-B(OC<sub>7</sub>H<sub>15</sub>)<sub>2</sub> (**3b**) also yielded very poorly soluble material. Solubility was improved through the use of increased side chain lengths (polymers **4c,d**), branched side chains (polymer **4e**), and oligomeric ether side chains (**4f**).

The soluble fractions from polymers **4c-f** were analyzed by <sup>1</sup>H NMR and GPC to determine degree of polymerization (Table 4.1); BEDOT-B(OC<sub>12</sub>H<sub>25</sub>)<sub>2</sub> (**3c**) yielded soluble trimer (9 rings), while monomers **3d-f** yielded soluble tetramer to pentamer (12 to 15 rings). For all of the polymers, significant fractions (30-60%) of insoluble materials were obtained that could be due to either poor solubility of the higher molecular weight polymers or possibly overoxidized or crosslinked materials.

The structures of the neutral polymers obtained from ferric chloride-induced polymerizations were studied by FT-IR. The absorption associated with the thiophene  $\alpha$ -C-H stretch apparent in the monomers (*ca.* 3100 cm<sup>-1</sup>) is absent in the polymers, while the absorption from the phenylene C-H stretch (*ca.* 2850 cm<sup>-1</sup>) remains. The <sup>1</sup>H NMR spectra of the polymers support this, as the ratio of the thiienyl hydrogens to phenyl hydrogens differs from that observed in the monomers, while the ratio of phenyl hydrogens to ethylenedioxy bridge hydrogens remains the same. These results indicate that polymerization occurred through the thiophene  $\alpha$ -carbon, as expected.

**Table 4.1:** Molecular weights of polymers prepared by ferric chloride-induced oxidative polymerization

Polymer <sup>a</sup>	$M_w$ (g/mol)	$M_n$ (g/mol)	$M_w/M_n$	GPC $X_n^b$	Number of rings <sup>c</sup>	$^1\text{H}$ NMR $X_n^d$
<b>4a</b>	insoluble					
<b>4b</b>	insoluble					
<b>4c</b>	2900	2300	1.3	3.1	9	3
<b>4d</b>	4600	4000	1.4	4.8	14	4
<b>4e</b>	3700	2800	1.3	4.6	14	4
<b>4f</b>	2300	1900	1.2	3.1	9	e

<sup>a</sup> Prepared using 2.5 moles  $\text{FeCl}_3$  per mole of monomer

<sup>b</sup> Determined by  $M_n/M_{rep}$

<sup>c</sup> Determined by multiplication of GPC values of  $X_n$  by the number of rings (3) per repeat unit

<sup>d</sup> Determined by the ratio of phenyl H to terminal thietyl H

e End group peak too small to quantitate

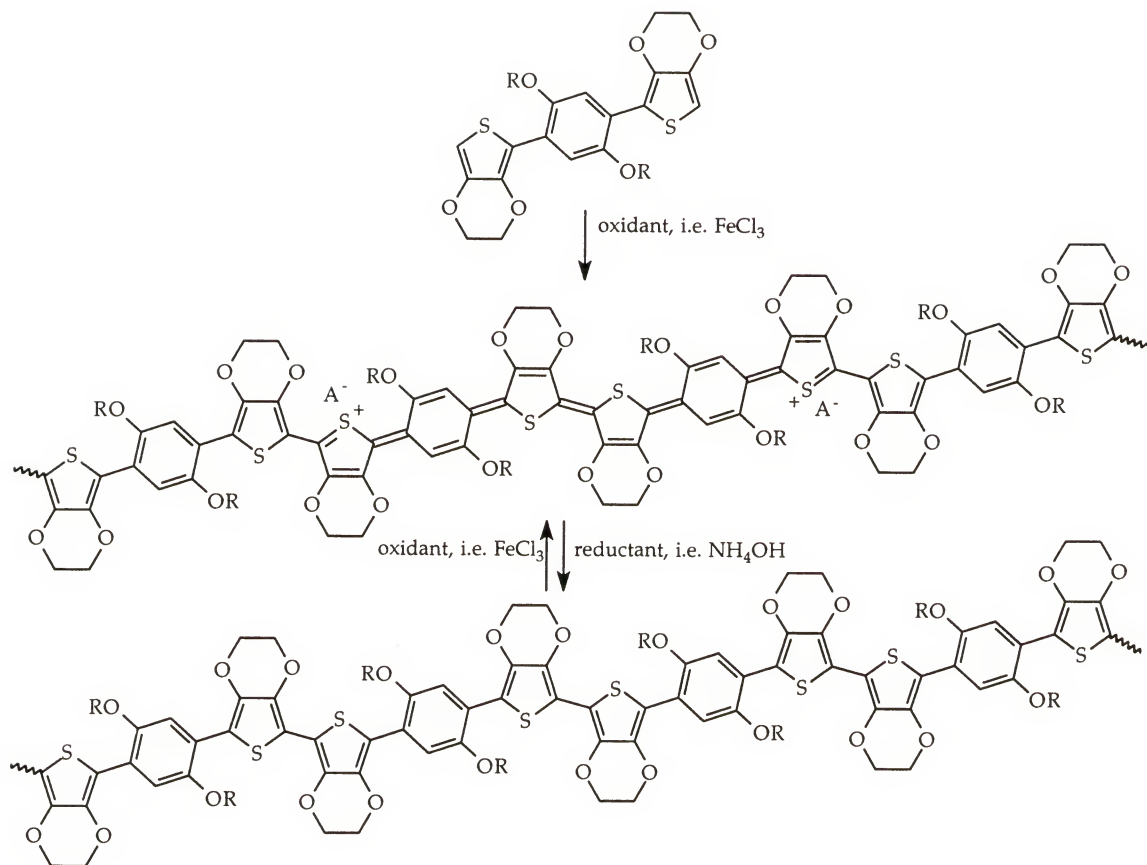


**Figure 4.2:** Oxidative polymerization of BEDOT-B(OR)<sub>2</sub> monomers (**3a-f**)

#### 4.2.3 Oxidative Polymerization of BEDOT-B(OC<sub>16</sub>H<sub>33</sub>)<sub>2</sub> with Various Oxidants

To study the effect of oxidant on polymer solubility and molecular weight, Fe(ClO<sub>4</sub>)<sub>3</sub>, CuBr<sub>2</sub> and FcPF<sub>6</sub> were used to polymerize BEDOT-B(OC<sub>16</sub>H<sub>33</sub>)<sub>2</sub> (**3d**). This monomer was chosen for the polymerization study due to its relative ease of preparation as compared to the oligomeric ether- and 2-ethylhexyl-substituted monomers (**4e,f**), which yielded similar molecular weights in the ferric chloride polymerizations discussed above. Two moles of oxidant per mole of monomer were used in all cases, and

oxidation with  $\text{FeCl}_3$  was repeated concurrently; reduction of the oxidized polymers was accomplished using hydrazine monohydrate as opposed to ammonium hydroxide.

Vastly varied results were obtained with the different oxidants, but results from the ferric chloride polymerization used in this case agreed well with those of previous ferric chloride polymerizations (as in section 4.2.2). The best results were those obtained from oxidation using  $\text{Fe}(\text{ClO}_4)_3$ ; the polymer dissolved completely within 5 minutes. GPC revealed a material with fairly low polydispersity (1.7) and high molecular weight; the number average molecular weight  $M_n$  was 13,500g/mol, which corresponds to 16 repeat units, or 48 conjugated rings. This is nearly four times higher in molecular weight than that of the soluble fraction obtained from the ferric chloride polymerization ( $X_n=4.8$ ), even though the two materials had the same  $\text{Fe}^{3+}$  oxidant. This suggests that counterion effects are important and should be studied.

In the case of  $\text{FcPF}_6$ , while a solid was collected from the reaction mixture, reduction with hydrazine yielded a red-brown oil that could not be purified further. The polymer prepared from  $\text{CuBr}_2$  was very poorly soluble; GPC of the soluble fraction (Table 4.2) revealed a broad molecular weight distribution ( $M_w/M_n=3.5$ ), with a degree of polymerization ranging from 4 to 13 (from  $M_n$  to  $M_w$ ).  $\text{Cu}^{2+}$  introduced during synthesis of polythiophenes has been shown to be difficult to remove, resulting in poorly soluble materials;

the authors attribute this effect to coordination of copper to the thiophene sulfur atoms on multiple polymer chains.<sup>191,192,193,194</sup>

The molecular weights of these polymers were also examined using <sup>1</sup>H NMR. While the polymer prepared from CuBr<sub>2</sub> was too poorly soluble to obtain useful molecular weight information, CDCl<sub>3</sub> soultions of polymers prepared from FeCl<sub>3</sub> and Fe(ClO<sub>4</sub>)<sub>3</sub> provided useful <sup>1</sup>H NMR spectra. In the case of the polymer prepared from FeCl<sub>3</sub>, 4.6 phenyl H were found for every thienyl H, corresponding to approximately 5 repeat units. The polymer prepared from Fe(ClO<sub>4</sub>)<sub>3</sub> had 14.1 phenyl H per thienyl H, or 14 repeat units. These numbers agree fairly well with the values obtained using GPC.

The reason for improved molecular weight in the ferric perchlorate case is unclear. While FeCl<sub>3</sub> and Fe(ClO<sub>4</sub>)<sub>3</sub> both have the same formal oxidation charge, Cl<sup>-</sup> is more coordinating than ClO<sub>4</sub><sup>-</sup>, allowing Fe(ClO<sub>4</sub>)<sub>3</sub> to act as a stronger oxidant than FeCl<sub>3</sub>. It is also possible that the larger perchlorate ions might prevent chain aggregation during polymerization, allowing higher molecular weights to be attained before maximum solubility is reached. The polymer obtained from Fe(ClO<sub>4</sub>)<sub>3</sub> polymerization had no insoluble fraction, yet it had much higher molecular weight than the polymers obtained using other oxidants. The large fractions of insoluble materials obtained during ferric chloride polymerizations are typically attributed to a combination of higher molecular weight fractions and crosslinked materials. This may indicate that all the insolubles in polymers

obtained from ferric chloride (and CuBr<sub>2</sub>) are crosslinked material, or that polymers obtained from ferric chloride (and CuBr<sub>2</sub>) are highly aggregated.

**Table 4.2:** Effect of oxidant choice on molecular weight of PBEDOT-B(OC<sub>16</sub>H<sub>33</sub>)<sub>2</sub> (**4d**)

Oxidant <sup>a</sup>	$M_w$ (g/mol)	$M_n$ (g/mol)	$M_w/M_n$	GPC $X_n$ <sup>b</sup>	Number of rings <sup>c</sup>	<sup>1</sup> H NMR $X_n$ <sup>d</sup>
FeCl <sub>3</sub>	4600	4000	1.1	4.8	14	4.6
FeClO <sub>4</sub>	23000	13500	1.7	16	48	14.1
CuBr <sub>2</sub>	11000	3000	3.5	3.6	11	e

<sup>a</sup> 2 moles per mole **3d**

<sup>b</sup> Determined by  $M_n/M_{rep}$

<sup>c</sup> Determined by multiplication of GPC values of  $X_n$  by the number of rings (3) per repeat unit

<sup>d</sup> Determined by the ratio of phenyl H to terminal thietyl H

<sup>e</sup> Too poorly soluble to be determined

### 4.3 Non-Oxidative Coupling Polymerizations

While oxidative polymerization has been widely used in the synthesis of conducting polymers, irregular backbones, side reactions and solubility-limited molecular weights are recurrent problems (see section 1.3). Non-oxidative routes to conducting polymers can be used to avoid those and other problems, yielding well-defined, soluble polymers. These polymerizations typically involve transition metal-mediated coupling reactions, as described in section 2.2.2 for monomer synthesis.

Many of the coupling polymerizations require the use of dihalogenated phenylenes or heterocycles. To use BEDOT-B(OR)<sub>2</sub> in these reactions, it was necessary to find an effective halogenation route. Direct bromination with Br<sub>2</sub> was unsuccessful, producing insoluble black powder that may be crosslinked polymer. Addition of N-bromosuccinimide (NBS) at room temperature with or without acid catalyst also produced insoluble black powder. However, addition of NBS at -78°C to methoxy- and hexadecyloxy-substituted monomers **3a,d** followed by stirring at 0°C for 18h produced dibrominated monomers Br<sub>2</sub>BEDOT-B(OR)<sub>2</sub> (**5a,d**) (Figure 4.3) in reasonable yields: 90% for Br<sub>2</sub>BEDOT-B(OCH<sub>3</sub>)<sub>2</sub> (**5a**) and 63% for Br<sub>2</sub>BEDOT-B(OC<sub>16</sub>H<sub>33</sub>)<sub>2</sub> (**5d**). Similar attempts to dibrominate glyme monomer **3f** at 0°C also yielded insoluble black powder. With the availability of **5d** it is possible to utilize a wide variety of coupling reactions to produce both homopolymers and copolymers.

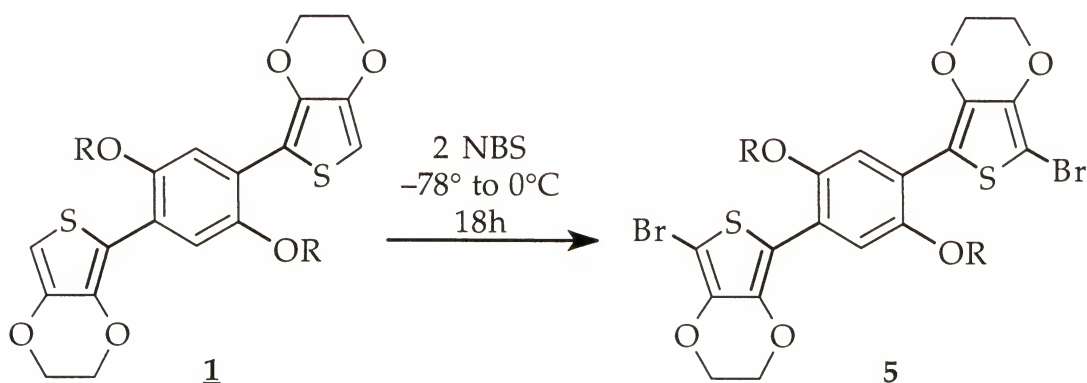


**Figure 4.3:** Monomer bromination [where R=CH<sub>3</sub> (**5a**) or C<sub>16</sub>H<sub>33</sub> (**5d**)]

#### 4.3.1 Homocoupling Polymerizations

Ullmann polycondensation. Aryl halides (or heteroarylhalides) can be dimerized using the Ullmann coupling reaction; similarly, aryl dihalides can be polymerized (Figure 4.4). Homopolymerizations have been relatively successful using this technique.<sup>195,196,197</sup>

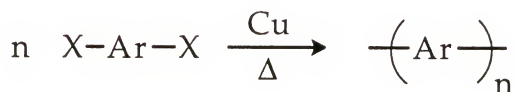


**Figure 4.4:** General Ullmann coupling polymerization

While it has been nearly one hundred years since the discovery of the Ullmann reaction,<sup>198</sup> the reaction mechanism remains unknown. The general process the reaction is thought to follow is shown in Figure 4.5,<sup>199</sup> though the pathways to the intermediates, as well as the geometries of the intermediates, are unknown. The first step of the reaction is generally thought to be initiated by copper abstracting a halogen atom from an aromatic (or heteroaromatic) species, but subsequent steps are widely contested. Suggestions for the reactive intermediates include aryl free radicals,<sup>200,201</sup> copper-aryl species,<sup>202,203</sup> or surface-bound aryl groups,<sup>204,205</sup> and evidence for all three types of intermediates has been found. While specifics of this

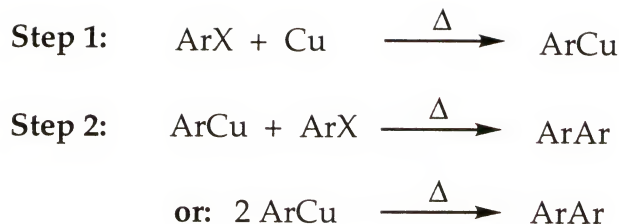


**Figure 4.5:** Pathway of the Ullmann coupling reaction

mechanism are beyond the scope of this work, it is important to note that a wide variety of copper species have been used successfully, ranging from freshly precipitated copper powder to copper (I) species. Recent work suggests that either clean copper metal<sup>206</sup> or copper (I) species<sup>203</sup> (which may be generated in solution by dissolution of the copper metal or oxide<sup>207,208</sup>) is the active constituent.

The Ullmann coupling reaction was used in attempts to polymerize Br<sub>2</sub>BEDOT-B(OC<sub>16</sub>H<sub>33</sub>)<sub>2</sub> (**5d**). The reaction was attempted using freshly prepared copper powder, activated copper-bronze, CuCl<sub>2</sub>, and CuI, all of which have been shown to be useful in aryl coupling reactions. Specifically, CuI has been particularly useful in the coupling of aryl bromides.<sup>209</sup> Greatly improved coupling yields from aryl bromides using CuI may be due to exchange of bromine for iodine, producing the more reactive aryl iodide. While Ullmann coupling polymerizations of **5d** using freshly prepared copper powder, activated copper-bronze, and CuCl<sub>2</sub> were all unsuccessful (returning starting material in each case), polymerization of **5d** using CuI yielded polymer **6d**, as

shown in Figure 4.6. Importantly, this polymer has a repeat unit identical to that prepared by oxidative polymerization of **3d**.

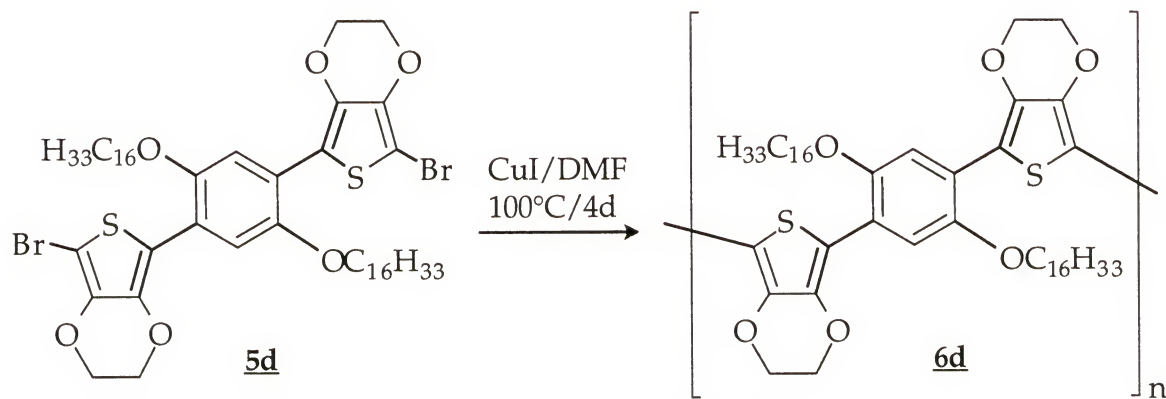


**Figure 4.6:** Ullmann coupling polymerization of **5d**

Theoretically, the end groups in this reaction should be a combination of bromine and hydrogen, with the latter resulting from hydrolysis of metal-coordinated chain ends during quenching. However, in the cases of polypyrroles<sup>195</sup> and polythiophenes<sup>196</sup> prepared using Ullmann coupling reactions, no bromine remained in the polymers. Pomerantz and coworkers state that no bromine was found by elemental analysis of the polythiophenes they prepared,<sup>196</sup> and Meijer's group used <sup>1</sup>H NMR to determine that the endgroups in their polypyrroles were entirely hydrogens.<sup>195</sup> Since their reactions were not exposed to water, they attribute the hydrogen end groups to reductive debromination of the chain ends by the solvent, DMF, which was the only source of hydrogen available.

<sup>1</sup>H NMR analysis of polymer **6d** revealed three phenyl H per thiaryl H, which would correspond to a trimer with H end groups. With a  $M_w$  of 3000

and a  $M_n$  of 2900 ( $M_w/M_n=1.1$ ), the GPC trace is also suggestive of a trimer ( $X_n=3.5$ , ~10 rings); the product also has a very low polydispersity. The solution UV-Vis-nIR spectrum of **6d** revealed a band gap of 2.08eV, virtually identical to that observed in oxidatively prepared polymer **4d** with the same repeat (2.1eV in solution).

#### Modified Ullmann polycondensation.

A modification of the Ullmann coupling reaction allows for lithiated aromatics (or heteroaromatics) to undergo copper-mediated coupling.<sup>210</sup> Because the copper-mediated coupling immediately follows lithiation in a one-pot synthesis, this method appears more attractive than the coupling of brominated species, since often the brominated species must be prepared from the aromatic species and purified before subsequent coupling reactions can occur. However, the inability to purify the lithiated species prior to coupling may limit molecular weights in polymerizations, as it is difficult to ensure exact stoichiometry.

To evaluate the use of the modified Ullmann coupling polymerization in the synthesis of polybisEDOTdialkoxybenzenes, several attempts were made to polymerize the monomers with activated copper (Figure 4.7). Both dodecyl- (**3c**) and hexadecyl- (**3d**) substituted monomers were reacted with nBuLi and then exposed to activated copper-bronze. In each case, no polymerization occurred; starting materials were isolated. Believing that this might be a lithiation problem, the reaction was repeated with *sec*-BuLi and **3d**.

Again, only starting material (>95% recovery) was isolated; a trace amount of dimer was detected by HRMS.

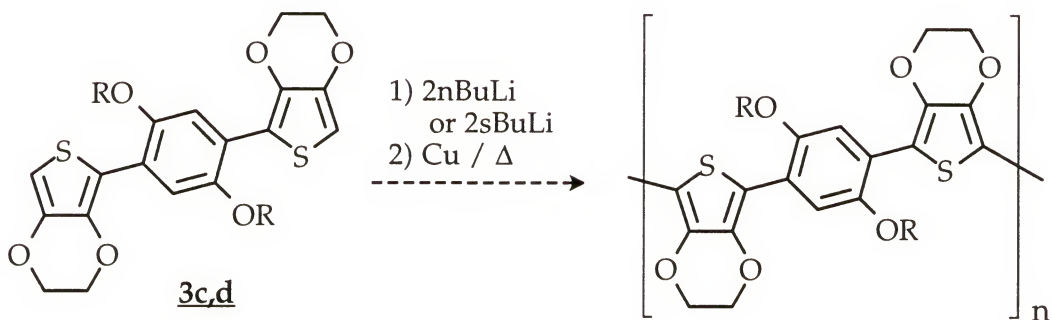


**Figure 4.7:** Attempts at modified Ullmann coupling polymerization of **3c,d**

The inability to lithiate these compounds is not unprecedented; other groups have reported difficulties in standard lithiations of thiophene oligomers, noting that the longer and more electron rich the oligomer, the more difficult lithiation becomes.<sup>211,212</sup> To better understand the difficulties encountered during lithiation attempts, an NMR study was conducted. Three samples of compound **3d** were dissolved in deuterated THF under inert atmosphere, and their <sup>1</sup>H NMR spectra were observed. The samples were then chilled to -78°C, where **3d** precipitated from solution. At this temperature, *n*-, *sec*-, and *tert*-butyl lithium were added to the samples (to examine the effectiveness of stronger lithiating agents), which were allowed to warm to room temperature with mixing. NMR spectra of all samples were examined, both immediately and after ten minutes. With all the samples, only partial lithiation occurred immediately, as evidenced by a partial

decrease in the thienyl  $^1\text{H}$  NMR absorbance accompanied by splitting of the ethylenedioxy and phenyl  $^1\text{H}$  NMR absorbances. Almost no change was observed after ten minutes, indicating that the reaction is not rapid, even with *tert*-butyl lithium at room temperature. Evidence of undesirable side reactions was found in the *sec*- and *tert*-butyl lithiation spectra, where small peaks unattributable to the monomer evolved, accompanied by splitting of the expected alkyl  $^1\text{H}$  NMR absorbances.

Further examination after an hour at room temperature in inert atmosphere revealed that lithium-deuterium exchange had occurred, presumably by deuterium abstraction from THF- $\text{d}_8$ . These results suggest that only partial lithiation of **3d** is possible before hydrogen exchange occurs (Figure 4.8). The increased solubility of **3a** in THF at  $-78^\circ\text{C}$  makes lithiation possible at lower temperatures, avoiding hydrogen exchange.

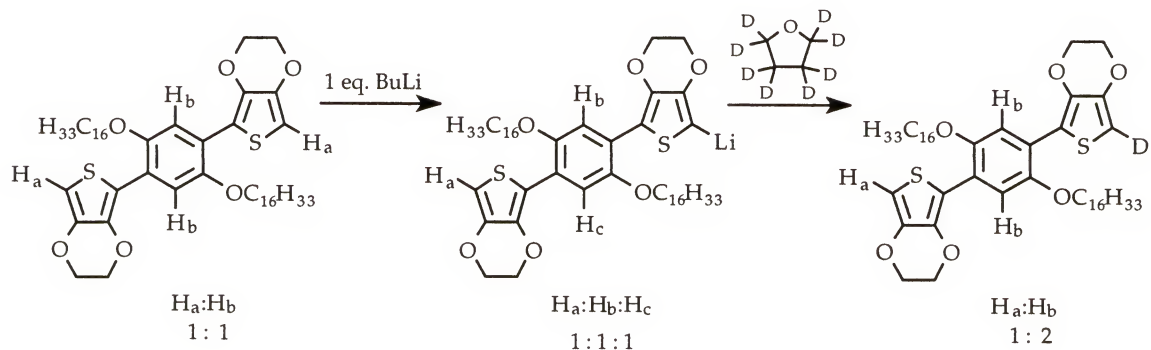


**Figure 4.8:** Lithiation of **3d** and subsequent deuterium exchange

#### 4.3.2 Heterocoupling Polymerizations

Stille coupling polymerizations. In non-oxidative chemical polymerizations to yield thiophene-based conducting polymers, the highest molecular weights have been obtained using the Stille reaction.<sup>38,116</sup> This reaction involves the palladium-catalyzed coupling of a bistrialkylstannylarylene with an aryl dihalide (see Chapter 2 for more information on the mechanism of this type of aryl-aryl coupling reactions). The Stille reaction is advantageous because it can tolerate a wide variety of functional groups and the organometallic species (a trialkylstannylarylene) is relatively stable, allowing it to be purified (hence the higher molecular weights) and stored prior to use.<sup>115</sup> For these reasons, the Stille coupling reaction has been widely used in the synthesis of conjugated polymers.<sup>41,117,213,214,215,216,217</sup>

2, 5-Bis(trimethylstannyl)EDOT (**8**) was prepared for use in coupling with **2d** (Figure 4.9) as well as with **5d** (Figure 4.10). The polymers produced from these reactions have, respectively, one-to-one and three-to-one EDOT-to-dialkoxybenzene. Together with the Ullmann-coupled polymer **6d** (two-to-one), which has a repeat unit identical to that of the oxidatively-prepared polymer **4d**, these polymers could be used to examine the effect of increasing EDOT content in the polymer chain. While organic tin compounds are more stable than their zinc halide or magnesium halide counterparts, 2, 5-bis(trimethylstannyl)EDOT decomposes fairly rapidly

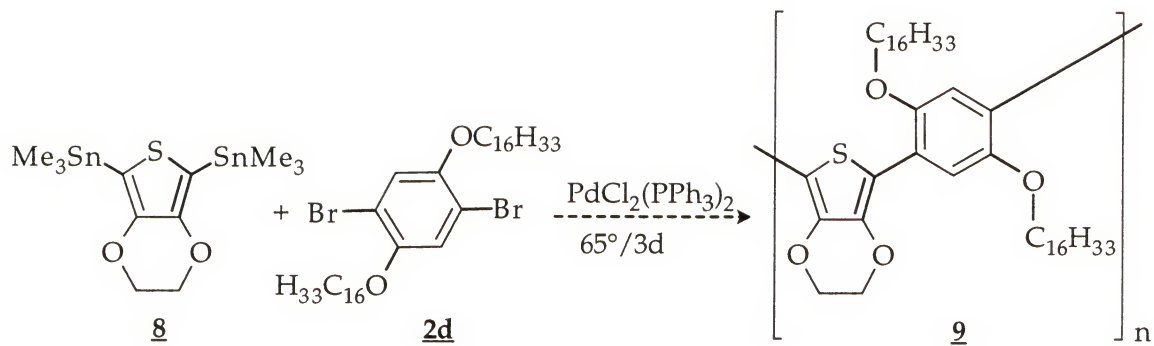


**Figure 4.9:** Attempted Stille coupling polymerization using dibrominated phenylene **2d**

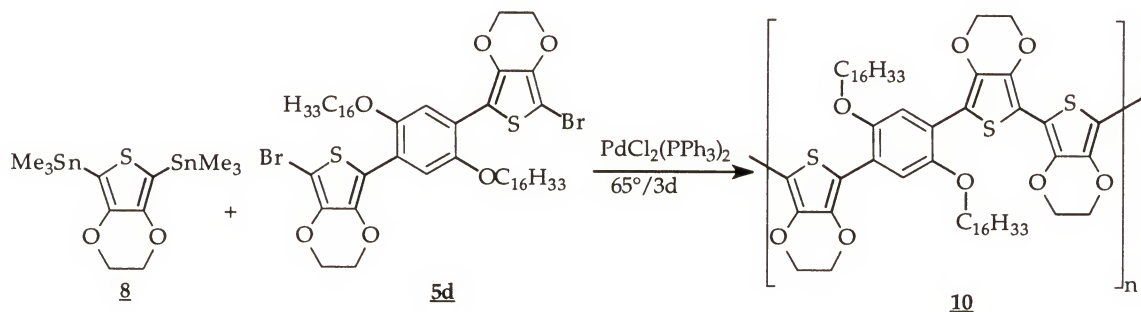


**Figure 4.10:** Stille coupling polymerization using dibrominated compound **5d**

(discoloration begins within 24h in inert atmosphere at 0°C in the dark), and it must be used immediately.

Repeated attempts to polymerize **8** with **2d** were unsuccessful, yielding only starting material. Reports of successful Stille coupling polymerizations of 1,4-dialkoxy-2,5-dibromobenzenes with 2,5-bistrialkylstannylthiophenes can be found in the literature,<sup>215,218</sup> suggesting that unfavorable steric or electronic interactions with the ethylenedioxy bridge prevent the coupling shown in Figure 4.9.

Polymerization of **8** with **5d** was successful, yielding polymer **10**. GPC of the polymer revealed three repeat units (corresponding to 12 rings), with relatively low polydispersity ( $M_w/M_n=3500/2900=1.2$ ).  $^1\text{H}$  NMR showed broadened peaks in the anticipated locations; no terminal thiaryl H was visible for confirmation of the GPC results.

The UV-Vis spectrum of **10** in chloroform revealed a band gap of 1.7eV, considerably lower than those of all the other polymers reported here, which typically exhibit band gaps around 2.0eV. The lower band gap is consistent with the increased EDOT content of **10** (polyEDOT exhibits a bandgap of 1.6eV<sup>67</sup>).

Suzuki coupling polymerizations. The Suzuki polymerization, which has been widely used in the synthesis of poly-*p*-phenylenes,<sup>219,220,221,222,223</sup> can also be used in the synthesis of thiylene/phenylene polymers.<sup>39,224</sup> In this reaction, a benzene diboronic acid (or diboronic ester for greater stability) is polymerized with a dibromoarylene in the presence of a palladium catalyst<sup>225</sup> (for a general mechanism applicable to this reaction, see Figure 2.4).

In a successful test of this premise, 1,4-bis(2-bisthiaryl)benzene (**12**) was prepared in 85% yield from bisneopentylglycol-1,4-phenylene diboronate (**11**) and 2-bromothiophene (Figure 4.11). Compound **5d** was then polymerized with compound **11** (Figure 4.12) to give a chloroform-soluble polymer with five repeat units, or 20 rings ( $M_w=5200$ ,  $M_n=4700$ , polydispersity 1.1).

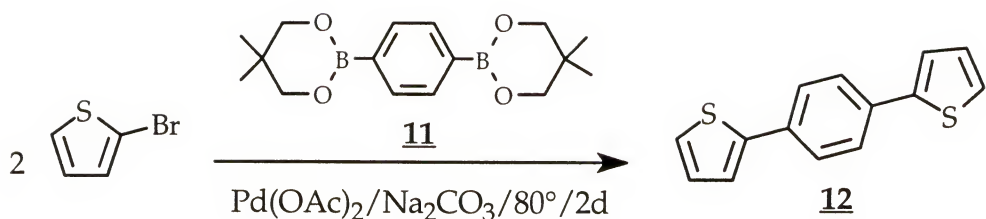


**Figure 4.11:** Suzuki model reaction

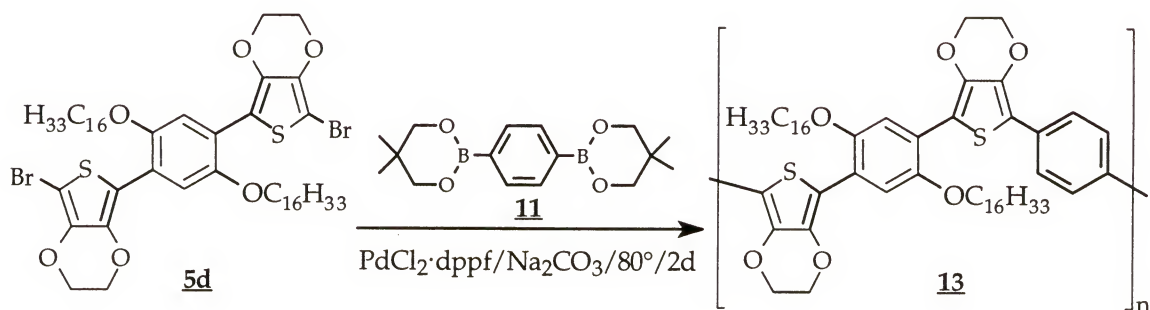


**Figure 4.12:** Suzuki polymerization of 5d

The <sup>1</sup>H NMR spectrum of this polymer, which readily dissolves in chloroform, reveals broad peaks and complex splitting in the phenylene region. This is expected due to the presence of three types of phenylene hydrogens in the repeat unit of the polymer; additional complexity should arise from asymmetries at the chain ends. It is not possible to obtain definitive information about molecular weight from the NMR spectrum, as the terminal phenyl hydrogens could not be discerned from internal phenyl hydrogens. A very small thienyl hydrogen peak is present, integrating at one per every forty phenylene hydrogens. This corresponds fairly well to a polymer containing one phenylene and one thiophene chain end, with six

repeat units (37 phenylene H per thiophene H) and is within one repeat unit of the GPC results.

Polymer **13** differs from all the other polymers described here in that it contains a phenylene that is not alkoxy-substituted. The polymer is therefore less electron-rich than the other polymers, and the change in the electronics can be seen in the UV-Vis spectrum of the polymer. The UV-Vis-nIR spectrum of this polymer in CHCl<sub>3</sub> reveals a band gap of 2.4eV. The other polymers studied here are more electron-rich, with band gaps ranging from 1.8 to 2.0eV (or around 2.1eV in solution). Indeed, while the other polymers are red or orange in their reduced states, polymer **13** is brilliant yellow in color.

#### 4.4 Comparison of Polymer Properties

The ability to prepare many structurally similar polymers using a variety of techniques makes it possible to examine the effects of polymer structure on properties. PBEDOT-B(OC<sub>16</sub>H<sub>33</sub>)<sub>2</sub> (**4d**, **6d**) has been prepared using electrochemical and chemical oxidations as well as using non-oxidative coupling techniques, specifically the Ullmann coupling reaction. A variety of molecular weights have been attained, from nearly monodisperse trimer (**6d**) to broad polydisperse polymer prepared electrochemically, to narrow polydispersity polymers of various molecular weights from chemical oxidations.

With the variety of molecular weights (Table 4.3) available in PBEDOT-B( $\text{OC}_{16}\text{H}_{33}$ )<sub>2</sub> (**4d** and **6d**), it is possible to examine the effect of molecular weight on optical properties of the polymer. GPC of electrochemically prepared **4d** reveals a very broad molecular weight distribution ( $M_w/M_n=19,500/2,600=7.5$ ), with the number of repeats ranging from 3 to 23. With only 3 or 4 repeat units in some of the chemically-prepared polymers described here, it seems possible that a higher conjugation length might occur in the electrochemically-prepared polymers, and that their interesting electronic properties are a result of the higher molecular weight fractions. However, a comparison of the onset of the  $\pi$  to  $\pi^*$  transitions in the solution spectra of the monomer, trimer, and the hexadecamer prepared using  $\text{Fe}(\text{ClO}_4)_3$  reveals that this is not the case. BEDOT-B( $\text{OC}_{16}\text{H}_{33}$ )<sub>2</sub> (**3d**) exhibits a single absorption in the UV-Vis-nIR spectrum, beginning around 3.1eV and peaking at 3.4eV. The polymer prepared by Ullmann polymerization is a nearly monodisperse trimer, with  $E_g=2.1\text{eV}$ . Both the electrochemically-prepared and  $\text{Fe}(\text{ClO}_4)_3$ -prepared polymers also exhibit solution  $E_g=2.1\text{eV}$ . This means that maximum conjugation length is attained somewhere between four and nine rings.

Also available for study are polymers similar to PBEDOT-B( $\text{OC}_{16}\text{H}_{33}$ )<sub>2</sub> (**4d**), which possess either an additional EDOT (Stille polymer **10**) or an unsubstituted phenylene (Suzuki polymer **13**). While all of the PBEDOT-B( $\text{OR}$ )<sub>2</sub> (**4a-f**, **6d**) exhibit similar band gaps (*ca.* 2.0eV), inclusion of these

**Table 4.3:** Molecular weights of polymers derived from BEDOT-B(OC<sub>16</sub>H<sub>33</sub>)<sub>2</sub>

Method	Polymer	$M_w$ (g/mol)	$M_n$ (g/mol)	$M_w/M_n$	$X_n^a$	# of rings <sup>b</sup>	$E_g$ (eV) <sup>c</sup>
Electrochemical	<b>4d</b>	19500	2600	7.5	3.1	9	2.1
FeCl <sub>3</sub>	<b>4d</b>	4400	4000	1.1	4.8	15	2.1
Fe(ClO <sub>4</sub> ) <sub>3</sub>	<b>4d</b>	23000	13500	1.7	16	48	2.1
CuBr <sub>2</sub>	<b>4d</b>	11000	3000	3.5	3.6	12	<sup>d</sup>
Ullmann	<b>6d</b>	3000	2900	1.1	3.5	9	2.1
Stille	<b>10</b>	3500	2900	1.2	3.2	12	1.7
Suzuki	<b>13</b>	5300	4700	1.1	5.2	20	2.4

<sup>a</sup> Determined by  $M_n/M_{rep}$ <sup>b</sup> Determined by multiplication of GPC  $X_n$  values by the number of rings per repeat unit<sup>c</sup> For polymer solutions in CHCl<sub>3</sub><sup>d</sup> Could not be determined

additional groups shifts the bandgap by varying the electron density of the polymer. The incorporation of an additional, electron-rich EDOT lowers the bandgap to 1.7, and incorporation of a single electron-deficient *p*-phenylene ring (notably different from the electron-rich alkoxy-substituted phenylene rings incorporated in monomer **3d**) raises the bandgap to 2.4eV, which is significant enough to shift the color of the polymer from red to yellow (Figure 4.13).

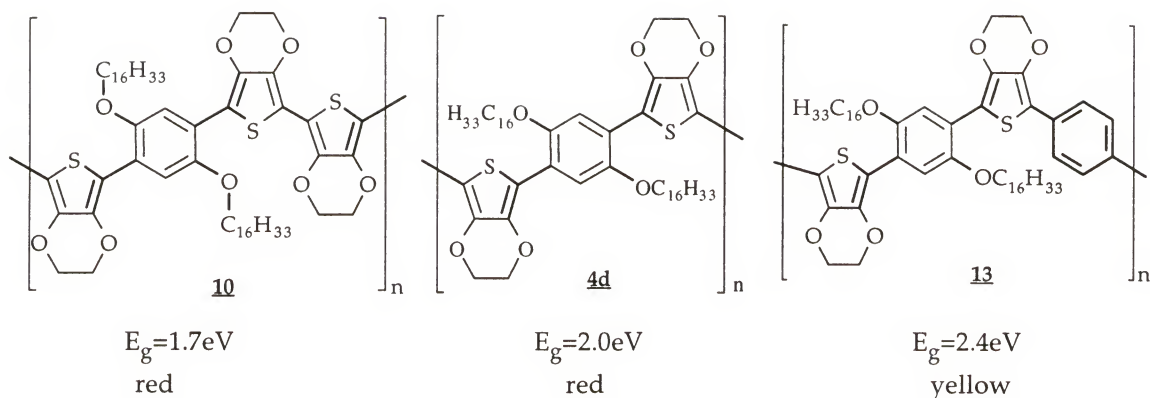


**Figure 4.13:** Effect of structural modification on bandgap

## 4.5 Experimental

### 4.5.1 Materials

Compounds **1** and **3a-f** were prepared and purified as described in Chapter 2.  $\text{FeCl}_3$ , activated Cu-bronze,  $\text{CuI}$ ,  $\text{CuBr}_2$ ,  $\text{FcPF}_6$ ,  $\text{Fe}(\text{ClO}_4)_3$ ,  $\text{SnMe}_3\text{Cl}$  in THF (1.0M).  $\text{Pd}(\text{OAc})_2$ ,  $\text{Pd}(\text{PPh}_3)_4$ ,  $\text{NiCl}_2\text{:dppp}$ , 1-bromoeicosane, hydrazine monohydrate, and 2-bromothiophene were obtained from Aldrich and used as received. THF, DMF, *n*-BuLi, *sec*-BuLi, and *tert*-BuLi were obtained from Aldrich in Sure Seal bottles and used as received.  $\text{NH}_4\text{OH}$ ,  $\text{CHCl}_3$ ,  $\text{CH}_3\text{OH}$ ,  $\text{NaHCO}_3$ , HCl, KOH, acetone, Celite, and  $\text{Na}_2\text{SO}_3$  were obtained from Fisher Scientific and used as received. NBS was purchased from Aldrich, recrystallized from water and stored *in vacuo* prior to use. Dichloro[1,1'-bis(diphenylphosphino)ferrocene]palladium (II) ( $\text{PdCl}_2\text{:dpff}$ ) was purchased from Strem and used as received. EDOT was obtained from AG Bayer and

purified as outlined in section 2.3.3. Bisneopentylglycol-1,4-phenylene diboronate (**11**) was prepared according to a literature procedure.<sup>112</sup>

#### 4.5.2 Characterization

NMR spectra were obtained in solution and recorded on a Gemini 300 MHz or a VXR 300 MHz FT-NMR spectrophotometer. Elemental analyses were obtained from Robertson Microlit Laboratories, Inc., Madison, NJ. Mass spectra were obtained using a Finnigan MAT 95Q mass spectrometer.

Gel permeation chromatography (GPC) was performed using a Waters Associates Liquid Chromatograph 757 UV absorbance detector at 500nm and a Perkin-Elmer LC-25 RI detector. All molecular weights are relative to polystyrene standards. Polymer samples were prepared in CHCl<sub>3</sub> (10mg/mL), passed through a 50μm filter, and injected successively through 5 × 10<sup>3</sup> Å and 5 × 10<sup>4</sup> Å Phenogel columns (crosslinked polystyrene gel) at a flow rate of 1mL/min. Retention times were calibrated against polystyrene standards (Scientific Polymer Products, Inc.). The molecular weights ( $M_p$ ) of the polystyrene standards used were the following: 1,900, 7,700, 12,000, 30,000, 48,900, 59,000, 79,000, 139,400, 650,000 g/mol. All polydispersities ( $M_w/M_n$ ) of the polymer standards used were less than 1.07.

#### 4.5.3 Synthesis

Poly{1,4-bis[2-(3,4-ethylenedioxy)thienyl]-2,5-didodecyloxybenzene} (4c).

A solution of  $\text{FeCl}_3$  ( $2.75 \times 10^{-3}$  mol) in  $\text{CHCl}_3$  (5mL) was added dropwise to a stirring solution of **3c** ( $6.88 \times 10^{-4}$  mol) in chloroform (15mL). The black mixture was stirred under argon for 24h, then added dropwise to rapidly stirring methanol (200mL). The black solid was collected by filtration and washed with successive portions of methanol and water. The black powder was reduced by rapid stirring in concentrated ammonium hydroxide (75mL) and  $\text{CHCl}_3$  (75mL) for 20h. The red  $\text{CHCl}_3$  solution was isolated, washed with water until neutral, and concentrated under reduced pressure. The solution was then precipitated into rapidly stirring methanol to yield a brick red powder that was collected by filtration and washed with methanol, then dried under vacuum. The resultant brick-red powder was insoluble or very poorly soluble in a broad range of organic solvents, with highest solubility in  $\text{CHCl}_3$ . [no mp below 300°C, 92% yield].

Poly{1,4-bis[2-(3,4-ethylenedioxy)thienyl]-2,5-dihexadecyloxybenzene}

(4d). Compound **4d** was prepared according to the procedure described for **4c** using **3d** ( $2.98 \times 10^{-4}$  mol) and  $\text{FeCl}_3$  ( $2.98 \times 10^{-4}$  mol to  $5.96 \times 10^{-4}$  mol), resulting in a poorly soluble brick red powder. [no mp below 300°C, 91% yield].

Poly{1,4-bis[2-(3,4-ethylenedioxy)thienyl]-2,5-di(2-ethyl)hexyloxy-

benzene} (4e). Compound **4e** was prepared according to the procedure

described for **4c** using **3e** ( $8.19 \times 10^{-4}$  mol) and  $\text{FeCl}_3$  ( $8.19 \times 10^{-4}$  mol), resulting in a poorly soluble brick red powder. [no mp below 300°C, 91% yield].

Poly[1,4-bis[2-(3,4-ethylenedioxy)thienyl]-2,5-di(1,4,7-trioxanonyl)-benzene] (4f). Compound **4f** was prepared according to the procedure described for **4c** using **3f** ( $8.20 \times 10^{-4}$  mol) and  $\text{FeCl}_3$  ( $1.64 \times 10^{-3}$  mol), resulting in a poorly soluble brick red powder. [no mp below 300°C, 87% yield].

Poly[1,4-bis[2-(3,4-ethylenedioxy)thienyl]-2,5-dihexadecyloxybenzene] (4d) prepared using various oxidants. Samples of monomer **3d** were dissolved in  $\text{CHCl}_3$  (5mL) to give pale yellow solutions and deaerated with nitrogen. Oxidants were dissolved in acetone and added dropwise to the monomer solutions, causing the reaction mixtures to turn deep blue instantly. After deaerating with nitrogen, the reaction mixtures were sealed and stirred 18h at room temperature. The mixtures were then concentrated under reduced pressure and precipitated into methanol, yielding blue-black flakes in solutions of various colors (yellow for  $\text{CuBr}_2$  and  $\text{FcPF}_6$ , green for  $\text{FeCl}_3$ , and purple for  $\text{Fe}(\text{ClO}_4)_3$ ). These black solids were collected by filtration, dissolved (partially) in  $\text{CHCl}_3$ , and reduced with hydrazine hydrate. The mixtures all turned red within 1min; even after stirring 24h in 50mL  $\text{CHCl}_3$ , none of the samples dissolved completely except for the polymer from  $\text{Fe}(\text{ClO}_4)_3$ . The mixtures were washed with water until neutral and concentrated under reduced pressure to give viscous red-black liquids that were precipitated into methanol. The resultant brick-red precipitates were

collected by filtration, washed with methanol, and dried under vacuum. (Exception: polymer from  $\text{FcPF}_6$  would not precipitate and could not be analyzed further.) [no mp below 300°C for isolated solids, yields given in Table 4.4 below].

**Table 4.4:** Concentrations used in oxidative polymerization of BEDOT-B( $\text{OC}_{16}\text{H}_{33}$ )<sub>2</sub> with various oxidants

Oxidant	Moles oxidant	Moles <b>3d</b>	% Yield of <b>4d</b>
$\text{FeCl}_3$	$1.229 \times 10^{-4}$	$6.494 \times 10^{-5}$	88
$\text{CuBr}_2$	$1.332 \times 10^{-4}$	$6.660 \times 10^{-5}$	82
$\text{FcPF}_6$	$1.213 \times 10^{-4}$	$6.065 \times 10^{-5}$	—
$\text{Fe}(\text{ClO}_4)_3$	$1.172 \times 10^{-4}$	$5.862 \times 10^{-5}$	91

1,4-Bis[2-(5-bromo-3,4-ethylenedioxy)thienyl]-2,5-dimethoxy-benzene

**(5a).** A solution of **3a** ( $2.39 \times 10^{-3}$  mol) in THF (60mL) was chilled to  $-78^\circ\text{C}$  under argon, and NBS ( $5.26 \times 10^{-3}$  mol) was slowly added under positive argon flow. This pale yellow mixture was warmed to  $0^\circ\text{C}$ , causing the reaction mixture to darken to a deep green color. The reaction mixture was stirred at  $0^\circ\text{C}$  for 18h, and then  $\text{Na}_2\text{SO}_3$  ( $1.59 \times 10^{-2}$  mol) was added. After stirring for an additional 10 minutes, the reaction mixture was filtered through paper and concentrated under reduced pressure to give a tan solid which was recrystallized from THF/methanol to give **5a** [no mp below 375°C, 90% yield]. Anal. calcd for  $\text{C}_{20}\text{H}_{16}\text{Br}_2\text{O}_6\text{S}_2$ : C, 41.69; H, 2.80; Br, 27.73; O, 16.66; S, 11.13. Found: C, 41.89; H, 2.87; Br, 27.54; S, 11.04.  $^1\text{H}$  NMR ( $\text{C}_6\text{D}_6$ , ppm): 7.91 (s), 3.55 (s), 3.34 (m). HRMS calcd for  $\text{C}_{20}\text{H}_{16}\text{Br}_2\text{O}_6\text{S}_2$ : 573.8755; found, 573.8796.

1,4-Bis[2-(5-bromo-3,4-ethylenedioxy)thienyl]-2,5-dihexadecyloxy-

benzene (5d). Compound **5d** was prepared according to the procedure described for **5a** using **3d** ( $1.19 \times 10^{-3}$  mol), NBS ( $2.62 \times 10^{-3}$  mol), and  $\text{Na}_2\text{SO}_3$  ( $1.59 \times 10^{-2}$  mol), resulting in a yellow solid that was recrystallized from THF/methanol [mp 127-129°C, 63% yield]. Anal calcd. for  $\text{C}_{50}\text{H}_{76}\text{Br}_2\text{O}_6\text{S}_2$ : C, 60.23; H, 7.68; Br, 16.03; O, 9.63; S, 6.43. Found: C, 60.07; H, 7.59; Br, 15.61; S, 6.51.  $^1\text{H}$  NMR ( $\text{CDCl}_3$ , ppm): 7.67 (s), 4.30 (s), 4.02 (t), 1.83 (p), 1.52 (p), 1.23 (m), 0.86 (t).  $^{13}\text{C}$  NMR ( $\text{CDCl}_3$ , ppm): 148.57, 139.33, 137.84, 120.42, 113.76, 112.69, 88.18, 75.94, 69.91, 64.77, 55.84, 31.91, 29.70, 29.42, 29.35, 29.26, 26.27, 22.67, 14.11. HRMS calcd for  $\text{C}_{50}\text{H}_{76}\text{Br}_2\text{O}_6\text{S}_2$ : 994.3450; found, 994.3450.

Poly{1,4-bis[2-(3,4-ethylenedioxy)thienyl]-2,5-dihexadecyloxybenzene}

(6d). DMF (50mL) was added to **5d** ( $5.015 \times 10^{-4}$  mol) under argon to give a pale green mixture. Upon heating to 60°C, all solids dissolved, giving a pale orangebrown, nonfluorescent solution. The solution was heated to 100°C, and CuI ( $2.6254 \times 10^{-4}$  mol) was added. Within 5h, the reaction mixture began to fluoresce under UV light. Greenbrown solid had precipitated, and the reaction had become brighter orange. After a complete reaction time of 4d, the reaction mixture was concentrated under reduced pressure, allowed to cool to room temperature, and poured into ice water. After melting, the mixture was extracted with  $\text{CH}_2\text{Cl}_2$ , and the organic layer was dried over  $\text{MgSO}_4$ , filtered through paper, and concentrated under reduced pressure to give a cloudy orange mixture that upon cooling yielded an orange-red

precipitate. This was collected by vacuum filtration, washed with methanol, and dried under vacuum [no mp below 300°C, 93% yield]. Anal. calcd for C<sub>50</sub>H<sub>76</sub>O<sub>6</sub>S<sub>2</sub>: C, 71.73; H, 9.15; O, 11.47; S, 7.66; Br, 0. Found: C, 55.22; H, 7.98; Br, 2.38. <sup>1</sup>H NMR (CDCl<sub>3</sub>, ppm): 7.65 (d), 6.95 (s), 4.36 (m), 4.25 (bm), 4.08 (s), 1.86 (bm), 1.55 (bm), 1.23 (s), 0.85 (t).

2,5-Bis(trimethylstannyl)-3,4-ethylenedioxythiophene (8). EDOT (5.0g, 0.035 mol) was dissolved in anhydrous diethyl ether (50 mL) and cooled to -78 °C, then *n*-butyl lithium (28.1 mL of a 2.5 M solution in hexanes) was added via syringe. The reaction mixture was allowed to stir for 1h before a solution of trimethylstannyl chloride (140 mL of 1M solution in methylene chloride) was added. After stirring 1h at 78°C, the reaction mixture was allowed to warm to room temperature, where it was stirred an additional 24h. The reaction mixture was concentrated under reduced pressure, and the remaining brown oil was distilled under vacuum to yield a white solid [bp 110°C at 0.1 torr, 64% yield]. <sup>1</sup>H NMR (CDCl<sub>3</sub>, ppm): 0.33 (s), 4.14 (s). This compound is not very stable to storage under inert atmosphere at 0°C, precluding full characterization. Compound **8** was therefore used immediately after distillation.

Poly(5,5'-{1,4-bis[2-(3,4-ethylenedioxy)thienyl]-2,5-dihexadecyloxy- benzene}-alt-2,5-(3,4-ethylenedioxythiophene) (10). Compound **5d** ( $2.939 \times 10^{-4}$  mol) was combined with **8** ( $2.779 \times 10^{-4}$  mol) and PdCl<sub>2</sub>(PPh<sub>3</sub>)<sub>2</sub> ( $5.7 \times 10^{-6}$  mol)

and dissolved in THF (50mL) under argon. The yellow, non-fluorescent reaction mixture was heated at reflux with stirring for 3d, after which time it had darkened to a deep red and fluoresced under UV light. Activated charcoal and Celite were then added and allowed to stir for an additional 2h, and the mixture was filtered through paper. The filtrate was concentrated under reduced pressure and precipitated into acetone/water (equal volumes) to give a red-black precipitate which was collected by filtration to yield 200mg crude polymer. This product was extracted repeatedly with refluxing acetone to remove starting materials, and the remaining acetone-insoluble polymer was collected and dried under vacuum [no mp below 300°C, 51% yield]. Anal. calcd for  $C_{56}H_{80}O_8S_3$ : C, 73.97; H, 8.42; O, 13.09; S, 9.84; Br, 0. Found: C, 60.80. H, 8.57; Br, 0.  $^1H$  NMR ( $CDCl_3$ , ppm): 7.65 (d), 4.30 (s), 4.02 (t), 1.86 (p), 1.54 (m), 1.23 (m), 0.855 (t).

1,4-Bis(2-thienyl)benzene (12). Compound **11** ( $1.66 \times 10^{-3}$ mol),  $Na_2CO_3$  ( $9.93 \times 10^{-3}$ mol), and  $Pd(OAc)_2$  ( $2.78 \times 10^{-4}$ mol) were combined and deaerated with argon. An argon-deaerated solution of 2-bromothiophene ( $3.97 \times 10^{-3}$ mol) in DMF/ $H_2O$  (24mL/12mL) was added to the solids, giving a colorless solution that quickly darkened to dark brown. The reaction mixture was heated at 80°C under argon for 48h, with additional  $Pd(OAc)_2$  ( $2.78 \times 10^{-4}$ mol) added after 24h. The reaction mixture was cooled, precipitated into water, and filtered to yield a gray solid that was dissolved in  $CH_2Cl_2$ , washed with water, and dried over  $MgSO_4$ . Charcoal was added to absorb palladium salts, and the mixture

was filtered through Celite and concentrated under reduced pressure to yield a tan powder that was recrystallized from methanol. [mp 130-132°C, dec (lit.<sup>54,226</sup> mp 128-131°C, dec), 78% yield]. <sup>1</sup>H NMR (CDCl<sub>3</sub>, ppm): 7.63 (s), 7.35 (dd), 7.30 (dd), 7.10 (t).

Poly(5,5'-{1,4-bis[2-(3,4-ethylenedioxy)thienyl]-2,5-dihexadecyloxy-benzene}-alt-1,4-phenylene) (13). Compound **5d** (7.361x10<sup>-4</sup>mol), compound **11** (7.361x10<sup>-4</sup>mol), sodium bicarbonate (7.36x10<sup>-3</sup>mol), and PdCl<sub>2</sub>dppf (1.01 x 10<sup>-5</sup>mol) were combined and deaerated by evacuating and filling with argon three times. Water (5mL) and THF (30mL) were deaerated with argon for 30 minutes and added to the reaction flask. The mixture was stirred and heated at 75°C for 3 days. The reaction solution fluoresced yellow/green upon illumination with a UV lamp shortly after reaching the desired temperature. The reaction mixture was cooled and concentrated under reduced pressure. The solution was precipitated into cold methanol and collected by filtration. The red material was rinsed with methanol and water, dried in an air stream, and then dried *in vacuo* at 60°C. [63% yield]. Anal. calcd for C<sub>56</sub>H<sub>80</sub>S<sub>2</sub>O<sub>6</sub>: C, 73.64; H, 8.83; S, 7.02. Found: C, 68.86; H, 8.68; S, 5.95; Br, 5.12. <sup>1</sup>H NMR (CDCl<sub>3</sub>, ppm): 0.86 (bm), 1.24 (bm), 1.50 (bm), 1.82 (bm), 4.03 (bm), 4.30 (bm), 6.36 (s), 7.67 (bm).

## CHAPTER 5 CONCLUDING REMARKS

### 5.1 Monomer Synthesis

Through the use of a modified bromination reaction, 1,4-dibromohydroquinone can be prepared in good purity from hydroquinone. The ability to prepare large amounts of this compound makes possible the synthesis of 1,4-dialkoxy-2,5-dibromobenzenes (**2a-f**) in fewer total reactions.

These 1,4-dialkoxy-2,5-dibromobenzenes have been used to prepare highly electron-rich monomers, 1,4-bis[2-(3,4-ethylenedioxy)thienyl]-2,5-dialkoxybenzenes (BEDOT-B(OR)<sub>2</sub>, **3a-f**). For modification of polymer solubility, alkoxy substituents have been varied from the short-chain methoxy substituent (**3a**) to longer chain heptoxy- (**3b**), dodecyloxy- (**3c**), and hexadecyoxy- (**3d**) substituents, as well as the branched 2-ethylhexyl substituent (**3e**) and an oligomeric ether substituent (**3f**). In the synthesis of these compounds, Negishi coupling reactions of EDOT-ZnCl with 1,4-dialkoxy-2,5-dibromobenzenes (**2a-f**) were necessary rather than the more commonly preferred (and shorter) Yamamoto coupling reactions due to the highly electron rich nature of this system. Yields in these were reactions were

for the most part good, with difficulty isolating the glyme-substituted monomer **3f** due to partial solubility of the monomer in water.

## 5.2 Electrochemistry

The monomers prepared in Chapter 2 efficiently electropolymerize at potentials considerably lower than conventional polyheterocycles to yield highly electroactive, electrochromic polymers. The majority of the polymers exhibit only one redox process, with oxidation occurring well below 0.0V. Most of the polymers are stable up to *ca.* 1.0V, leaving a broad potential window in which the polymers are stable conductors. Additionally, the polymers retain electroactivity over many redox cycles, allowing them to be used as polymer modified electrode materials.

The oligomeric ether-substituted polymer, **4f**, exhibits strong ion effects; while redox switching of **4f** in many perchlorate-based electrolytes yielded polymer oxidation peak potentials ( $E_{a,p}$ ) *ca.* -0.45V vs. Ag/Ag<sup>+</sup>, the peak potential was shifted to -0.15V in Ba(ClO<sub>4</sub>)<sub>2</sub>. To obtain a better understanding of these effects, further research is needed, including the examination of the effects of other electrolytes on  $E_{a,p}$ . The effect of ion concentration on the shift in  $E_{a,p}$  should also be investigated to determine the usefulness of this polymer in molecular recognition, as should the effect of changing electrolytes from polymerization to polymer switching.

Additionally, the effect of electrolyte choice on the polymer's UV-Vis-nIR spectrum should be examined.

These polymers are electrochromic, switching from red in the reduced state to blue when oxidized. All the electrochemically-prepared polymers exhibit solid state band gaps around 2.0eV, and band gaps are shifted to slightly higher energy in solution. Vibronic coupling visible in the spectra of films of polymers **4b-f** disappear in solution, as solid state interactions are eliminated.

An in-situ EPR study of several of these polymers revealed that the doping process which occurs upon oxidation is highly solvent dependent. In the presence of methylene chloride, polarons are formed during oxidation, with further oxidation resulting in near complete conversion of polarons into bipolarons. When only acetonitrile is used, the EPR-electrochemistry reveals that the polarons formed during oxidation are only partially converted into bipolarons. In either case, reduction results in complete regeneration of polarons, with further reduction resulting in complete conversion of polarons to the neutral state.

To further understand the nature of solvent-dependent polaron stability, end-capped monomers and dimers could be used to model the EPR-electrochemistry solution properties of the polymers. End-capping with groups that are inactive toward oxidative polymerization (at the relatively low potentials of interest here) would yield compounds that would be unable to polymerize, reversibly forming radical cations and perhaps (in the case of

end-capped dimers) dications. The EPR-electrochemistry of these compounds could be used to verify that the stable polarons seen in the absence of CH<sub>2</sub>Cl<sub>2</sub> are a result of film morphology; morphology effects would be limited in solution, and solvent effects on EPR-electrochemistry could easily be studied. Perhaps more importantly, the model study would also answer definitively whether bipolarons can be stabilized over six rings, based on the EPR-electrochemistry of the end-capped six-ring dimers. Toward this end, the synthesis of alkyl- and phenyl-capped monomers and dimers is currently underway.

The potential dependence of conductivity was explored for several of these polymers. Extremely low polymer oxidation potentials make PBEDOT-B(OR)<sub>2</sub> useful conductors over a much broader potential window than their thiophene analogs. Conductivity in propylene carbonate/tetrahydrofuran increases all the way through the polymer redox process, but this can not be used to determine the principal charge carrier in these materials (i.e. polaron or bipolaron), since the solvent dependence of polaron stability is so strong.

The interesting electronic and optoelectronic properties of these materials are likely to lead to further study in the areas of electrochromic devices, molecular recognition, and modified electrodes.

### 5.3 Chemical Polymerizations

Using a variety of polymerization techniques, soluble oligomers based on BEDOT-B(OR)<sub>2</sub> have been prepared. Oxidative polymerization using ferric perchlorate as an oxidizing agent produced soluble polymers with much higher molecular weights (16 repeat units, or 48 rings) than were obtained using any of the other chemical polymerization techniques. Further studies may determine the optimal ferric perchlorate concentration for maximum molecular weight and high solubility. The use of other oxidants may also be investigated to further study the effect of the anion on polymer properties; polymerizations using ferric tosylate and ferric dodecylbenzenesulfonate might be particularly interesting.

The dibromination of **4d** made possible a variety of non-oxidative coupling polymerizations. These reactions yielded polymers of similar molecular weights to those obtained using the most commonly used chemical oxidant, ferric chloride (3 to 5 repeat units, or 9 to 15 rings). Incorporation of an additional EDOT into the PBEDOT-B(OC<sub>16</sub>H<sub>33</sub>)<sub>2</sub> repeat unit lowers the polymer (**10**) bandgap to 1.7eV, while incorporation of a phenylene group raises the polymer (**13**) bandgap to 2.4eV. The availability of these non-oxidative coupling techniques should make it possible to prepare a wide range of homopolymers and copolymers. In this way, polymer properties can be finely tuned for a variety of applications.

APPENDIX  
X-RAY CRYSTAL DATA FOR BEDOT-B(OG)<sub>2</sub>

**Table A-1:** Crystal data and structure refinement for BEDOT-B(OG)<sub>2</sub>

Parameter	Attributes
Empirical formula	C <sub>30</sub> H <sub>38</sub> O <sub>10</sub> S <sub>2</sub>
Formula weight	622.72
Temperature	173(2) K
Wavelength	0.71073 Å
Crystal system	Monoclinic
Space group	P2(1)/n
Unit cell dimensions	a = 8.628(2) Å α = 90° b = 7.608(1) Å β = 93.96(1)° c = 22.422(3) Å γ = 90°
Volume, Z	1468.4(5) Å <sup>3</sup> , 2
Density (calculated)	1.408 Mg/m <sup>3</sup>
Absorption coefficient	0.239 mm <sup>-1</sup>
F(000)	660
Crystal size	0.32 x 0.28 x 0.17 mm
Theta range for data collection	1.82 to 27.50°
Limiting indices	-11≤h≤8, -9≤k≤9, -16≤l≤29
Reflections collected	10331
Independent reflections	3347 [R(int) = 0.0271]
Absorption correction	Integration
Max. and min. transmission	0.964 and 0.935
Refinement method	Full-matrix least-squares on F <sup>2</sup>
Data / restraints / parameters	3347 / 0 / 191
Goodness-of-fit on F <sup>2</sup>	1.062
Final R indices [I>2sigma(I)]	R1 = 0.0328, wR2 = 0.0836 [3059]
R indices (all data)	R1 = 0.0369, wR2 = 0.0871
Extinction coefficient	0.0022(12)
Largest diff. peak and hole	0.281 and -0.274 e.Å <sup>-3</sup>

**Table A-2:** Atomic coordinates ( $\times 10^4$ ) and equivalent isotropic displacement parameters ( $\text{\AA}^2 \times 10^3$ ) for BEDOT–B(OG)<sub>2</sub>: U(eq) is defined as one third of the trace of the orthogonalized  $U_{ij}$  tensor.

Atom	x	y	z	U(eq)
S	2563(1)	9588(1)	113(1)	32(1)
O1	2243(1)	6798(1)	1554(1)	26(1)
C1	1939(1)	7801(2)	519(1)	22(1)
O2	4102(1)	9935(1)	1772(1)	30(1)
C2	2512(1)	7974(2)	1107(1)	22(1)
O3	671(1)	7916(1)	-660(1)	32(1)
C3	2607(2)	7540(2)	2139(1)	28(1)
O4	675(1)	9706(1)	-2131(1)	27(1)
C4	4153(2)	8446(2)	2168(1)	29(1)
O5	1487(1)	9871(1)	-3376(1)	31(1)
C5	3435(2)	9500(2)	1217(1)	25(1)
C6	3568(2)	10489(2)	721(1)	33(1)
C7	960(1)	6387(2)	251(1)	22(1)
C8	309(2)	6451(2)	-342(1)	24(1)
C9	623(2)	4886(2)	583(1)	24(1)
C10	301(2)	7953(2)	-1287(1)	25(1)
C11	1018(2)	9632(2)	-1503(1)	24(1)
C12	1442(2)	11134(2)	-2396(1)	32(1)
C13	897(2)	11279(2)	-3045(1)	31(1)
C14	971(2)	10002(2)	-3992(1)	34(1)
C15	1537(2)	8431(2)	-4324(1)	44(1)

**Table A-3:** BEDOT-B(OG)<sub>2</sub> bond lengths

Bond	Length (Å)	Bond	Length (Å)
S-C1	1.7414(13)	C7-C8	1.409(2)
O1-C2	1.3745(14)	C8-C9#1	1.383(2)
O1-C3	1.4432(14)	C9-C8#1	1.383(2)
C1-C2	1.383(2)	C9-H9A	0.9500
C1-C7	1.469(2)	C10-C11	1.513(2)
O2-C5	1.374(2)	C10-H10A	0.9900
O2-C4	1.439(2)	C10-H10B	0.9900
C2-C5	1.420(2)	C11-H11A	0.9900
O3-C8	1.371(2)	C11-H11B	0.9900
O3-C10	1.4207(14)	C12-C13	1.502(2)
C3-C4	1.499(2)	C12-H12A	0.9900
C3-H3A	0.9900	C12-H12B	0.9900
C3-H3B	0.9900	C13-H13A	0.9900
O4-C11	1.4206(14)	C13-H13B	0.9900
O4-C12	1.424(2)	C14-C15	1.507(2)
C4-H4A	0.9900	C14-H14A	0.9900
C4-H4B	0.9900	C14-H14B	0.9900
O5-C13	1.418(2)	C15-H15A	0.9800
O5-C14	1.426(2)	C15-H15B	0.9800
C5-C6	1.355(2)	C15-H15C	0.9800
C6-H6A	0.9500		

**Table A-4:** BEDOT-B(OG)<sub>2</sub> bond angles

Bond	Angle (°)	Bond	Angle (°)
C6-S-C1	93.17(6)	C7-C9-H9A	119.1
C2-O1-C3	111.81(9)	O3-C10-C11	105.31(10)
C2-C1-C7	128.04(11)	O3-C10-H10A	110.7
C2-C1-S	108.69(9)	C11-C10-H10A	110.7
C7-C1-S	123.27(9)	O3-C10-H10B	110.7
C5-O2-C4	111.25(10)	C11-C10-H10B	110.7
O1-C2-C1	124.47(11)	H10A-C10-H10B	108.8
O1-C2-C5	121.73(11)	O4-C11-C10	106.75(10)
C1-C2-C5	113.80(11)	O4-C11-H11A	110.4
C8-O3-C10	119.19(10)	C10-C11-H11A	110.4
O1-C3-C4	110.88(10)	O4-C11-H11B	110.4
O1-C3-H3A	109.5	C10-C11-H11B	110.4
C4-C3-H3A	109.5	H11A-C11-H11B	108.6
O1-C3-H3B	109.5	O4-C12-C13	109.67(11)
C4-C3-H3B	109.5	O4-C12-H12A	109.7
H3A-C3-H3B	108.1	C13-C12-H12A	109.7
C11-O4-C12	111.91(10)	O4-C12-H12B	109.7
O2-C4-C3	110.26(10)	C13-C12-H12B	109.7
O2-C4-H4A	109.6	H12A-C12-H12B	108.2
C3-C4-H4A	109.6	O5-C13-C12	110.65(11)
O2-C4-H4B	109.6	O5-C13-H13A	109.5
C3-C4-H4B	109.6	C12-C13-H13A	109.5
H4A-C4-H4B	108.1	O5-C13-H13B	109.5
C13-O5-C14	110.83(10)	C12-C13-H13B	109.5
C6-C5-O2	123.73(12)	H13A-C13-H13B	108.1
C6-C5-C2	112.92(12)	O5-C14-C15	109.44(12)
O2-C5-C2	123.34(11)	O5-C14-H14A	109.8
C5-C6-S	111.42(10)	C15-C14-H14A	109.8
C5-C6-H6A	124.3	O5-C14-H14B	109.8
S-C6-H6A	124.3	C15-C14-H14B	109.8
C9-C7-C8	116.36(11)	H14A-C14-H14B	108.2
C9-C7-C1	120.94(11)	C14-C15-H15A	109.5
C8-C7-C1	122.69(11)	C14-C15-H15B	109.5
O3-C8-C9#1	122.83(11)	H15A-C15-H15B	109.5
O3-C8-C7	115.40(11)	C14-C15-H15C	109.5
C9#1-C8-C7	121.77(11)	H15A-C15-H15C	109.5
C8#1-C9-C7	121.87(11)	H15B-C15-H15C	109.5
C8#1-C9-H9A	119.1		

Symmetry transformations used to generate equivalent atoms:  
 #1 -x,-y+1,-z

**Table A-5:** Anisotropic displacement parameters ( $\text{Å}^2 \times 10^3$ ) for BEDOT-B(OG)<sub>2</sub>: the anisotropic displacement factor exponent takes the form:  
 $-2 \pi^2 [h^2 a^{*2} U_{11} + \dots + 2 h k a^* b^* U_{12}]$

Atom	U <sub>11</sub>	U <sub>22</sub>	U <sub>33</sub>	U <sub>23</sub>	U <sub>13</sub>	U <sub>12</sub>
S	47(1)	29(1)	21(1)	3(1)	-1(1)	-15(1)
O1	36(1)	25(1)	17(1)	2(1)	-3(1)	-9(1)
C1	26(1)	21(1)	20(1)	1(1)	2(1)	-3(1)
O2	41(1)	26(1)	23(1)	-1(1)	-6(1)	-9(1)
C2	24(1)	21(1)	21(1)	1(1)	2(1)	-2(1)
O3	51(1)	26(1)	17(1)	4(1)	-4(1)	-14(1)
C3	37(1)	29(1)	17(1)	-1(1)	-2(1)	-4(1)
O4	34(1)	27(1)	19(1)	5(1)	-1(1)	-9(1)
C4	34(1)	27(1)	24(1)	1(1)	-6(1)	-2(1)
O5	38(1)	28(1)	28(1)	6(1)	7(1)	7(1)
C5	29(1)	23(1)	23(1)	-3(1)	-1(1)	-4(1)
C6	44(1)	28(1)	27(1)	0(1)	-2(1)	-15(1)
C7	25(1)	22(1)	18(1)	-1(1)	1(1)	-3(1)
C8	30(1)	22(1)	18(1)	2(1)	2(1)	-4(1)
C9	30(1)	26(1)	17(1)	1(1)	-1(1)	-4(1)
C10	31(1)	26(1)	17(1)	3(1)	-2(1)	-4(1)
C11	29(1)	25(1)	20(1)	1(1)	-1(1)	-2(1)
C12	39(1)	28(1)	29(1)	5(1)	5(1)	-10(1)
C13	41(1)	23(1)	29(1)	7(1)	9(1)	3(1)
C14	41(1)	33(1)	28(1)	4(1)	7(1)	2(1)
C15	55(1)	39(1)	42(1)	-6(1)	16(1)	-1(1)

**Table A-6:** Hydrogen coordinates ( $\times 10^4$ ) and isotropic displacement parameters ( $\text{Å}^2 \times 10^3$ ) for BEDOT-B(OG)<sub>2</sub>.

Atom	x	y	z	U(eq)
H3A	2625	6594	2443	33
H3B	1791	8392	2231	33
H4A	4428	8842	2582	35
H4B	4962	7613	2053	35
H6A	4146	11550	712	40
H9A	1046	4786	984	29
H10A	-839	7960	-1377	30
H10B	743	6917	-1482	30
H11A	574	10663	-1306	29
H11B	2156	9623	-1408	29
H12A	2580	10942	-2357	38
H12B	1214	12240	-2187	38
H13A	-252	11260	-3086	37
H13B	1251	12410	-3206	37
H14A	1379	11094	-4163	40
H14B	-178	10050	-4034	40
H15A	1181	8520	-4748	67
H15B	1122	7354	-4155	67
H15C	2675	8397	-4285	67

## REFERENCES

<sup>1</sup> Natta, G.; Mazzanti, G.; Corradini, P. *Atti Acad. Naz. Lincei, Cl. Sci. Fis. Mat. Nat. Rend.* **1958**, 25, 3.

<sup>2</sup> Ito, T.; Shirakawa, H.; Ikeda, S. *J. Polym. Sci. Polym. Chem. Ed.* **1974**, 12, 11.

<sup>3</sup> Shirakawa, H.; Louis, E. J.; MacDiarmid, A. G.; Chiang, C. K.; Heeger, A. J. *J. Chem. Soc., Chem. Commun.* **1977**, 578.

<sup>4</sup> Chiang, C. K.; Fincher, C. R. Jr.; Park, Y. W; Heeger, A. J.; Shirakawa, H.; Louis, E. J.; Gau, S. C.; MacDiarmid, A. G. *Phys. Rev. Lett.* **1977**, 39, 1098.

<sup>5</sup> Shirakawa, H. *Synthetic Metals* **1995**, 69, 3.

<sup>6</sup> Shirakawa, H. in *Handbook of Conducting Polymers*, 2nd ed.; Skotheim, T. A.; Elsenbaumer, R. L.; Reynolds, J. R., Eds.; Marcel Dekker: New York, 1998, Ch. 7.

<sup>7</sup> Okada, T.; Ogata, T.; Ueda, M. *Macromolecules* **1996**, 29, 7645.

<sup>8</sup> Toshima, N.; Hara, S. *Prog. Polym. Sci.* **1995**, 20, 155.

<sup>9</sup> Kovacic, P.; Jones, M. B. *Chem. Rev.* **1987**, 87, 357.

<sup>10</sup> Ueda, M.; Aba, T.; Awano, H. *Macromolecules* **1992**, 25, 5125.

<sup>11</sup> Baughman, R. H.; Bredas, J. L.; Chance, R. R.; Elsenbaumer, R. L.; Shacklette, L. W. *Chem. Rev.* **1982**, 82, 209.

<sup>12</sup> Elsenbaumer, R. L; Jen, K. -Y.; Oboodi, R. *Synthetic Metals* **1986**, 15, 169.

<sup>13</sup> Miller, G. G.; Elsenbaumer, R. L. *J. Chem. Soc., Chem. Commun.* **1986**, 1346.

<sup>14</sup> Sato, M.; Tanaka, S.; Kaeriyama, K. *J. Chem. Soc., Chem. Commun.* **1986**, 873.

<sup>15</sup> Hotta, S.; Rughooputh, S. D. D. V.; Heeger, A. J.; Wudl, F. *Macromolecules* **1987**, *20*, 212.

<sup>16</sup> Sato, M.; Morii, H. *Macromolecules* **1991**, *24*, 1196.

<sup>17</sup> Sato, M.; Morii, H. *Polym. Commun.* **1991**, *32*, 42.

<sup>18</sup> Krivoshei, I. V.; Skorobogatov, V. M. *Polyacetylene and Polyarylenes: Synthesis and Conductive Properties*; Polymer Monographs Vol. 10; Huglin, M. B., Ed.; Gordon and Breach Science Publishers: Philadelphia, PA, 1991; Ch. 4.

<sup>19</sup> Winokur, M. J. in *Handbook of Conducting Polymers*, 2nd ed.; Skotheim, T. A.; Elsenbaumer, R. L.; Reynolds, J. R., Eds.; Marcel Dekker: New York, 1998, Ch. 25.

<sup>20</sup> McCullough, R. D.; Ewbank, P. C. in *Handbook of Conducting Polymers*, 2nd ed.; Skotheim, T. A.; Elsenbaumer, R. L.; Reynolds, J. R., Eds.; Marcel Dekker: New York, 1998, Ch. 9.

<sup>21</sup> McCullough, R. D. *Adv. Mater.* **1998**, *10*, 93.

<sup>22</sup> McCullough, R. D.; Tristam-Nagle, S.; Williams, S. P.; Lowe, R. D.; Jayaraman, M. *J. Am. Chem. Soc.* **1993**, *115*, 4910.

<sup>23</sup> Chen, T. -A.; Wu, X.; Rieke, R. D. *J. Am. Chem. Soc.* **1995**, *117*, 233.

<sup>24</sup> McCullough, R. D.; Lowe, R. D. *J. Chem. Soc., Chem. Commun.* **1992**, 70.

<sup>25</sup> Chen, T. -A.; Rieke, R. D. *J. Am. Chem. Soc.* **1992**, *114*, 10087.

<sup>26</sup> Andersson, M. R.; Selse, D.; Berggren, H.; Jarvinen, H.; Hjertberg, T.; Ingäas, O.; Wennerstrom, O.; Osterholm, J. E. *Macromolecules* **1994**, *27*, 6503.

<sup>27</sup> Levesque, I.; Leclerc, M. *J. Chem. Soc., Chem. Commun.* **1995**, 2293.

<sup>28</sup> Ivory, D. M. *J. Chem. Phys.* **1979**, *71*, 1506.

<sup>29</sup> Diaz, A. F.; Kanazawa, K. K.; Gardini, G. P. *J. Chem. Soc., Chem. Commun.* **1979**, 635.

<sup>30</sup> Edwards, J. H.; Feast, W. J. *Polymer* **1980**, *21*, 595.

<sup>31</sup> Edwards, J. H.; Feast, W. J.; Bott, D. C. *Polymer* **1984**, *25*, 395.

<sup>32</sup> Gagnon, D. R.; Capistran, J. D.; Karasz, F. E. and Lenz, R. W. *Polym. Bull.* **1984**, 12, 293.

<sup>33</sup> Murase, I.; Ohnishi, T.; Noguchi, T.; Hirooka, M. *Polym. Commun.* **1984**, 25, 327.

<sup>34</sup> Murase, I.; Ohnishi, T.; Noguchi, T.; Hirooka, M. ; Murakami, S. *Mol. Cryst. Liq. Cryst.* **1985**, 118, 333.

<sup>35</sup> Ballard, D. G. H.; Courtis, A.; Shirley, I. M.; Taylor, S. C. *J. Chem. Soc., Chem. Commun.* **1983**, 954.

<sup>36</sup> Wessling, R. A. *J. Polym. Chem., Polym. Symp.* **1985**, 72, 55.

<sup>37</sup> Ballard, D. G. H.; Courtis, A.; Shirley, I. M.; Taylor, S. C. *Macromolecules* **1988**, 21, 294.

<sup>38</sup> Schlüter, A. -D.; Wegner, G. *Acta Polymer.* **1993**, 44, 59.

<sup>39</sup> Pelter, A.; Jenkins, I.; Jones, D. E. *Tetrahedron* **1997**, 53, 10357.

<sup>40</sup> McCullough, R. D.; Williams, S. P.; Tristam-Nagle, S.; Jayaraman, M.; Ewbank, P. C.; Miller, L. *Synthetic Metals* **1995**, 69, 279.

<sup>41</sup> Chan, W. -K.; Chen, Y.; Peng, Z.; Yu, L. *J. Am. Chem. Soc.* **1995**, 115, 11735.

<sup>42</sup> Evans, G. in *Advances in Electrochemical Science and Engineering*, Vol. 1 Gerischer, H. and Tobias, C. W., Eds.; VCH: New York, 1990; Ch. 1.

<sup>43</sup> Ferraris, J. P. and Guerrero, D. J. in *Handbook of Conducting Polymers*, 2nd ed.; Skotheim, T. A.; Elsenbaumer, R. L.; Reynolds, J. R., Eds.; Marcel Dekker: New York, 1998, Ch. 10.

<sup>44</sup> Diaz, A. F.; Crowley, J.; Bargon, J.; Gardini, G. P.; Torrance, J. B. *J. Electroanal. Chem.* **1981**, 121, 355.

<sup>45</sup> Marque, P.; Roncali, J.; Garnier, F. *J. Electroanal. Chem.* **1987**, 218, 107.

<sup>46</sup> Roncali, J. in *Handbook of Conducting Polymers*, 2nd ed.; Skotheim, T. A.; Elsenbaumer, R. L.; Reynolds, J. R., Eds.; Marcel Dekker: New York, 1998, Ch. 12.

<sup>47</sup> Su, W. -P.; Schrieffer, J. R.; Heeger, A. J. *Phys. Rev. B* **1980**, 28, 1138.

<sup>48</sup> Su, W. -P. in *Handbook of Conducting Polymers*, 1st ed.; Skotheim, T. A., Ed.; Marcel Dekker: New York, 1986; p. 757.

<sup>49</sup> Bloor, D. in *Comprehensive Polymer Science*, Vol 2 Allen, G; Bevington, J. C., Eds.; Booth, C.; Price, C., Volume Eds.; Pergamon Press: Elmsford, NY, 1989; Ch. 22.

<sup>50</sup> Brédas, J. L.; Chance, R. R.; Silbey, R. *Mol. Cryst. Liq. Cryst.* **1981**, 77, 319.

<sup>51</sup> Bishop, A. R.; Campbell, D. K.; Fesser, K. *Mol. Cryst. Liq. Cryst.* **1981**, 77, 253.

<sup>52</sup> Irvin, D. J.; Dudis, D. S.; Reynolds, J. R. *Polymer Preprints* **1997**, 38, 318.

<sup>53</sup> Jen, K.; Miller, G. G.; Elsenbaumer, R. L. *J. Chem. Soc., Chem. Commun.* **1986**, 1346.

<sup>54</sup> Reynolds, J. R.; Ruiz, J. P.; Child, A. D.; Nayak, K.; Marynick, D. S. *Macromolecules*, **1991**, 24, 678.

<sup>55</sup> Ruiz, J. P.; Dharia, J. R.; Reynolds, J. R.; Buckley, L. J. *Macromolecules* **1992**, 25, 849.

<sup>56</sup> Child, A. D.; Sankaran, B.; Larmat, F.; Reynolds, J. R. *Macromolecules*, **1995**, 28, 6571.

<sup>57</sup> LeClerc, M.; Daoust, D. *J. Chem. Soc., Chem. Commun.* **1990**, 273.

<sup>58</sup> LeClerc, M.; Daoust, D. *Synthetic Metals* **1991**, 41, 529.

<sup>59</sup> Weder, C.; Wrighton, M. S. *Macromolecules* **1996**, 29, 5157.

<sup>60</sup> Wudl, F.; Allemand, P. -M.; Srđanov, G.; Ni, Z.; McBranch, D. in *Materials for Nonlinear Optics: Chemical Perspectives*; ACS Symposium Series #455; Marder, S. R.; Sohn, J. E. and Stucky, G. D., Eds.; American Chemical Society: Washington, D. C., 1991; Ch. 46.

<sup>61</sup> Bhowmik, P. K.; Garay, R. O.; Lenz, R. W. *Makromol. Chem.* **1991**, 192, 415.

<sup>62</sup> Lenz, R. W.; Furukawa, A.; Bhowmik, P. K.; Garay, R. O. and Majnusz, J. *Polymer* **1991**, 32, 1703.

<sup>63</sup> Garay, R. O.; Mayer, B.; Karasz, F. E.; Lenz, R. W. *J. Polym. Sci., Polym. Chem. Ed.* **1995**, 33, 525.

<sup>64</sup> Reichardt, C. *Solvents and Solvent Effects in Organic Chemistry*, 2nd ed.; VCH: New York, 1988, Chapter 2.

<sup>65</sup> Roncali, F.; Garnier, F.; Garceau, R.; Lemaire, M. *J. Chem. Soc., Chem. Commun.* **1987**, 1500.

<sup>66</sup> Elsenbaumer, R. L.; Jen, K. Y.; Miller, G. G.; Shacklette, L. M. *Synthetic Metals* **1989**, *18*, 277.

<sup>67</sup> Dietrich, M.; Heinze, J.; Heywang, G.; Jonas, F. *J. Electroanal. Chem.* **1994**, *369*, 87.

<sup>68</sup> Jonas, F.; Heywang, G. *Electrochimica Acta* **1994**, *39*, 1345.

<sup>69</sup> Jonas, F.; Heywang, G.; Schraldtberg, W.; Heinze, J.; Dietrich, M. *United States Patent* **1991**, 5,035,926.

<sup>70</sup> Heywang, G.; Jonas, F. *Adv. Mat.* **1992**, *4*, 116.

<sup>71</sup> Sotzing, G. A.; Reynolds, J. R.; Steel, P. J. *Adv. Mater.* **1997**, *9*, 795.

<sup>72</sup> Kumar, A.; Reynolds, J. R. *Macromolecules* **1996**, *29*, 7629.

<sup>73</sup> Sankaran, B.; Reynolds, J. R. *Macromolecules* **1997**, *30*, 2582.

<sup>74</sup> Bruce, J.; Challenger, F.; Gibson, H. B.; Allenby, W. E. *J. Inst. Petrol.* **1948**, *34*, 226.

<sup>75</sup> Meisel, S. L.; Johnson, G. C.; Hartough, H. D. *J. Am. Chem. Soc.* **1950**, *72*, 1910.

<sup>76</sup> Kovacic, P.; McFarland, K. N. *J. Polym. Sci., Polym. Chem. Ed.* **1979**, *17*, 1963.

<sup>77</sup> Yamamoto, T.; Sanechika, K.; Yamamoto, A. *J. Polym. Sci., Polym. Lett. Ed.* **1980**, *180*, 13.

<sup>78</sup> Tourillon, G.; Garnier, F. *J. Electroanal. Chem.* **1982**, *135*, 173.

<sup>79</sup> Hotta, S.; Hosaka, T.; Shimotsuma, W. *Synthetic Metals* **1983**, *6*, 69.

<sup>80</sup> Souto Maior, R. M.; Hinkelmann, K.; Eckert, H.; Wudl, F. *Macromolecules* **1990**, *23*, 1268.

<sup>81</sup> Cunningham, D. D.; Galal, A.; Pham, C. V.; Lewis, E. T.; Burkhardt, A.; Laguren-Davidson, L.; Nkansah, A.; Ataman, O. Y.; Zimmer, H.; Mark, H. B. Jr. *J. Electrochem. Soc.: Electrochem. Sci. Technol.* **1988**, *135*, 2750.

<sup>82</sup> Havinga, E. E.; van Horssen, L. W. *Makromol. Chem., Makromol. Symp.* **1989**, *24*, 67.

<sup>83</sup> Roncali, J.; Gorgues, A.; Jubault, M. *Chem. Mater.* **1993**, *1*, 1456.

<sup>84</sup> Zotti, G.; Gallazi, M. C.; Zerbil, G.; Meille, S. V. *Synthetic Metals* **1995**, *73*, 213.

<sup>85</sup> Sotzing, G. A.; Reynolds, J. R.; Steel, P. J. *Chem. Mater.* **1996**, *8*, 882.

<sup>86</sup> Danieli, R.; Ostoja, R.; Tiecco, M.; Zamboni, R.; Taliani, C. *J. Chem. Soc., Chem. Commun.* **1986**, 1473.

<sup>87</sup> Mitsuhara, T.; Tanaka, S. and Kaeriyama, K. *J. Chem. Soc., Chem. Commun.* **1987**, 764.

<sup>88</sup> Tanaka, S.; Kaeriyama, K.; Hiraide, T. *Makromol. Chem., Rapid Commun.* **1988**, *9*, 743.

<sup>89</sup> Chung, T.; Kaufman, J.; Heeger, A. J.; Wudl, F. *Phys. Rev. B* **1984**, *30*, 702.

<sup>90</sup> Eckhart, H.; Shacklette, L. M.; Jen, K. Y.; Elsenbaumer, R. L. *J. Chem. Phys.* **1989**, *91*, 1303.

<sup>91</sup> Sotzing, G. A.; Reynolds, J. R. *J. Chem. Soc., Chem. Commun.* **1995**, 703.

<sup>92</sup> Reddinger, J. L.; Sotzing, G. A.; Reynolds, J. R. *Chem. Commun.* **1996**, 1777.

<sup>93</sup> Sapp, S. A.; Sotzing, G. A.; Reddinger, J. L.; Reynolds, J. R. *Adv. Mater.* **1996**, *8*, 808.

<sup>94</sup> Cheng, Y.; Elsenbaumer, R. L. *J. Chem. Soc., Chem. Commun.* **1995**, 1451.

<sup>95</sup> Sotzing, G. A.; Thomas, C. A.; Reynolds, J. R.; Steel, P. J. *Macromolecules* **1998**, *31*, 3750.

<sup>96</sup> Sotzing, G. A.; Reddinger, J. L.; Katritzky, A. R.; Soloducho, J.; Musgrave, R.; Reynolds, J. R. *Chem. Mater.* **1997**, *9*, 1578.

<sup>97</sup> Irvin, D. J.; Reynolds, J. R. *Polymers for Advanced Technologies* **1998**, *9*, 260.

<sup>98</sup> Reynolds, J. R.; Child, A. D.; Gieselman, M. B. in *Kirk-Othmer Encyclopedia of Chemical Technology*. Vol. 9, 4th ed.; Wiley and Sons: New York, 1994, p. 77.

<sup>99</sup> Colaneri, N. F.; Shacklette, L. W. *IEEE Trans. Intr. Meas.* 1 **1986**, 82, 1259.

<sup>100</sup> Matsunaga, T.; Daifuku, H.; Nakajima, T.; Kawagoe, T. *Polymers for Advanced Technologies* **1990**, 1, 33.

<sup>101</sup> Lu, W-K; Basak, S.; Elsenbaumer, R. L. in *Handbook of Conducting Polymers*, 2nd ed.; Skotheim, T. A.; Elsenbaumer, R. L.; Reynolds, J. R., Eds.; Marcel Dekker: New York, 1998, Ch. 31.

<sup>102</sup> Gregory, R. V.; Kimbell, W. C.; Kuhn, H. H. *Synthetic Metals* **1989**, 28, C823.

<sup>103</sup> Gregory, R. V.; Kimbell, W. C.; Kuhn, H. H. *J. Coated Fabrics* **1991**, 20, 1.

<sup>104</sup> Kincal, D.; Kumar, A.; Child, A. D.; Reynolds, J. R. *Synthetic Metals* **1998**, 92, 53.

<sup>105</sup> Kuhn, H. H.; Child, A. D. in *Handbook of Conducting Polymers*, 2nd ed.; Skotheim, T. A.; Elsenbaumer, R. L.; Reynolds, J. R., Eds.; Marcel Dekker: New York, 1998, Ch. 35.

<sup>106</sup> Foulds, N. C.; Lowe, C. R. *J. Chem. Soc., Faraday Trans.* **1986**, 82, 1259.

<sup>107</sup> Guiseppi-Elie, A.; Wallace, G. G.; Matsue, T. in *Handbook of Conducting Polymers*, 2nd ed.; Skotheim, T. A.; Elsenbaumer, R. L.; Reynolds, J. R., Eds.; Marcel Dekker: New York, 1998, Ch. 34.

<sup>108</sup> Otero, T. F.; Grande, H. -J. in *Handbook of Conducting Polymers*, 2nd ed.; Skotheim, T. A.; Elsenbaumer, R. L.; Reynolds, J. R., Eds.; Marcel Dekker: New York, 1998, Ch. 36.

<sup>109</sup> Zinger, B.; Miller, L. L. *J. Am. Chem. Soc.* **1984**, 106, 6861.

<sup>110</sup> Miller, L. L. *Mol. Cryst. Liq. Cryst.* **1988**, 160, 297.

<sup>111</sup> Norris, R.; Sternell, S. *Aust. J. Chem.* **1973**, 26, 333.

<sup>112</sup> Balandra, P. B.; Ph.D. Dissertation, University of Florida, Gainesville, 1997.

<sup>113</sup> *Comprehensive Organic Synthesis: Selectivity, Strategy, and Efficiency in Modern Organic Chemistry*, 1st ed; Trost, B. M. and Fleming, I., Eds.; Pergamon: New York, 1991; Ch 2.

<sup>114</sup> Yamamoto, T.; Hayashi, Y.; Yamamoto, A. *Bull. Chem. Soc. Jpn.* **1978**, *51*, 2091.

<sup>115</sup> Stille, J. K. *Angew. Chem. Int. Ed. Engl.* **1986**, *25*, 508.

<sup>116</sup> Bochmann, M.; Kelly, K.; Lu, J. *J. Polym. Sci., Polym. Chem. Ed.* **1992**, *30*, 2511.

<sup>117</sup> Swager, T. M.; Marsella, M. J.; Zhou, Q.; Goldfinger, M. B. *J. M. S.-Pure Appl. Chem.* **1994**, *A31*, 1893.

<sup>118</sup> Gronowitz, S.; Peters, D. *Heterocycles* **1990**, *30*, 645.

<sup>119</sup> Inganäs, O.; Salanek, W. R.; Osterholm, J. -E.; Laasko, J. *Synth. Met.* **1988**, *22*, 395.

<sup>120</sup> Negishi, E. *Am. Chem. Soc. Div. Pet. Chem. Prepr.* **1979**, *24*, 226.

<sup>121</sup> Negishi. E *Acc. Chem. Res.* **1982**, *15*, 340.

<sup>122</sup> Yamamoto, T.; Morita, A.; Miyazaki, Y.; Maruyama, T.; Wakayama, H.; Zhou, Z.; Nakamura, Y.; Kanbara, T.; Sasaki, S.; Kubota, K. *Macromolecules* **1992**, *25*, 1214.

<sup>123</sup> Yamamoto, T.; Miyazaki, Y.; Fukuda, T.; Zhou, Z.; Maruyama, T.; Kanbara, T.; Osakada, K. *Synth. Met.* **1993**, *55–57*, 1214.

<sup>124</sup> Zimmerman, E. K.; Stille, J. K. *Macromolecules* **1985**, *18*, 321.

<sup>125</sup> Bolognesi, A.; Catellani, M.; Porzio, W, Speroni, F.; Galarini, R.; Musco, A.; Pontelli, R. *Polymer* **1993**, *34*, 4150.

<sup>126</sup> Miyaura, N.; Yanagi, T.; Suzuki, A. *Synth. Commun.* **1981**, *11*, 513.

<sup>127</sup> Miler, R. B.; Dugar, S. *Organometallics*, **1984**, *3*, 1261.

<sup>128</sup> Deeter, G. A.; Moore, J. S. *Macromolecules* **1993**, *26*, 2535.

<sup>129</sup> Bondi, A. J. *J. Phys. Chem.* **1964**, *68*, 441.

<sup>130</sup> Irvin, D. J.; Ph.D. Dissertation, University of Florida, Gainesville, 1998.

<sup>131</sup> Salmon, M.; Kanazawa, K. K.; Diaz, A. F.; Krounbi, M. *J. Polym. Sci.* **1982**, *20*, 187.

<sup>132</sup> Street, G. G.; Clarke, T. C.; Krounbi, M.; Kanazawa, K.; Lee, V.; Pfluger, P.; Scott, J. C.; Weiser, G. *Mol. Cryst. Liq. Cryst.* **1982**, *83*, 1285.

<sup>133</sup> Shimidzu, T.; Ohtani, A.; Iyoda, T.; Honda, K. *J. Chem. Soc., Chem. Commun.* **1986**, 1414.

<sup>134</sup> Abruña, H. *Coordination Chemistry Reviews* **1988**, *86*, 135.

<sup>135</sup> Lane, R. F.; Hubbard, A. T. *J. Phys. Chem.* **1973**, *77*, 1401.

<sup>136</sup> Laviron, E. *J. Electroanal. Chem.* **1972**, *39*, 1.

<sup>137</sup> Sawyer, D. T.; Sobkowiak, A.; Roberts, J. L. Jr. *Electrochemistry for Chemists*, 2nd ed.; John Wiley and Sons: New York, 1995; Ch. 5.

<sup>138</sup> Nowak, M.; Rughooputh, S.; Hotta, S.; Heeger, A. *Macromolecules* **1987**, *20*, 965.

<sup>139</sup> McCullough, R. D.; Williams, S. P. *J. Am. Chem. Soc.* **1993**, *115*, 11608.

<sup>140</sup> Miyazaki, Y.; Kanbara, T.; Osakada, K.; Yamamoto, T.; Kubota, K. *Polymer J.* **1994**, *26*, 509.

<sup>141</sup> Bäurle, P.; Scheib, S. *Acta Polymer.* **1995**, *46*, 124.

<sup>142</sup> Marsella, M. J.; Newland, R. J.; Carroll, P. J.; Swager, T. M. *J. Am. Chem. Soc.* **1995**, *117*, 9842.

<sup>143</sup> Leclerc, M.; Faid, K. *Adv. Mater.* **1997**, *9*, 1087.

<sup>144</sup> Rimmel, G.; Bäurle, P. in the International Conference on Science and Technology of Synthetic Metals July, 1998, reprint to be published in the conference proceedings in *Synthetic Metals* in 1999.

<sup>145</sup> Pyo, M.; Reynolds, J. R.; Warren, L. F.; Marcy, H. O. *Synthetic Metals* **1994**, *68*, 71.

<sup>146</sup> Rughooputh, S. D. D. V.; Hotta, S.; Heeger, A. J.; Wudl, F. *J. Polym. Sci. B: Polym. Phys.* **1987**, *25*, 1071.

<sup>147</sup> Chen, S. -A.; Ni, J. -M. *Macromolecules* **1992**, *25*, 1071.

<sup>148</sup> Rasmussen, S. C.; Pickens, J. C.; Hutchison, J. E. *Chem. Mater.* **1998**, *10*, 1990.

<sup>149</sup> Sotzing, G.; Reynolds, J.; Steel, P. *Chem. Mater.* **1996**, *8*, 882.

<sup>150</sup> Roncali, J.; Garreau, R.; Yassar, A.; Marque, P.; Garnier, F.; Lemaire, M. *J. Phys. Chem.* **1987**, *91*, 6706.

<sup>151</sup> Murray, R. W. in *Electroanalytical Chemistry*, Vol. 13; Bard, A. J., Ed.; Marcel Dekker: New York, 1984; p. 191.

<sup>152</sup> Abruña, H. D. *Coord. Chem. Rev.* **1988**, *86*, 135.

<sup>153</sup> Merz, A. *Topics Curr. Chem.* **1990**, *152*, 49.

<sup>154</sup> Leech, D. in *Electroactive Polymer Electrochemistry, Part 2: Methods and Applications*; Lyons, M. E. G., Ed.; Plenum Press: New York, 1996; p. 271.

<sup>155</sup> Child, A. D.; Reynolds, J. R. *J. Chem. Soc., Chem. Commun.* **1991**, 1779.

<sup>156</sup> Lee, J. -W.; Park, D. -S.; Shim, Y. -B.; Park, S. -M. *J. Electrochem. Soc.* **1992**, *139*, 3507.

<sup>157</sup> Sun, Z. W.; Frank, A. J. *J. Chem. Phys.* **1991**, *94*, 4600.

<sup>158</sup> Hoier, S. N.; Park, S. -M. *J. Phys. Chem.* **1992**, *96*, 5188.

<sup>159</sup> Oudard, J. F.; Allendoerfer, R. D.; Osteryoung, R. A. *J. Electroanal. Chem.* **1988**, *241*, 231.

<sup>160</sup> Wertz, J. E.; Bolton, J. R. *Electron Spin Resonance: Elementary Theory and Practical Applications* Chapman and Hall: New York, 1986; Ch. 1.

<sup>161</sup> Gourley, K. D.; Lillya, C. P.; Reynolds, J. R.; Chien, J. C. W. *Macromolecules* **1984**, *17*, 1025.

<sup>162</sup> Reynolds, J. R.; Schlenoff, J. B.; Chien, J. C. W. *J. Electrochem. Soc.: Electrochem. Sci. Tech.* **1985**, *132*, 1131.

<sup>163</sup> Genoud, F.; Guglielmi, M.; Nechtschein, M.; Genies, E.; Slamon, M. *Phys. Rev. Lett. B* **1985**, *55*, 118.

<sup>164</sup> Chen, J.; Heeger, A. J.; Wudl, F. *Solid State Commun.* **1986**, *58*, 251.

<sup>165</sup> Oudard, J. F.; Allendoerfer, R. D.; Osteryoung, R. A. *J. Electroanal. Chem.* **1988**, *241*, 231.

<sup>166</sup> Zotti, G.; Schiavon, G. *Synth. Met.* **1989**, *31*, 347.

<sup>167</sup> Zotti, G.; Schiavon, G. *Chem. Mater.* **1991**, *3*, 62.

<sup>168</sup> Piette, L. H.; Ludwig, P.; Adams, R. N. *J. Am. Chem. Soc.* **1961**, *83*, 2671.

<sup>169</sup> Piette, L. H.; Ludwig, P.; Adams, R. N. *J. Am. Chem. Soc.* **1962**, *84*, 4212.

<sup>170</sup> Heeger, A. J. in "Conjugated Polymers and Related Materials: The Interconnection of Chemical and Electronic Structure," Oxford University Press: New York, 1993; Chap. 4.

<sup>171</sup> Kittlesen, G. P.; White, H. S.; Wrighton, M. S. *J. Am. Chem. Soc.* **1984**, *106*, 7389.

<sup>172</sup> Paul, E. W.; Ricco, A. J.; Wrighton, M. S. *J. Phys. Chem.* **1985**, *89*, 1441.

<sup>173</sup> Schiavon, G.; Sitran, S.; Zotti, G. *Synth. Met.* **1989**, *32*, 209.

<sup>174</sup> Ye, S.; Bélanger, D. *J. Electroanal. Chem.* **1993**, *344*, 395.

<sup>175</sup> Morvant, M. C.; Reynolds, J. R. *Synth. Met.* **1998**, *92*, 57.

<sup>176</sup> Quirk, R. P.; Lynch, T. *Macromolecules* **1993**, *26*, 1206.

<sup>177</sup> Zhang, H.; Rankin, A.; Ward, I.M. *Polymer* **1996**, *37*, 1079.

<sup>178</sup> Ferraris, J. P.; Newton, M. D. *Polymer* **1992**, *33*, 391.

<sup>179</sup> Quirk, R. P.; Schock, L. E. *Macromolecules* **1991**, *24*, 1237.

<sup>180</sup> Adams, P. N.; Apperley, D. C.; Monkman, A. P. *Polymer* **1993**, *34*, 328.

<sup>181</sup> Johncock, P.; Cunliffe, A. V. *Polymer* **1993**, *34*, 1933.

<sup>182</sup> Miura, K.; Kitayama, T.; Hatada, K.; Nakata, T. *Polymer Journal* **1990**, *22*, 67.

<sup>183</sup> Odian, G. *Principles of Polymerization*, 2nd ed.; Wiley Interscience: New York, 1991, Ch. 1.

<sup>184</sup> Askadskii, A. A. *Polym. Sci. USSR* **1989**, *31*, 2356.

<sup>185</sup> Hotta, S.; Hosaka, T.; Soga, M.; Shimotsuma, W. *Synthetic Metals* **1984/5**, *10*, 5.

<sup>186</sup> Jen, K.-Y.; Oboodi, R.; Elsenbaumer, R. L. *Polym. Mat. Sci. Eng.* **1985**, *53*, 79.

<sup>187</sup> Pomerantz, M.; Tseng, J. J.; Zhu, H.; Sproull, S. J.; Reynolds, J. R.; Uitz, R.; Arnott, H. J.; Haider, M. I. *Synthetic Metals* **1991**, *41–43*, 825.

<sup>188</sup> Müllen, K.; Wegner, G. *Electronic Materials: The Oligomer Approach*; Wiley–VCH: New York, 1998.

<sup>189</sup> Benoit, H.; Grubisic, Z.; Rempp, P.; Decker, D.; Zilliox, J. G. *J. Chim. Phys.* **1966**, *63*, 1507.

<sup>190</sup> Grubisic, Z.; Rempp, P.; Benoit, H. *J. Polym. Sci. Part B* **1967**, *5*, 753.

<sup>191</sup> Czerwinski, A.; Zimmer, H.; Amer, A.; Chiem, V. P.; Pons, S.; Mark, H. B. *J. Chem. Soc. Chem. Commun.* **1985**, 1158.

<sup>192</sup> Czerwinski, A.; Zimmer, H.; Chiem, V. P.; Amer, A.; Schrader, J. R.; Mark, H. B. *Anal. Lett. A* **1985**, *18*, 673.

<sup>193</sup> Chiem, V. P.; Czerwinski, A.; Zimmer, H.; Mark, H. B. *J. Polym. Sci. C* **1986**, *24*, 103.

<sup>194</sup> Czerwinski, A.; Cunningham, D. D.; Amer, A.; Schrader, J. R.; Chiem, V. P.; Zimmer, H.; Mark, H. B.; Pons, S. *J. Electrochem. Soc.* **1987**, *134*, 1158.

<sup>195</sup> Groendaal, L.; Peerlings, H. W. I.; van Dongen, J. L. J.; Havinga, E. E.; Vekemans, J. A. J. M.; Meijer, E. W. *Macromolecules* **1995**, *28*, 116.

<sup>196</sup> Pomerantz, M.; Yang, H.; Cheng, Y. *Macromolecules* **1995**, *28*, 5706.

<sup>197</sup> Yoshizawa, K.; Ito, A.; Tanaka, K.; Yamabe, T. *Synthetic Metals* **1992**, *48*, 271.

<sup>198</sup> Ullmann, F.; Bielecki, J. *Ber. Dtsch. Chem. Ges.* **1901**, *34*, 2174.

<sup>199</sup> March, J. *Advanced Organic Chemistry: Reactions, Mechanisms, and Structure*, 3rd ed.; John Wiley and Sons: New York, 1985; pp. 597–598.

<sup>200</sup> Nursten, H. E. *J. Chem. Soc.* **1955**, 3081.

<sup>201</sup> Rule, H. G.; Smith, F. R. *J. Chem. Soc.* **1937**, 1096.

<sup>202</sup> Tamura, M.; Kochi, J. K. *J. Organomet. Chem.* **1972**, *42*, 205.

<sup>203</sup> Paine, A. J. *J. Am. Chem. Soc.* **1987**, *109*, 1496.

<sup>204</sup> Xi, M.; Bent, B. E. *Surf. Sci.* **1992**, *278*, 19.

<sup>205</sup> Xi, M.; Bent, B. E. *J. Am. Chem. Soc.* **1993**, *115*, 7426.

<sup>206</sup> Suslick, K. S.; Casadonte, D. J.; Doktycz, S. J. *Chem. Mater.* **1989**, *1*, 6.

<sup>207</sup> Fanta, P. E. *Chem. Rev.* **1946**, *38*, 139.

<sup>208</sup> Fanta, P. E. *Synthesis* **1974**, 9.

<sup>209</sup> Björklund, C. *Acta Chem. Scand.* **1971**, *25*, 2825.

<sup>210</sup> Niziurski-Mann, R. E.; Cava, M. P. *Adv. Mater.* **1993**, *5*, 547.

<sup>211</sup> Li, W.; Maddux, T.; Yu, L. *Macromolecules* **1996**, *29*, 7329.

<sup>212</sup> Zhu, S. S.; Swager, T. M. *J. Am. Chem. Soc.* **1997**, *119*, 12568.

<sup>213</sup> Bolognesi, A.; Catellani, M.; Musco, A.; Pontellini, R. *Synthetic Metals* **1993**, *55–57*, 1255.

<sup>214</sup> Musfeldt, J. L.; Reynolds, J. R.; Tanner, D. B.; Ruiz, J. P.; Wang, J.; Pomerantz, M. *J. Polym. Sci., Polym. Chem. Ed.* **1994**, *32*, 2395.

<sup>215</sup> Bao, Z.; Chan, W. K.; Yu, L. *J. Am. Chem. Soc.* **1995**, *117*, 12426.

<sup>216</sup> Kanbara, T.; Miyazaki, Y.; Yamamoto, T. *J. Polym. Sci., Polym. Chem. Ed.* **1995**, *33*, 999.

<sup>217</sup> Zhang, Q. T.; Tour, J. M. *J. Am. Chem. Soc.* **1998**, *120*, 5355.

<sup>218</sup> Bao, Z.; Chan, W.; Yu, L. *Chem. Mater.* **1993**, *5*, 2.

<sup>219</sup> Sniekus, V. *Chem. Rev.* **1990**, *90*, 925.

<sup>220</sup> Kalinin, V. N. *Synthesis* **1992**, 413.

<sup>221</sup> Kim, Y. H.; Webster, O. W. *Macromolecules* **1992**, *25*, 5561.

<sup>222</sup> Child, A. D.; Reynolds, J. R. *Macromolecules* **1994**, *27*, 1975.

<sup>223</sup> Rulkens, R.; Schulze, M.; Wegner, G. *Macromol. Rapid Commun.* **1994**, *15*, 669.

<sup>224</sup> Fréchette, M.; Belletete, M.; Bergeron, J.-Y.; Durocher, G.; Leclerc, M. *Macromol. Chem. Phys.* **1997**, *198*, 1709.

<sup>225</sup> Kowitz, C.; Wegner, G. *Tetrahedron* **1997**, *53*, 15553.

<sup>226</sup> Power, K. L.; Vries, T. R.; Havinga, E. E.; Meijer, E. W.; Wynberg, H. J. *Chem. Soc., Chem. Commun.* **1988**, 1432.

## BIOGRAPHICAL SKETCH

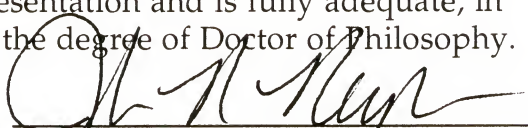
Jennifer Allison Ash Irvin was born on July 4, 1969, in Chicago, Illinois, but she spent most of her life in Texas. She met her future husband, David, while a high school freshman, and they married in 1991.

Jennifer began her undergraduate education in the fall of 1987 at Southwest Texas State University, San Marcos, Texas, where she obtained a B. S. in chemistry in 1991. She continued her studies at Southwest Texas State University, obtaining an M. S. in chemistry in August, 1993. Under the guidance of Dr. Patrick Cassidy from 1988 until 1993, Jennifer studied the synthesis and characterization of highly fluorinated aromatic polyethers.

In the fall of 1993, Jennifer began her graduate studies at the University of Florida. She joined the group of Professor John R. Reynolds, where she conducted research in the area of electroactive polymers. Jennifer completed her Ph.D. in organic chemistry in September, 1998.

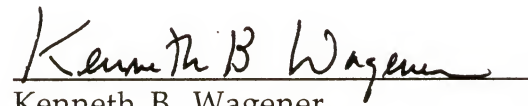
Jennifer is eager to apply her skills at Sandia National Laboratory in Livermore, California, as a postdoctoral chemist. In this position, Jennifer will continue to work in the area of conducting polymer synthesis and characterization.

I certify that I have read this study and that in my opinion it conforms to acceptable standards of scholarly presentation and is fully adequate, in scope and quality, as a dissertation for the degree of Doctor of Philosophy.



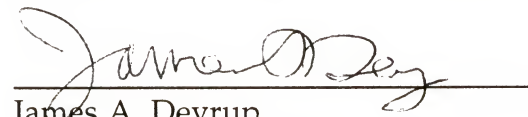
John R. Reynolds, Chairman  
Professor of Chemistry

I certify that I have read this study and that in my opinion it conforms to acceptable standards of scholarly presentation and is fully adequate, in scope and quality, as a dissertation for the degree of Doctor of Philosophy.



Kenneth B. Wagener  
Professor of Chemistry

I certify that I have read this study and that in my opinion it conforms to acceptable standards of scholarly presentation and is fully adequate, in scope and quality, as a dissertation for the degree of Doctor of Philosophy.



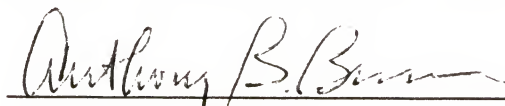
James A. Deyrup  
Professor of Chemistry

I certify that I have read this study and that in my opinion it conforms to acceptable standards of scholarly presentation and is fully adequate, in scope and quality, as a dissertation for the degree of Doctor of Philosophy.



Robert T. Kennedy  
Professor of Chemistry

I certify that I have read this study and that in my opinion it conforms to acceptable standards of scholarly presentation and is fully adequate, in scope and quality, as a dissertation for the degree of Doctor of Philosophy.



---

Anthony B. Brennan  
Associate Professor of Materials  
Science and Engineering

This dissertation was submitted to the Graduate Faculty of the Department of Chemistry in the College of Liberal Arts and Sciences and to the Graduate School and was accepted as partial fulfillment of the requirements for the degree of Doctor of Philosophy.

December, 1998

---

Dean, Graduate School